Antarctic sea ice algae:
Primary production and carbon allocation

A thesis submitted in fulfilment of the requirements
of the Degree of Doctorate of Philosophy
by

Sarah Caroline Ugalde

Bachelor of Environmental Science
Graduate Diploma of Agriculture Science (Honours)

Antarctic Climate and Ecosystems Cooperative Research Centre
Institute for Marine and Antarctic Studies
University of Tasmania

September 2015

Antarctic sea ice core with a dense bottom ice microbial community

Image: Sarah C. Ugalde

Declaration of Originality

This thesis contains no material which has been accepted for a degree or diploma by the University or any other institution, except by way of background information and duly acknowledged in the thesis, and to the best of my knowledge and belief no material previously published or written by another person except where due acknowledgement is made in the text of the thesis, nor does the thesis contain any material that infringes copyright.

Sarah C. Ugalde

15 September 2015

Authority of Access

This thesis may be made available for loan and limited copying and communication in accordance with the Copyright Act 1968.

Sarah C. Ugalde

15 September 2015

Statement Regarding Published Work

Statement of Co-authorship

Paper 1: Thesis Chapter 2

Title of Paper	Photosynthetic carbon allocation of an Antarctic sea ice diatom (*Fragilariopsis cylindrus*)
Publication Status	Published
Publication Details	Ugalde SC, Meiners KM, Davidson AT, Westwood KJ, McMinn A (2013). Photosynthetic carbon allocation of an Antarctic sea ice diatom (*Fragilariopsis cylindrus*). Journal of Experimental Marine Biology and Ecology. 446:228-235.

The following people and institutions contributed to the publication of work undertaken as part of this thesis:

Name of Principal Author (Candidate)	Ms. Sarah C. Ugalde (75 %)
Contribution to the Paper	Designed experimental set-up Performed analysis / prepared all samples Analysed and interpreted the data Wrote the manuscript Acted as corresponding author

Name of Co-author	Dr. Klaus M. Meiners (10 %)
Contribution to the Paper	Conceptualisation of work Funded the research Manuscript evaluation / editing

Name of Co-author	Dr. Andrew T. Davidson (5 %)
Contribution to the Paper	Interpretation of the data Trained the candidate in scientific writing Manuscript evaluation / editing

Name of Co-author	Dr. Karen J. Westwood (5 %)
Contribution to the Paper	Interpretation of the data Trained the candidate in C^{14} methods Manuscript evaluation / editing

Name of Co-author	Prof. Andrew McMinn (5 %)
Contribution to the Paper	Interpretation of the data Manuscript evaluation / editing

Paper 2: Thesis Chapter 3

Title of Paper	Extracellular organic carbon dynamics during a bottom ice algal bloom (Antarctica)
Publication Status	Published
Publication Details	Ugalde SC, Martin A, Meiners KM, McMinn A, Ryan KG. Extracellular organic carbon dynamics during a bottom-ice algal bloom (Antarctica). Aquatic Microbial Ecology. 73(3):195 – 210.

The following people and institutions contributed to the publication of work undertaken as part of this thesis:

Name of Principal Author (Candidate)	Ms. Sarah C. Ugalde (75 %)
Contribution to the Paper	Designed field sampling Collected field samples Performed analysis / prepared all samples Analysed and interpreted the data Wrote the manuscript Acted as corresponding author

Name of Co-author	Dr. Andrew Martin (5 %)
Contribution to the Paper	Field team leader Sourced some field equipment Manuscript evaluation / editing

Name of Co-author	Dr. Klaus M. Meiners (5 %)
Contribution to the Paper	Funded the research Interpretation of the data Manuscript evaluation / editing

Name of Co-author	Prof. Andrew McMinn (10 %)
Contribution to the Paper	Conceptualisation of work Interpretation of the data Manuscript evaluation / editing

Name of Co-author	Assoc. Prof. Ken G. Ryan (5 %)
Contribution to the Paper	Field project leader Manuscript evaluation / editing

Paper 3: Thesis Chapter 4

Title of Paper	Characteristics and primary productivity of East Antarctic pack ice during winter-spring transition
Publication Status	Submitted for publication
Publication Details	Ugalde SC, Westwood KJ, van den Enden R, McMinn A, Meiners KM. Characteristics and primary productivity of East Antarctic pack ice during the winter-spring transition. Deep Sea Research II. Submitted (special edition).

The following people and institutions contributed to the publication of work undertaken as part of this thesis:

Name of Principal Author (Candidate)	Ms. Sarah C. Ugalde (66 %)
Contribution to the Paper	Conceptualisation of work Designed field sampling Field work Performed analysis / prepared samples Analysed and interpreted the data Wrote the manuscript Acted as corresponding author

Name of Co-author	Dr. Karen J. Westwood (12 %)
Contribution to the Paper	Designed field sampling Field work Interpretation of the data Manuscript evaluation / editing

Name of Co-author	Mr. Rick van den Enden (5 %)
Contribution to the Paper	Field work Prepared some samples

Name of Co-author	Prof. Andrew McMinn (5 %)
Contribution to the Paper	Interpretation of the data Manuscript evaluation / editing

Name of Co-author	Dr. Klaus M. Meiners (12 %)
Contribution to the Paper	Field team/project leader Conceptualisation of work Funded the research Designed field sampling Interpretation of the data Manuscript evaluation / editing

We the undersigned agree with the above stated proportion of work undertaken for each of the above published (or submitted) peer-reviewed manuscripts contributing to this thesis:

Signed:

Date: 2/11/2015

Prof. Andrew McMinn
Primary supervisor
Institue for Marine and Antarctic Studies
University of Tasmania

Signed:

Date: 2/11/15

Prof. Craig Johnson
Director
Marine and Antarctic Futures Centre
Institute for Marine and Anarctic Studies
University of Tasmania

List of Abbreviations

A	surface albedo constant
AAD	Australian Antarctic Division
ACE CRC	Antarctic Climate and Ecosystems Cooperative Research Centre
ASPeCt	Antarctic Sea Ice Processes and Climate
Bact	bacteria
bd	below detection
C	carbon
C:N	carbon:nitrogen (molar)
chl *a*	chlorophyll *a*
CHO_{Mono}	carbohydrates (monosaccharides)
CHO_{Poly}	carbohydrates (polysaccharides)
cm	centimetre
CO_2	carbon dioxide
COLLOC	colloidal organic carbon
CSL	Central Science Laboratory
d	day
DIC	dissolved inorganic carbon
DOC	dissolved organic carbon
DPM	disintegrations per minute
E	light intensity at which carbon-uptake is maximal

EDOC	extracellular dissolved organic carbon
E_k	light saturation index
EOC	extracellular organic carbon
EPS	extracellular polymeric substances
Fe	iron
Fluoro	fluorometry
F_v/F_m	maximum quantum photosynthetic yield
h	hour
HNA	high nucleic acid
HPLC	high performance liquid chromatography
I_0	maximum incoming irradiance
ISPOL	Ice Station Polarstern
I_z	irradiance invident at a given depth
kg	kilogram
k_i	ice attenuation coefficient
km	kilometre
k_s	snow attenuation coefficient
l	litre
LNA	low nucleic acid
m	metre
mg	milligram
min	minute
MIZ	marginal sea ice zone
ml	millilitre

N	nitrogen
n	number
$NaHCO_3$	sodium bicarbonate
NH_4^+	ammonium
NO_2^-	nitrite
NO_3^-	nitrate
NO_x	sum of nitrate and nitrite
O_2	oxygen
P	rate of primary productivity
PAM	pulse amplitude modulation
PAR	photosynthetically active radiation
pCO_2	partial pressure of carbon dioxide
P-E	photosynthesis-irradiance
P_{max}	light satuated photosynthetic rate
PO_4	phosphate
POC or PON	particulate organic carbon or nitrogen
s	second
$Si(OH)^4$	silicic acid
SIMCO	sea ice microbial community organism
SIPEX	Sea Ice Physics and Ecosystems eXperiment
stderr or SE	standard error
TA	total alkalinity
TC	total carbon
TCHO	total carbohydrates

TDL	theoretical dilution lines
TEOC	total extracellular organic carbon
Tg	tetragram
TIN or TN	total inorganic nitrogen or total nitrogen
TPP	total primary production or productivity
TPTZ	2,4,6-tri pyridyl-*s*-triazine
V_b/V	brine volume fraction (V_b) to total brine volume (V)
WWOS	Winter Weddell Outflow Study
z_i	ice depth
z_s	snow depth
^{14}C	radiocarbon (carbon-14)
$\delta^{13}C$	stable carbon isotopes, expressed by the equation:

$$\delta^{13}C = \left(\frac{\left(\frac{^{13}C}{^{12}C}\right)\text{sample}}{\left(\frac{^{13}C}{^{12}C}\right)\text{standard}} - 1 \right) * 1000\ ‰$$

$\delta^{18}O$	stable oxygen isotopes, expressed by the equation:

$$\delta^{18}C = \left(\frac{\left(\frac{^{18}O}{^{16}O}\right)\text{sample}}{\left(\frac{^{18}O}{^{16}O}\right)\text{standard}} - 1 \right) * 1000\ ‰$$

µg	microgram
µl	microlitre
µm	micrometre
µmol	micromol

ABSTRACT

Antarctic sea ice algae: Primary production and carbon allocation

by

Sarah Caroline Ugalde

Sea ice is a semi-solid matrix of brine-filled channels, typically displaying strong vertical gradients in temperature, salinity, light, and space. Prolonged biological activity within the confines of the brine channels itself alters the micro-environment and physicochemistry. To be able to cope with these changes, ice algae display a complex suite of physiological and metabolic adaptations. One such adaptation is the exudation of photosynthetically-derived organic carbon.

Research undertaken for the thesis details primary production and carbon allocation of ice algal communities in laboratory and field conditions, and discusses the relationships between microbial growth dynamics, responses to physicochemical change, and ecosystem dynamics.

The thesis finds that sea ice algae are capable of exuding large quantities of photosynthetically-derived organic carbon. Allocation to exuded organic carbon is highest during times of adverse conditions, such as challenging biochemical and physicochemical conditions. The composition of exuded carbon varies between

defined pools, including dissolved organic carbon, colloidal organic carbon, and extracellular polymeric substances. The observed magnitude of changes in carbon allocation indicates that each extracellular carbon pool imparts different ecological roles and/or benefits to the producer organism.

The thesis highlights the complexity of sea ice primary productivity, subsequent carbon allocation, and the driving factors within the diverse sea ice habitat. With an increased ability to quantify direct exudation of organic carbon, the contribution of sea ice algae to total primary production and carbon flux dynamics across ice-covered seas could now be estimated.

Acknowledgements

The thesis would not have come to fruition if not for the dedication, support, and collective knowledge from many people – to you all, thankyou.

First and foremost, I would like to express the deepest appreciation to my supervisors; Prof. Andrew McMinn, Dr. Klaus Meiners, and Dr. Karen Westwood, whose outlook, accumulative knowledge, and at times, brutal honesty is a substance of genius and inspiration.

My appreciation to the Antarctic Climate and Ecosystems Cooperative Research Centre, Institute for Marine and Antarctic Studies (University of Tasmania), and the Australian Antarctic Division for the facilities, support, and scientific community.

To my army of mentors, coaches, and sympathisers for offering time, words wisdom, and incomparable opportunities, in particular those who influenced the foundations of this thesis; Dr. Andrew Martin, Dr. Andrew Davidson, Prof. Michael Stoddart, and Dr. Tony Press.

To those who have offered imperative technical assistance, both in the laboratory and field, and provided information, patience, forgiveness, and pure grunt; Dr. Thomas Rodeman (Central Science Laboratories), Ms. Debbie Lang (Australian Antarctic Division), Ms. Chris Thorn (Victorian University of Wellington), Mr.

Neville Higgison (Victorian University of Wellington), and Mr. Rick van den Enden (Australian Antarctic Division) to name a few.

A very special mention to Prof. Gustaaf Hallegraeff for the mentorship, understanding, and truly exciting opportunities – I look forward to our future endevours.

To my fellow postgraduate candidates, past and present, whose innovations, triumphs, and at times, turmoils, maintained my motivations and interests. I am sure many of us will be crossing paths in our future endeavours.

To the Millhouse family (Leslie Vale) for providing a roof over my head during a difficult time, and for introducing me to a beautiful and unforgettable landscape.

And finally, to my dearest family and friends, two- and four-legged, I dedicate this thesis to you for your unconditional love, patients, continuous moral support, and contribution throughout this seemingly never-ending adventure. Here's to you all!

TABLE OF CONTENTS

List of Figures and Tables

Chapter 1

Chapter 2

Chapter 3

Chapter 4

Chapter 5

CHAPTER 1

General Introduction

Antarctic sea ice is an extensive, yet ephemeral, habitat covering approximately 4.1 to 6.1 % of the total surface area of the global ocean (Arrigo 2014). Unlike freshwater ice, frozen seawater forms a semi-solid matrix of brine-filled channels, typically exhibiting strong vertical gradients in temperature, salinity, light, and importantly, space (Thomas and Dieckmann 2010). Despite these challenging conditions, photosynthetic microbes exist within sea ice, often concentrating at the ice-water interface, and are capable of reaching high standing stocks (Saenz and Arrigo 2014). Sea ice primary production and cell metabolism can be high during autumn ice formation, and then slow with the approaching winter in response to altering brine physicochemical conditions (Krell et al. 2008; McMinn and Martin 2013). With the onset of spring, light levels increase and primary production resumes to reach a maximum rate in spring – early summer (Arrigo et al. 1997; McMinn et al. 2010, Petrou and Ralph 2011).

The primary production rate of any photosynthetic biomass is largely determined by two factors; the amount of biomass and the amount of light available to that biomass (Antoine and Morel 1996). But it is also sensitive to a multitude of other factors, including temperature, nutrient availability, and carbonate chemistry. In

the sea ice habitat, a consequence of photosynthetic activity within the confines of brine channels is that the fluid becomes increasingly depleted in dissolved CO_2, with high concentrations of dissolved organic matter, low concentrations of inorganic nutrients, high ammonia concentrations, and elevated pH (Gleitz et al. 1995; Papadimitriou et al. 2007; Thomas and Dieckmann 2010). To not only cope with, but to thrive in such extreme and variable conditions, microbial survival and functioning requires a complex suite of physiological and metabolic adaptations. Today, little is understood about these putative microbial adaptations, and how they are linked to ecosystem function and environmental change.

One such adaptation expressed by sea ice algae is the exudation of photosynthetically-derived organic carbon. Sea ice algae are believed to exude large quantities of organic carbon, based on observations that concentrations of extracellular organic carbon in sea ice may be much higher than those in the underlying water column (Meiners et al. 2003; Riedel et al. 2006; Underwood et al. 2010). However, the ecological advantage of exuding organic carbon, both on a cellular and community level is not clear. There have been very few attempts to quantify sea ice algal exudation rates and composition, and incorporation of this source of bio-active energy into ecosystem function.

Organic carbon exudation associated with sea ice algae may be diverse and variable. Exuded cell-associated organic carbon is thought to be important for aiding cellular attachment and motility (Decho 2000), and may also provide a

protective coating capable of buffering adverse physicochemical conditions, such as temperature, salinity, pH, and nutrients (Krembs and Deming 2008; Krembs et al. 2011; Underwood et al. 2004). Carbon-based material may also provide a substrate for an active bacterial loop, whereby bacteria utilise the material and in turn, replenish vitamins and minerals required for algal growth (Giesenhagen et al. 1999; Martin et al. 2009, 2011). Sea ice algae can also take up extracellular organic carbon, independent of light availability (Palmisano and Garrison 1993), presenting a potential advantage under conditions of light limitation during overwinter survival. Structurally complex molecules (i.e. extracellular polymeric substances, EPS) may have the potential to influence the sea ice micro-morphology, creating a more suitable algal habitat by increasing concentrations of organic carbon that restrict the flow of fluid within the brine channel system, increasing bulk salinity (thereby reducing the brine freezing temperature), and increasing brine channel structural complexity (Ewert and Deming 2013; Krembs and Deming 2008; Krembs et al. 2001, 2002, 2011). Finally, exuded organic carbon may be an end-product of an overflow metabolism, whereby cells release the carbon derived from primary production that is excessive to their growth requirements (Fogg 1983).

Not surprisingly, quantities of extracellular organic carbon in sea ice show high spatial and temporal variation, and are positively correlated with algal biomass, represented through both particulate organic carbon and chlorophyll *a* (Meiners et al. 2003; Riedel et al. 2006, 2007, Van der Merwe et al. 2009). However, this apparent association between intra- and extracellular organic carbon pools has not

been well explored, and the level of dependence between them is not known. This is important, because if exudation of organic carbon reflects an ecological adaptation, then the exudation ratio between intra- and extracellular organic carbon could very well vary depending on physiological and metabolic pressures.

The thesis consists of three data studies, each incorporating a different methodological approach. The methods applied in each study had their strengths, as well as possible limitations, and a different set of assumptions and uncertainties. Each study is reported in the thesis as a separate chapter. Study 1 (chapter 2) was carried out in a controlled laboratory environment, and is well suited to test initial biogeochemical hypotheses. Study 2 (chapter 3) expands methods and experimental protocols to a relatively homogenous small-scale field station. Finally, study 3 (chapter 4) contributes to a large-scale ecosystem study and was undertaken as part of an interdisciplinary voyage. Therefore, the thesis demonstrates the evolution of technical methods, accumulation of new knowledge, and increasing logistical complexity.

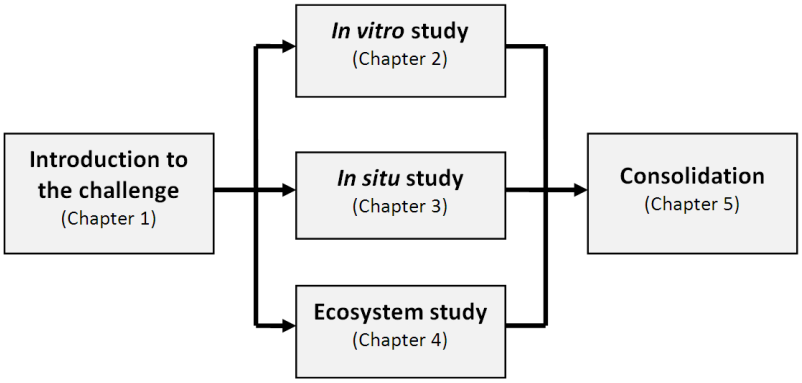

Figure 1.1: Thesis mind map indicating three phases; *in vitro* study (Chapter 2), *in situ* study (Chapter 3), and ecosystem study (Chapter 4).

The aim of the thesis is to examine and quantify primary production and subsequent carbon allocation of Antarctic sea ice algae. The objectives are to develop accurate methods of measuring primary production and carbon allocation of ice algal assemblages in laboratory and field conditions. The derived production measurements of algal assemblages are discussed in relation to microbial growth dynamics, responses to physicochemical change, and allocation of carbon into specified intra- and extracellular carbon pools. Therefore, the thesis spans variable spatial and temporal scales, encompassing multiple scientific disciplines and collaborations.

Chapter 2: This chapter quantifies primary production and carbon allocation by a common Antarctic sea ice diatom, *Fragilariopsis cylindrus*. The laboratory-based study was the first attempt to apply developed methods using a radioactive tracer (^{14}C), and determine production rates over the algal growth cycle while exposing assemblages to increasing biogeochemical stress.

Chapter 3: This chapter describes extracellular carbon dynamics of an Antarctic bottom ice algal assemblage. The study was conducted on fast ice in the vicinity of Turtle Rock (77° 44' S, 166° 46' E), McMurdo Sound, Antarctica, during the spring-summer transition (November to December 2011). A detailed description of the sea ice physicochemistry and microbial community, within 0.15 m from the ice-water interface is provided.

Chapter 4: This chapter quantifies primary production and carbon allocation by Antarctic bottom ice algal assemblages, using ^{14}C methods developed in chapter 1. The study was conducted in pack ice in East Antarctica (64.42 to 65.27 °S and 116.27 to 121.15 °E) during the winter-spring transition (October to September 2012). A description of pack ice physio-biogeochemical characteristics, and rates of primary production and carbon allocation within 0.02 m from the ice-water interface are provided.

Chapter 5: This chapter brings together the findings from each of the studies reported in the previous chapters to build a more comprehensive knowledge base on physio-biogeochemistry, primary production, and the synthesis of extracellular organic carbon dynamics in Antarctic sea ice.

At the time of submitting this thesis, chapters 2 and 3 have been published (journals: Experimental Marine Biology and Ecology and Aquatic Microbial Ecology). Chapter 4 has been submitted to a special edition (journal: Deep Sea

Research II). Differences between chapter text formats (e.g. reference structure) are attributed to requirements for journal submissions. Study citations are at the start of each chapter, and copies of published material are held inside the back cover of the thesis.

CHAPTER 2

Photosynthetic carbon allocation of an Antarctic sea ice diatom (*Fragilariopsis cylindrus*)

Citation: Ugalde SC, Meiners KM, Davidson AT, Westwood KJ, McMinn A (2013). Photosynthetic carbon allocation of an Antarctic sea ice diatom (*Fragilariopsis cylindrus*). Journal of Experimental Marine Biology and Ecology. 446:228–235.

2.1 ABSTRACT

Antarctic sea ice provides an ephemeral but important habitat for algal productivity and is characterised by extreme physicochemical variations. In this study, we assess the ability of a sea ice diatom (*Fragilariopsis cylindrus*) to cope with physicochemical changes through examination of physiological status and allocation of ^{14}C-incorporated organic carbon into particulate and extracellular fractions, using closed-bottle incubations over 49 d. Carbon allocation was found to vary with growth stage and shifts in the physicochemical environment, in particular the carbonate system. Total extracellular organic carbon was comprised of at least 85 % low molecular weight ^{14}C-colloidal organic carbon. The relative contribution of ^{14}C-extracellular polymeric substances and ^{14}C-total extracellular organic carbon to ^{14}C-total primary production varied from lag to senescent growth phases, increasing from 0 to 5.7 % and 32.9 % to 69.5 %, respectively.

Carbon allocation into ^{14}C-extracellular polymeric substances was correlated with a decline in CO_2 availability and increased pH. Overall, the results demonstrate that carbon exudation may play an important role in adaptive algal physiology by buffering cells against biogeochemical shifts within brine channels, induced through photosynthetic activity.

2.2 KEY WORDS

Antarctica

Carbon fractionation

Extracellular polymeric substances

Microalgae

pH

Primary production

Sea ice

2.3 INTRODUCTION

The variable extent of Antarctic sea ice is a significant seasonal event, advancing to ~18-19 x 10^6 km^2 at its maximum in September-October and retreating to ~3-4 x 10^6 km^2 each summer (Comiso 2010). This process has critical effects on ocean-atmosphere interactions (Thomas and Dieckmann 2010), and is integrally linked to productivity and ecosystem dynamics of the Southern Ocean (Bluhm et al. 2010; Frazer et al. 1997; Loeb et al. 1997).

Antarctic sea ice is structurally complex, comprised of a network of brine channels which provide an extensive habitat for microbial communities (Horner et al. 1992; Thomas and Dieckmann 2010). Pennate diatoms typically dominate the sea ice flora, comprising > 90 % of standing stocks during austral spring and often exceed 300 mg Chl *a* m^3 (Arrigo et al. 2010; Palmisano and Sullivan 1983; Trenerry et al. 2002). An abundant Antarctic diatom, *Fragilariopsis cylindrus* (Grunow) Krieger (Bacillariophyceae), occurs commonly in both sea ice and open water column assemblages (Kang and Fryxell 1992). It is therefore an ideal representative organism for physiological studies related to sea ice research (Mock and Valentin 2004).

Prolonged photosynthetic activity within the confines of brine channel systems can result in the alteration of brine biogeochemical properties, such as depletion of carbon dioxide, increased pH, reduced availability of nitrate and silicate, high ammonia concentrations, and high concentrations of dissolved organic matter (e.g. Gleitz et al. 1995; Thomas and Dieckmann 2010; Meiners et al. 2009; Papadimitriou et al. 2007). The mechanisms employed by sea ice algae to tolerate these biogeochemical extremes are poorly understood, however high cell abundances within brine channels infer significant adaptation.

Arctic and Antarctic sea ice characteristically contain high concentrations of mucilage and dissolved organic carbon, which is thought to be comprised of extracellular polymeric substances (EPS; Krembs et al. 2002; Meiners et al. 2003;

Underwood et al. 2010). EPS are produced by a range of micro-organisms, including bacteria and algae (Aslam et al. 2012a,b; Collins et al. 2010; Krembs and Deming 2008), and are defined as extracellular organic compounds that precipitate in a polar solvent, usually 70 % ethanol (Decho 1990; Underwood and Paterson 2003). The compounds are large and complex macromolecules, encompassing a wide range of polysaccharides, uronic acids, and sulphated sugars (Underwood and Paterson, 2003). Numerous studies have reported significant variability with respect to the abundance and composition of ice-associated EPS (Aslam et al. 2012a; Krembs et al.2002; Meiners et al. 2003; Underwood et al. 2010) and this is likely to reflect the spatial and temporal variability that characterises the sea ice matrix (Herborg et al. 2001; Kattner et al. 2004; Meiners et al. 2003).

In marine environments, EPS have multiple ecological functions, including aiding cell attachment and motility, buffering against pH/chemical variances, increasing grazer protection, and providing a mechanism for metabolic overflow (Cooksey and Wigglesworth-Cooksey 1995; Decho 1990; Hoagland et al. 1993; Riedel et al. 2006; Smith and Underwood, 1998, 2000; Staats et al. 2000). EPS may also affect sea ice microstructure, potentially influencing sea ice habitability and primary productivity (Krembs et al. 2011). Furthermore, EPS have an important carbon source in sea ice (Mock and Thomas, 2005), and are associated with higher rates of bacterial activity and growth (Martin et al. 2008, 2011; Meiners et al. 2008).

The aim of this study was to quantify photophysiology and organic carbon allocation by a common Antarctic sea ice diatom, *F. cylindrus*. It was hypothesised that increased physiological stress associated with photosynthetically-induced environmental changes would induce variation in carbon allocation between particulate and extracellular carbon fractions. To this end, we determined rates of ^{14}C-total primary production (TPP) and carbon allocation among ^{14}C-particulate organic carbon (POC) and ^{14}C-total extracellular organic carbon (TEOC; extracellular dissolved organic carbon [EDOC], colloidal organic carbon [COLLOC] and EPS) fractions. Rates were determined during lag, exponential, stationary and senescent phases of culture growth over 49 days. Changes in carbon allocation are related to coincident changes in the physicochemical environment, and results considered in terms of the ability of *F. cylindrus* to inhabit the sea ice environment.

2.4 METHODS

2.4.1 Experimental Set-up

Triplicate sterile polycarbonate vessels (Nalgene, 30 L) were inoculated with ca. 100 cells ml^{-1} *F. cylindrus* grown in f/2 medium (Guillard and Ryther 1962). The cultures were incubated for 49 days (d) at constant temperature (0 ± 1 °C) on an 18:6 light-dark cycle (irradiance: 40 μmol photons m^{-2} s^{-1}) using cool-white fluorescent tubes, and gently mixed daily. Subsamples were taken at intervals from 4 to 11 d for measurements of cell abundance, carbonate chemistry, photosynthetic physiology, and carbon allocation using ^{14}C bicarbonate

incorporation. Care was taken to ensure all subsamples were taken consistently at 12 ± 1 hours (h) into the light cycle. Until the final sampling day, less than 20 ± 3 % of the initial culture volumes had been removed.

2.4.2 Definition of Photosynthetically Produced Organic Carbon Fractions

For the purposes of this study, ^{14}C-total primary production (^{14}C-TPP) is defined as the sum of ^{14}C-particulate organic carbon (^{14}C-POC) and ^{14}C-total extracellular organic carbon (^{14}C-TEOC). ^{14}C-TEOC is defined as the sum of ^{14}C-extracellular dissolved organic carbon (^{14}C-EDOC) and ^{14}C-colloidal organic carbon (^{14}C-COLLOC). A subtracted proportion of ^{14}C-colloidal-OC was defined as ^{14}C-extracellular polymeric substances (^{14}C-EPS), and was precipitated using 70 % ethanol (Decho 1990; Underwood et al. 1995).

2.4.3 Fractionation of Photosynthetically Produced Organic Carbon

Organic carbon components (^{14}C-POC, ^{14}C-EDOC, ^{14}C-COLLOC, and ^{14}C-EPS) were isolated using a modified method of Goto et al. (1999). For each replicate culture, five 20 ml subsamples were inoculated with an aqueous antibiotic cocktail of penicillin (benzylpenicillin potassium, CSL Ltd, final concentration 75 µg ml^{-1}) and streptomycin (streptomycin sulfate, Sigma USA, final concentration 125 µg ml^{-1}), and incubated in glass vials for 1 h, according to Goto et al. (1999). One subsample was incubated in darkness, whilst the other four were exposed to the same incubation conditions as the parent cultures. After initial incubation, samples were spiked with 200 µl ^{14}C-$NaHCO_3$ (activity = 148 kBq ml^{-1}), and incubated for a further 10 h with gentle agitation.

At the termination of incubations, samples were filtered using GF/F (Whatman) filters under minimal light and low pressure (< 0.13 bar). 0.005 l of filtrate was then acidified with 200 µl 32 % HCl and bubbled with nitrogen for 20 min. This fraction was defined as ^{14}C-EDOC. Extracellular organic carbon was solubilized (^{14}C-EPS and ^{14}C-COLLOC) using the method of Decho (1993), whereby the remaining filter was submerged in 0.075 l of 4 nmol l^{-1} EDTA for 1 h at 40 ± 1 °C and gently agitated every 15 min. The extracellular organic carbon was then separated from algal cells by centrifugation (4000 x *g* for 10 min) and resuspended three times in the same supernatant. The supernatant was then filtered using GF/F (Whatman) filters under low pressure (< 0.13 bar). Hence, ^{14}C-COLLOC (low molecular weight) and ^{14}C-EPS (high molecular weight) are comprised of carbon extracted from both colloidal and cell-associated material.

The collected filtrate was acidified with 300 µl HCl and bubbled with nitrogen for 20 mins. Three ml of the acidified filtrate was placed in a scintillation vial and this fraction was defined as ^{14}C-COLLOC. Another 3 ml was placed in a capped 15 ml falcon tube and precipitated following Goto et al. (1999), in which cold (- 20 °C) ethanol (70 % final concentration) was added for 10 h and subsequently centrifuged (4000 x *g* for 10 min). This was followed by a single wash with cold 70 % ethanol and resuspended in distilled water. The extraction was repeated twice. The precipitate obtained was defined as ^{14}C-EPS. Allocation to ^{14}C-COLLOC was calculated by subtraction of the ^{14}C-EPS fraction.

The ^{14}C-POC fraction was determined from filters used to separate the supernatant for extracellular organic carbon determination. After removing the filtrate for ^{14}C-EPS and ^{14}C-COLLOC determination (see above), 0.05 l 2 % HCl was drawn through the ^{14}C-POC filter to acidify the remaining material. The filter was then placed in a scintillation vial for radioactive counts.

For radioactive counts of aqueous ^{14}C-EDOC and ^{14}C-COLLOC fractions, 0.015 l of Aquassure (Amersham) liquid scintillation cocktail was added to scintillation vials. For radioactive counts of ^{14}C-POC filters and ^{14}C-EPS precipitations, 0.002 l acetone was added to vials and allowed to solubilise for 24 h, with 0.010 l of Aquassure later added. All samples were briefly mixed and protected from the light prior to measurement. Radioactivity of each fraction was measured using a calibrated liquid scintillation counter (Beckman LS 6500), ensuring lumex errors were < 3.00 %. Radioactive decays per min (DPM) were used to calculate rates of production using the following equation:

$$P = \frac{\frac{DPM - DPM_{T=0}}{DPM_{100\,\%}} * DIC * k_1 * k_2}{T}$$

Where P was the rate of production, DPM was the count from the sample incubated in the light, $DPM_{T=0}$ was the background count, DIC was the dissolved inorganic carbon of the sample (µg l^{-1}), k_1 was the correction factor (1.05) for the

5 % metabolic discrimination for the uptake of ^{14}C relative to ^{12}C (Ertebjerg-Nielsen and Bresta 1984), k_2 was the correction factor for subsampling given that only part of the incubated sample was utilised, T was the incubation time, and $DPM_{100\%}$ was the total radioactivity added to each vial. Carbon uptake rates were then normalised to cell abundance (pg C $cell^{-1}$ h^{-1}) and chl *a* concentrations (mg C (mg chl *a*)$^{-1}$ d^{-1}).

2.4.4 Nutrient Parameters and Pigments

Filtered nutrients samples (NO_x [NO_2 + NO_3], NH_4, $Si(OH)_4$, and PO_4) were collected and stored at – 20 °C in acid washed polypropylene vials. Analysis was performed according to Eriksen (1997) using an Alpkem auto-analyser (Trevena et al. 2000). For determination of chl *a*, light-protected samples of 0.015 – 0.120 l were filtered onto GF/F (Whatman) filters and stored at -80 °C for fluorometric analysis. Chl *a* was later extracted in the dark at 4 °C using HPLC-grade methanol for 20 h. Concentrations were measured using a Turner Design Model 10-AU digital fluorometer calibrated against chl *a* standards (Sigma Chemicals Co., St Louis), according to Holm-Hansen et al. (1978).

2.4.5 Carbonate System

Culture pH was determined using a bench top meter (Mettler Toledo, S20-KS), calibrated daily using three-point standard buffer solutions. The carbonate system was also characterised by measuring total alkalinity (TA) and dissolved inorganic carbon (DIC) to calculate pCO_2. Acid washed glass bottles (0.25 l) were rinsed with sample then gently filled while avoiding air contact. For preservation, 100 µl

saturated mercuric chloride solution was then added and the bottles sealed using lids with convex inserts to exclude air. Samples were stored at 4 °C in the dark until analysis.

To quantify DIC concentrations, subsamples were drawn from bottles using a 0.025 l disposable syringe to avoid air contact. Each subsample was then filtered through a sterile 0.22 μm syringe filter (Pall Acrodisc). DIC was analysed using an Apollo SciTech's DIC analyser (USA), corrected against seawater certified reference material (prepared by A. G. Dickson, Scripps Institution of Oceanography). Multiple measurements of subsamples were taken and the results averaged.

`

TA was measured using the remaining sample (> 0.2 l) according to the potentiometric titration method described by Dickson (1981). pCO_2 was calculated using the software program CO_2sys (version 1.05 by E. Lewis and D.W.R Wallace, 2006), with dissociation constants for carbonic acid described by Roy et al. (1993).

2.4.6 Photophysiological Parameters, Algal and Bacterial Abundance

Photophysiological parameters were determined using a Water-Pulse Amplitude Modulated (PAM) fluorometer (Waltz, GmbH, Effeltrich, Germany; gain setting 5 - 25) on triplicate subsamples, dark-adapted for 30 min. Algal cell counts were determined from samples of 1 - 5 ml preserved with Lugol's iodine solution, and allowed to settle for at least 12 h in 27 mm diameter Utermöhl chambers. Cell

counts were performed on live cells at 400 x magnitude on a Zeiss Axiovert inverted microscope. Counts were conducted either over 20 random fields of view, or until at least 100 cells had been counted. Intrinsic growth rates were calculated according to Laundry and Hassett (1982).

For bacterial cell counts, samples were preserved with formaldehyde (3 % final concentration) and stored at – 20 °C. Thawed samples were subsequently stained with SYBR Green I nucleic acid gel (Molecular Probes, USA) spiked with green reference beads (Molecular Probes, USA), and incubated in the dark for 20 mins. Cells were then counted using a Becton Dickinson flow cytometer, according to Thomson et al. (2010).

2.4.7 Statistical analyses

Statistical analyses were performed using SAS (v9.2). One-way analysis of variance (ANOVA) and post-hoc Tukey tests were used to examine changes in culture characteristics and productivity in relation to the various carbon fractions and culture growth phases.

2.5 RESULTS

2.5.1 Culture Growth

Algal growth phases were identified based on statistically significant changes in algal cell abundance: 0 - 6 d lag phase, 17 – 25 d exponential phase, 33 - 37 d stationary phase, and 43 - 49 d senescent phase ($p < 0.001$). Algal intrinsic

growth rates fluctuated throughout the experiment, and was highest from 0 to 6 d ($\mu = 0.47\ d^{-1} \pm 0.02$), after which growth rates declined during the stationary phase ($\mu = 0.1\ d^{-1} \pm 0.03$ 33 – 37 d; Table 2.1). Algal abundance increased exponentially to 945 ± 49 cells ml^{-1} during exponential growth, and then declined by 26 % during the senescent phase (Figure 2.1). The initial bacterial count was 55.1 ± 10.5 x 10^3 cells ml^{-1}, and increased to a final abundance of 1496 ± 15.7 x 10^3 cells ml-1 (Figure 2.1). Algal and bacterial abundances were significantly correlated (Pearson's r = 0.657, $p < 0.001$, n = 24).

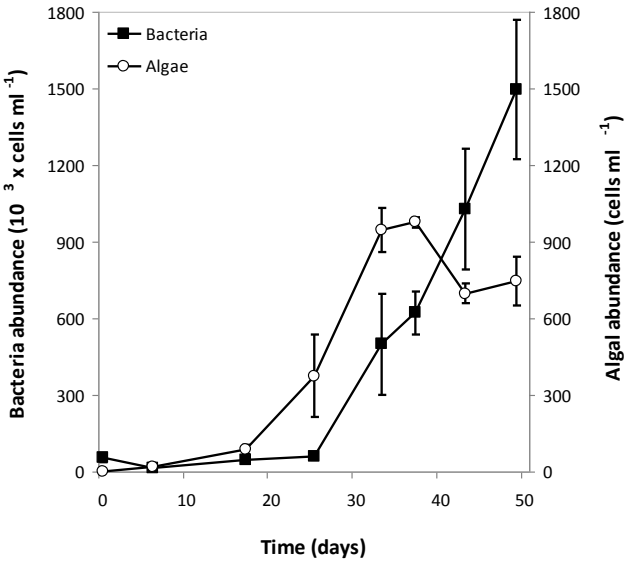

Figure 2.1: Temporal changes of *Fragilariopsis cylindrus* and bacterial cell abundance (means ± stderr).

2.5.2 Nutrients

NH_4 and $Si(OH)_4$ concentrations varied significantly between the lag to exponential phase, and the stationary to senescent phase ($p < 0.001$). NO_x and PO_4 declined significantly between the lag to exponential, stationary, and senescent phases ($p < 0.001$). Ammonium concentrations increased from an initial concentration of 0.48 ± 0.17 to 4.25 ± 0.53 μmol l^{-1} in the senescent phase (Table 2.1). $Si(OH)_4$ and NO_x were at initial concentrations of 60.4 ± 0.49 and 1142 ± 1.89 μmol l^{-1}, respectively, and reduced during exponential growth by 57 % and 15 %, respectively (Table 2.1). The initial concentration of phosphate was 36.4 ± 0.01 μmol l^{-1} which decreased by 41 % in the stationary phase. During the senescent phase, there was a slight increase to 21.1 ± 1.60 μmol l^{-1} (Table 2.1). NH_4, $Si(OH)_4$, NO_x, and PO_4 were correlated with algal cell abundance (Pearson's $r = 0.770, -0.923, -0.941, -0.778$, respectively; $p < 0.001$, $n = 24$).

2.5.3 Carbonate System

Media pH, DIC, and pCO_2 changed significantly between the lag, exponential, and stationary to senescent phases ($p < 0.001$). After an initial decline in pH during the lag phase (8.33 ± 0.2 to 8.05 ± 0.06), values increased rapidly to 9.29 ± 0.07 by the end of the exponential phase, and remained relatively constant thereafter (Figure 2.2). DIC declined from 1980 ± 14 μM kg^{-1} at the onset of exponential phase by 32 % during the stationary phase (Figure 2.2). Calculated values of pCO_2 were initially 379.5 ± 30.9, declining by 95 % during exponential growth (Figure 2.4). Media pH, DIC, and pCO_2 were negatively correlated with

algal cell abundance (Pearson's r = 0.940, -0.957, -0.926, respectively; $p < 0.001$, n = 24).

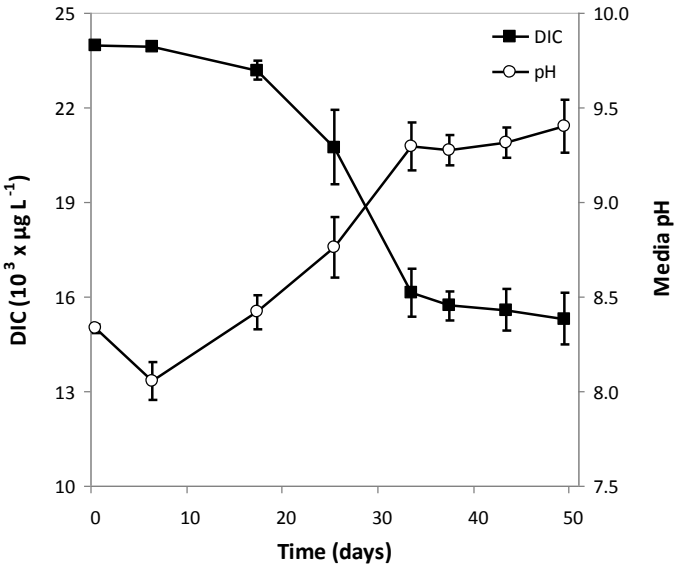

Figure 2.2: Temporal changes in the concentration of dissolved inorganic carbon (DIC) and media pH (means ± stderr)

2.5.4 Algal Photophysiology

Maximum potential photosynthetic yield (F_v/F_m) was below detection limits (gain = 25) during lag phase, but increased to a maximum of 0.63 ± 0.01 during exponential growth (25 d). Thereafter, the yield steadily declined and was 0.33 ± 0.04 by the end of the senescent phase (Figure 2.3). Chl *a* concentrations increased from an initial value of < 0.1 µg l^{-1} during the lag phase to 60.9 ± 0.3 µg l^{-1} in the senescent phase (Table 2.1). Cell-specific chl *a* increased from 20.6 ± 6.8 pg chl *a* $cell^{-1}$ in the lag phase to 99.6 ± 6.8 pg chl *a* $cell^{-1}$ during exponential growth. This then declined to 59.8 ± 8.3 pg chl *a* $cell^{-1}$ in stationary phase (Figure 2.4).

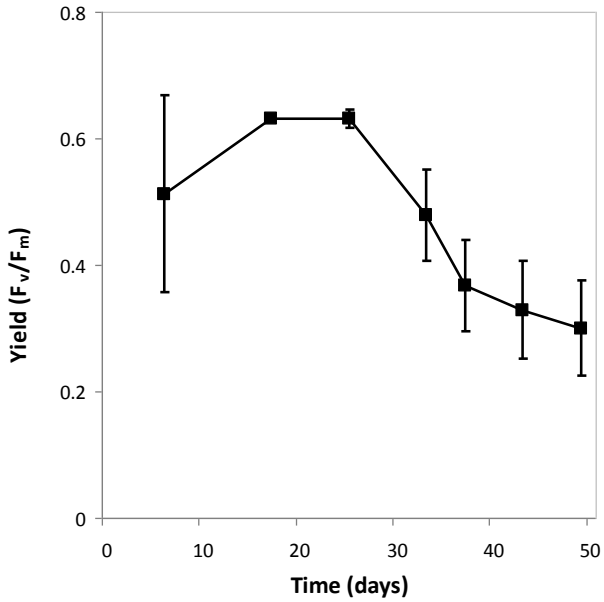

Figure 2.3: Temporal changes in maximum fluorescent yield (F_v/F_m) (means ± stderr)

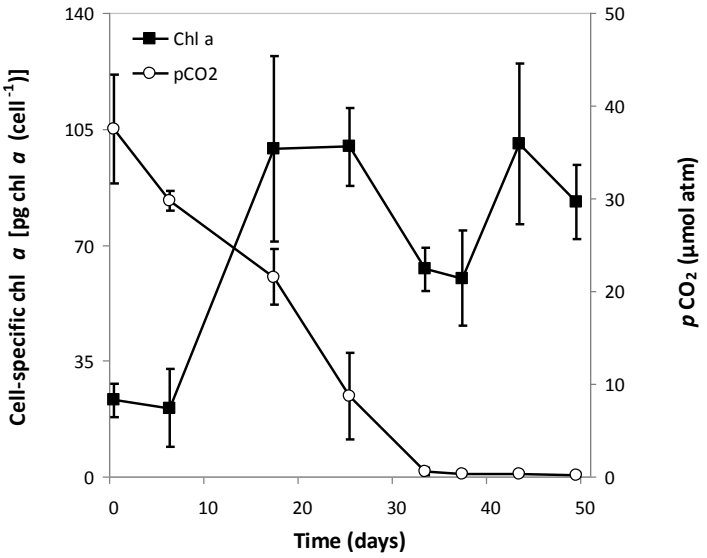

Figure 2.4: Temporal changes in pCO_2 (µmol atm) and chlorophyll *a* per cell (pg chl *a* cell $^{-1}$) (means ± stderr).

2.5.5 Rates of Total Primary Production and Extracellular Organic Carbon

To incorporate temporal changes in the cell-specific chlorophyll content (Figure 2.4), carbon uptake rates were normalised to both cell abundance (pg C cell^{-1} h^{-1}) and chl *a* (mg C (mg chl *a*)$^{-1}$ d^{-1}). Cell-specific rates of ^{14}C-TPP increased from an initial value of 61.8 ± 7.7 pg C cell-1 h^{-1} to 326.6 ± 60.4 pg C cell $^{-1}$ h^{-1} during the exponential phase (Table 2.2). Chl *a*-specific rates of ^{14}C-TPP decreased from an initial 80.12 ± 2.23 in the lag phase by 57 % at the early stationary phase. Thereafter, ^{14}C-TPP continued to decline with the exception of a peak in late stationary phase, at which time ^{14}C-TPP and ^{14}C-TEOC peaked at 126.90 ± 20.44 mg C (mg chl *a*)$^{-1}$ d^{-1} and 83.51 ± 11.03 mg C (mg chl *a*)$^{-1}$ d^{-1}, respectively (Table 2.2).

The relative contribution of chl *a*-specific production of ^{14}C-TEOC to ^{14}C-TPP increased from 33 ± 1 % at the end of the lag phase to 69 ± 4 % in the senescent phase (Figure 2.5; Table 2.2).

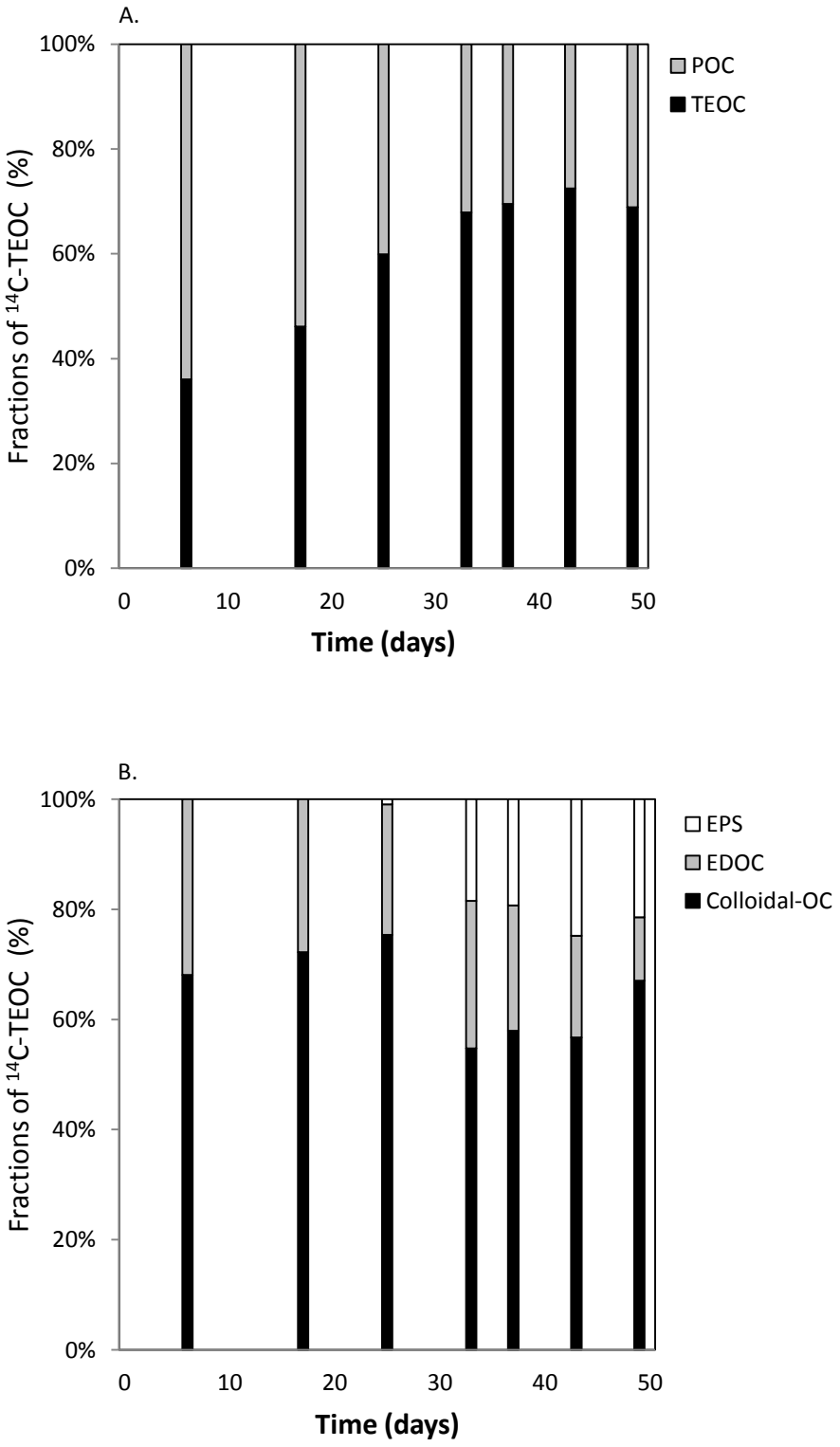

Figure 2.5: ^{14}C-total primary production fractions as ^{14}C-POC and ^{14}C-TEOC (%; A); and ^{14}C-TEOC fractions of ^{14}C-COLLOC, ^{14}C-EDOC, and ^{14}C-EPS (%; B).

2.5.6 ^{14}C-Colloidal Organic Carbon and ^{14}C-Particulate Organic Carbon

Cell-specific rates of ^{14}C-POC production peaked during early exponential phase at 174.4 ± 11.2 pg C cell^{-1} h^{-1}, and then reduced by 86 % during culture decline (Table 2.2). Similarly, cell-specific rates of ^{14}C-COLLOC production increased from 20.5 ± 2.9 pg C cell^{-1} h^{-1} during late lag phase by a factor of > 7 in late exponential phase (Table 2.2). Chl *a*-specific rates of ^{14}C-POC production were highest during early growth at 53.68 ± 9.79 mg C (mg chl *a*)$^{-1}$ d^{-1} (Table 2.2). They then generally declined to 6.66 ± 1.27 mg C (mg chl *a*)$^{-1}$ d^{-1} in the senescent phase, with the exception of a peak during the stationary phase (Table 2.2).

The relative contribution of ^{14}C-POC and ^{14}C-COLLOC to ^{14}C-TPP did not vary significantly throughout the experiment ($p = 0.187$; $p = 0.270$, respectively). The relative contribution of ^{14}C-POC to ^{14}C-TPP was highest at the end of the lag phase with 67 ± 1 %. This then declined during the stationary and senescent phases by 48 % and 55 %, respectively (Figure 2.5, Table 2.2). Accordingly, ^{14}C-TOEC contributed to 33 ± 1 % of ^{14}C-TPP at the end of the lag phase, and 65 to 69 % during the stationary and senescent phases. ^{14}C-COLLOC constituted at least 84 % of ^{14}C-TEOC throughout the study, with ^{14}C-EDOC contributing the remainder. At the end of the lag phase, ^{14}C-COLLOC accounted for 30 ± 2 % of ^{14}C-TPP, thereafter steadily increasing to 58 ± 1 % of ^{14}C-TPP during the stationary phase and 61 ± 2 % during senescent phase (Figure 2.5; Table 2.2).

Table 2.1: Chlorophyll *a* concentration (chl *a*), algal intrinsic growth rate (IGR) and nutrient concentrations (means ± SE) during growth phases.

	Time (days)							
	LAG		EXPONENTIAL		STATIONARY		SENESCENT	
	0 d	6 d	17 d	25 d	33 d	37 d	43 d	49 d
Chl *a* ($\mu g\ l^{-1}$)	0.0 ± 0.0	0.4 ± 0.1	8.7 ± 2.2	3.6 ± 7.9	58.8 ± 0.7	50.2 ± 2.3	60.9 ± 0.3	61.2 ± 2.5
Algal IGR ($\mu\ d^{-1}$)	.	0.5 ± 0.0	0.1 ± 0.0	0.2 ± 0.0	0.1 ± 0.0	0.0 ± 0.0	-0.1 ± 0.0	0.0 ± 0.0
$Si(OH)_4$ ($\mu mol\ l^{-1}$)	60.4 ± 0.5	65.6 ± 1.5	71.1 ± 0.3	59.2 ± 3.7	30.9 ± 2.0	27.5 ± 1.9	26.8 ± 1.5	25.9 ± 1.5
NO_x ($\mu mol\ l^{-1}$)	1142.0 ± 1.9	1142.0 ± 4.4	1128.0 ± 5.7	1082.0 ± 16.2	1008.0 ± 6.6	996.0 ± 13.7	994.0 ± 13.7	973.0 ± 15.9
PO_4 ($\mu mol\ l^{-1}$)	36.4 ± 0.0	34.9 ± 1.0	35.0 ± 1.1	30.2 ± 1.0	29.1 ± 0.3	25.9 ± 1.1	24.1 ± 1.8	21.1 ± 1.6
NH_4 ($\mu mol\ l^{-1}$)	0.5 ± 0.2	0.3 ± 0.1	0.5 ± 0.2	1.1 ± 0.1	3.0 ± 0.8	2.2 ± 0.5	3.3 ± 0.5	4.3 ± 0.5

Table 2.2: Carbon uptake rates and fractions (means ± SE) normalised to cell abundance (expressed as pg C $cell^{-1}$ h^{-1}) and chlorophyll *a* (expressed as mg C(mg chl *a*)$^{-1}$ d^{-1}). BD = below detection.

		Time (days)							
		LAG		EXPONENTIAL		STATIONARY		SENESCENT	
		0 d	6 d	17 d	25 d	33 d	37 d	43 d	49 d
pg C $cell^{-1}$ h^{-1}	^{14}C-TPP	BD	61.8 ± 7.7	326.2 ± 32.6	326.6 ± 60.4	98.1 ± 23.8	330.6 ± 39.3	98.9 ± 22.1	80.4 ± 10.8
	^{14}C-TEOC	BD	22.2 ± 2.7	151.8 ± 21.7	188.9 ± 16.1	65.9 ± 15.0	229.2 ± 24.5	70.8 ± 14.4	55.6 ± 8.2
	^{14}C-POC	BD	39.6 ± 5.1	174.4 ± 11.2	137.8 ± 47.2	32.1 ± 8.8	101.4 ± 16.4	28.1 ± 7.7	24.8 ± 2.6
	^{14}C-colloidal-OC	BD	20.5 ± 2.9	143.2 ± 20.6	178.7 ± 13.9	57.4 ± 13.3	206.1 ± 25.2	63.5 ± 14.4	52.0 ± 7.7
	^{14}C-EDOC	BD	1.7 ± 0.8	8.7 ± 1.4	8.2 ± 3.0	5.5 ± 1.3	13.3 ± 4.7	2.5 ± 0.6	1.2 ± 0.4
	^{14}C-EPS	BD	BD	BD	1.9 ± 0.6	3.0 ± 0.8	9.9 ± 1.7	4.8 ± 0.7	2.4 ± 0.4
mg C(mg chl *a*)$^{-1}$ d^{-1}	^{14}C-TPP	BD	80.1 ± 2.2	79.1 ± 11.7	73.9 ± 11.4	34.4 ± 6.8	126.9 ± 20.4	21.4 ± 2.8	21.7 ± 3.2
	^{14}C-TEOC	BD	26.4 ± 5.3	34.0 ± 6.3	40.7 ± 4.2	22.1 ± 4.0	83.5 ± 11.0	14.8 ± 1.6	14.3 ± 2.2
	^{14}C-POC	BD	53.7 ± 9.8	45.2 ± 5.7	33.2 ± 9.8	12.3 ± 2.9	43.3 ± 9.4	6.7 ± 1.3	7.4 ± 1.0
	^{14}C-colloidal-OC	BD	23.6 ± 4.0	31.7 ± 5.8	38.2 ± 3.9	18.8 ± 3.5	74.3 ± 12.5	12.9 ± 1.7	13.2 ± 2.1
	^{14}C-EDOC	BD	2.9 ± 2.0	2.3 ± 0.6	2.0 ± 0.6	2.2 ± 0.4	5.2 ± 1.2	0.7 ± 0.2	0.4 ± 0.1
	^{14}C-EPS	BD	BD	BD	0.5 ± 0.2	1.2 ± 0.3	4.1 ± 0.5	1.2 ± 0.2	0.7 ± 0.1

2.5.7 ^{14}C-Extracellular Organic Carbon and ^{14}C-Extracellular Polymeric Substances

Cell- and chl *a*-specific rates of ^{14}C-EDOC and ^{14}C-EPS exudation were undetectable in the early lag and the lag and the early exponential phases, respectively (Table 2.2). Rates of ^{14}C-EDOC exudation reached 13.3 ± 4.70 pg C cell^{-1} h^{-1} or 5.18 ± 1.16 mg C (mg chl *a*)$^{-1}$ d^{-1} during the stationary phase, but declined rapidly thereafter. Similarly, rates of ^{14}C-EPS exudation reached 9.90 ± 1.73 pg C cell^{-1} h^{-1} or 4.08 ± 0.69 mg C (mg chl *a*)$^{-1}$ d^{-1} during the stationary phase, then decreased by the end of the senescent phase by 76 % and 83 %, respectively (Table 2.2).

Percentages of ^{14}C-EPS exudation relative to ^{14}C-TPP changed significantly between the lag to exponential and stationary to senescent phases ($p < 0.001$). ^{14}C-EPS production increased from the first detectable value of 0.75 ± 0.31 % of ^{14}C-TPP (0.83 ± 0.25 % of ^{14}C-TEOC) during the late exponential phase to 3.4 ± 0.75 % (6.12 ± 0.60 % of ^{14}C-TEOC) during the stationary phase. It then increased further to 5.7 ± 0.75 % (1.74 ± 0.27 % of ^{14}C-TEOC) during the early senescent phase (Table 2.2). The relative contribution of ^{14}C-EPS to ^{14}C-TPP was strongly correlated with carbonate system components (Pearson's pH r = 0.846; DIC r = -0.879; pCO_2 r = -0.824; $p < 0.000$, n = 24), nutrient concentrations (Pearson's NH_4 r = 0.734; $Si(OH)_4$ r = -0.892; NO_x r = -0.849; PO_4 r = -0.776; $p < 0.000$, = 24), F_v/F_m (Pearson's r = -0.745, $p < 0.000$, n = 21), and biomass characteristics (Pearson's algal abundance r = 0.818; chl *a* r = 0.864; bacterial abundance r = 0.762; $p < 0.000$, n = 24).

2.6 DISCUSSION

This is the first study to quantify rates of carbon allocation among intra- and extracellular organic carbon fractions by a cultured Antarctic sea ice diatom under deteriorating carbonate conditions. Here, it is shown that increased physiological stress associated with photosynthetically-induced environmental changes has the potential to alter carbon allocation amongst particulate and extracellular carbon fractions.

Allocation into extracellular organic carbon is an important ecological strategy of diatoms to survive harsh environmental conditions, alter habitat structure and support increased biomass (Decho 1990; Hoagland et al. 1993; Krembs et al. 2011; Riedel et al. 2006; Smith and Underwood 1998, 2000). If this is the case, then a measurable shift in carbon allocation should be observed with changes in algal growth phase and physiological stress in our experiments. This is clearly demonstrated in our study by an observed increase in the relative contribution of ^{14}C-TEOC to ^{14}C-TPP between the lag phase (33 %) and the early senescent phase (69 %). Other studies on both temperate and polar species have also identified an increase in extracellular carbon allocation under changes in cell physiology and growth (e.g. Underwood et al. 2004; Aslam et al. 2012b). Goto et al. (1999) reported that the relative contribution of ^{14}C-TEOC to ^{14}C-TPP for a temperate tidal flat community increased from the exponential phase (22 %) to the stationary phase (51 %). Interestingly, ^{14}C-TEOC exudation in marine diatoms is generally low (Goto et al. 1999; Granum et al. 2002). One exception was the marine diatom *Chaetoceros affinis*, which was observed to excrete 10 to 58 % of

photosynthetically-produced carbon from the exponential to stationary phases, respectively (Myklestad et al. 1989). Thus, while the allocation of carbon into extracellular organic components may be species specific, in all cases the highest percentages were observed following exponential growth. This pattern in carbon allocation may reflect both a response to algal growth phase or increase in environmental stress, such as nutrient limitation or changes in carbonate chemistry.

This study shows that the sea ice diatom, *F. cylindrus*, may exude EPS and colloidal-OC at similar relative ratios when compared with other diatoms. Although total concentrations of high molecular weight material have recently been quantified for sea ice assemblages (Aslam et al. 2012a; Underwood et al. 2010), exudation rates have not previously been reported. In our study, the relative contributions of ^{14}C-EPS and ^{14}C-COLLOC to ^{14}C-TPP increased with growth phase from ca. 0 to 6 % and 30 to 61 %, respectively. These values are comparable to short-term radioactive labelling studies for estuarine benthic diatoms (^{14}C-COLLOC:^{14}C-TPP 30 – 60 %, ^{14}C-COLLOC:^{14}C-EPS 16 %; Smith and Underwood, 2000) and tidal flat diatoms (^{14}C-COLLOC:^{14}C-TPP 39 %, ^{14}C-COLLOC:^{14}C-EPS 41%; Goto et al. 1999). Studies using short pulse-chase incubations of intertidal epipelic diatoms have reported relatively low contributions of extracellular carbon fractions to ^{14}C-TPP values (^{14}C-COLLOC:^{14}C-TPP 8.0 – 11 %, ^{14}C-EPS:^{14}C-TPP 0.8 – 1.0 %; Smith and Underwood, 1998). However longer incubations, more comparable to the present

study, have indicated higher values (^{14}C-colloidal-OC:^{14}C-TPP 32 - 37 %, ^{14}C-EPS:^{14}C-TPP 4 - 18 %; Perkins et al. 2001).

For sea ice diatoms, cell-specific yields of extracellular polysaccharides of three common species (*Synedropsis* sp., *Fragilariopsis curta*, and *F. cylindrus*) were reported by Aslam et al. (2012a). While our results indicate extracellular carbon allocation increases with culture growth phase, Aslam et al. (2012a) reported carbon yields decrease from exponential growth (COLLOC:total carbohydrates 67, 75, 53 %, respectively) to the commencement of stationary phase (COLLOC:total carbohydrates 62, 35, 40 %, respectively). The contrasting results probably reflect differences in the methods used to isolate and quantify extracellular organic carbon fractions, but may also be due to growth-related changes in culture physiology and environmental factors (e.g. carbonate chemistry and nutrients). Overall our study supports the finding that growth phase and environmental factors have the potential to influence carbon allocation by cultured sea ice diatoms.

In our study, an increase in physiological stress was experienced by *F. cylindrus* as the culture matured. This was demonstrated by a decline in maximum potential photosynthetic yield (F_v/F_m) from exponential to senescent phases. During exponential growth, F_v/F_m measurements were comparable to the theoretical optimal of 0.65 for marine microalgae (Schreiber 2003). Previously reported values for Antarctic sea ice in early spring were 0.28 ± 0.13 and 0.37 ± 0.13 for sackhole and bottom communities, respectively (Meiners et al. 2009). Higher

values during spring for bottom ice communities have been reported for both Antarctic coastal fast ice (0.45 ± 0.15, McMinn et al. 2003) and East Antarctic offshore pack ice (0.47 ± 0.04, McMinn et al. 2007). The inconsistencies in these values may reflect the highly variable micro-environment of sea ice, which demonstrate seasonal shifts in algal community composition, and extremes of temperature, salinity, light, and chemistry. These shifts impose physiological stresses on biota, which can affect the physiological state of micro-organisms inhabiting the sea ice.

It is unlikely that macronutrient availability was limiting growth during our study. Sarthou et al. (2005) also reported half saturation constants for phytoplankton nutrient uptake as 1.6 ± 1.9 μmol l^{-1} for N, 0.24 ± 0.29 μmol l^{-1} for P, and 3.9 ± 5.0 μmol l^{-1} for Si. In our study, nutrient concentrations exceeded these half saturation constants during all phases of growth indicating that, despite draw-down during the incubation (Table 2.1), nutrients were not limiting. The observed increase in NH_4^+ concentrations observed during incubation was most possibly the result of bacterial nitrogen remineralisation (Table 2.1).

Physiological stress experienced by the *F. cylindrus* culture was likely caused through shifts in carbonate chemistry given that other factors remained sufficient (i.e. macronutrient, temperature and light availability). Throughout our study, the cultures experienced severely depleted CO_2, reduced DIC, and elevated pH (Figure 2.2, 2.4). These shifts were a consequence of photosynthesis within the confines of closed-bottle incubations and provide a useful proxy of processes

within a brine channel environment. Such shifts in the carbonate chemistry have the potential to inhibit algal growth and photosynthetic rates (Gleitz et al. 1995; Riebesell et al. 1993; Chen and Durbin, 1994). Although some diatoms have been shown to expend energy to increase the CO_2 concentrations (CO_2 concentrating mechanisms) in the proximity of RUBISCO (for example through utilising HCO_3^- ions), it is currently unclear if *F. cylindrus* has such potential (Giordano et al. 2005). Nonetheless, our study shows that photosynthetic-induced changes in carbonate chemistry within a closed system does not only affect algal production and growth, but also induces shifts in carbon allocation into particulate and extracellular organic carbon fractions, including EPS.

In both the sea ice and pelagic realm, extracellular organic carbon has been suggested to provide a potentially important link between algal and bacterial communities (Grossart et al. 2003; Junge et al. 2002; Plough and Grossart, 1999; Meiners et al. 2004, 2008). In our study bacterial cell abundance was observed to exponentially increase, with some evidence of nutrient remineralisation represented by an increase in NH_4 (Figure 2.1; Table 2.2). Consequently, aggregating bacterial colonies may have influenced some measured parameters. However, photosynthetic carbon allocation incubations were treated with antibiotics prior to the addition of ^{14}C, which was used to inhibit the bacterial uptake of algal extracellular organic carbon (Goto et al. 1999). Extracellular organic matter may serve as a carbon source for bacteria and account for high bacterial activity and diversity within sea ice systems (Bowman et al. 1997; Brown and Bowman, 2001; Martin et al. 2008). Colloidal organic carbon may

also provide an important substrate for bacteria, encouraging respiration and nutrient remineralisation compared with the surrounding water (Alldredge 2000; Ploug and Jørgensen 1999). Within sea ice, high bacterial activity could enhance remineralisation of nutrients, which is significant given inorganic carbon and nutrient replenishment are often restricted to the ice-water interface (McMinn et al. 2007, Vancoppenolle et al. 2010).

In our study EPS exudation was observed to increase with photosynthetically-induced environmental stress, which supports the hypothesis that extracellular organic carbon exudation is a response to unfavourable conditions. While algal growth phase and other potential factors (e.g. bacterial metabolites) may affect extracellular organic carbon exudation, our study strongly suggests that the carbonate system was the major driver of algal physiology. Previous studies on temperate diatoms have identified similar responses, and suggested that EPS may assist in the mediation of large shifts in pH (Braissant et al. 2007; Cummingham and Munns, 1984) and ion limitation (Mehta and Gaur 2007; Mohamed, 2001; Zinkevich et al. 1996). During unfavourable growth conditions, EPS exudation may be the consequence of metabolic over-flow, in which excess carbon dioxide is fixed relative to cellular growth requirements (Staats et al. 2000; Underwood et al. 2003). Although the concept of overflow metabolism has previously been applied to diatoms (Myklestad et al. 1989), this is an unlikely explanation of extracellular organic carbon allocation in this study as the culture experienced carbon limitation.

2.7 CONCLUSION

This is the first study to quantify rates of carbon allocation by an Antarctic sea ice diatom. The results provide an insight into allocation of carbon into particulate and extracellular organic fractions under increasing culture maturity and environmental stress induced by photosynthesis within confinement. This study shows that the physiology and carbon allocation of *F. cylindrus* is influenced by chemical shifts. Allocation of carbon into EPS and COLLOC fractions increased with environmental stress associated with carbonate chemistry, specifically elevated pH and the depletion of available DIC and CO_2. Although further work is clearly required, EPS exudation is thought to play an important role in algal physiology, and may represent an important adaptive response to the physiochemical extremes of the sea ice habitat and may facilitate sustained growth in sea ice algae.

2.8 ACKNOWLEDGEMENTS

We would like to thank the Australian Antarctic Division (Hobart, Australia) for providing support and infrastructure throughout this study. Recognition goes towards T. Rodemann (Central Science Laboratories, Hobart) for processing samples, supported by D. Davies who provided assistance and methodology. Nutrients were determined by D. Terhell, V. Latham and S. Reynolds (CSIRO Marine and Atmospheric Research, Hobart). Our gratitude goes towards A. Martin and anonymous reviewers for very valuable comments on the manuscript. This work was supported by the Australian Government's Cooperative Research Centre Program through the Antarctic Climate and Ecosystems Cooperative Research Centre (ACE CRC).

CHAPTER 3

Extracellular organic carbon dynamics during a bottom-ice algal bloom (Antarctica)

Citation: Ugalde SC, Martin A, Meiners KM, McMinn A, Ryan KG. Extracellular organic carbon dynamics during a bottom ice algal bloom (Antarctica). Aquatic Microbial Ecology. 73(3): 195 – 210.

3.1 ABSTRACT

Antarctic fast ice provides a habitat for diverse microbial communities, the biomass of which is mostly dominated by diatoms capable of growing to high standing stocks, particularly at the ice-water interface. While it is known that ice algae exude organic carbon in ecologically significant quantities, the mechanisms behind its distribution and composition are not well understood. The current study investigates extracellular organic carbon dynamics, microbial characteristics, and ice algal photophysiology during a bottom ice algal bloom at McMurdo Sound, Antarctica. Over a two week period (November – December, 2011), ice within 15 cm from the ice-water interface was collected and sliced into nine discrete sections. Over the observational period, the total concentrations of extracellular organic carbon components (dissolved organic carbon [DOC] and total carbohydrates [TCHO]; sum of monosaccharides [CHO_{Mono}] and polysaccharides [CHO_{Poly}]) increased, and were positively correlated with algal

biomass. However, when normalised to chlorophyll *a*, the proportion of extracellular organic carbon components substantially decreased from initial measurements. Concentrations of DOC generally consisted of < 20 % TCHO, typically dominated by CHO_{Mono} which decreased from initial measurements. This change was coincident with improved algal photophysiology (maximum quantum yield [F_v/F_m]) and an increase in sea ice brine volume fraction indicating an increased capacity for fluid transport between the brine channel matrix and the underlying seawater. Our study supports the suggestion that microbial exudation of organic carbon within the sea ice habitat is associated with vertical and temporal changes in brine physicochemistry.

3.2 KEY WORDS

Antarctica

Carbohydrates

Dissolved organic carbon

Microalgae

Nutrient limitation

Photophysiology

Sea ice

3.3 INTRODUCTION

Antarctic sea ice, permeated by a system of brine-filled pockets and channels, provides an extensive habitat for diverse microbial assemblages that play a significant role in the ecology and biogeochemistry of the Southern Ocean (Delille et al. 2002; Palmisano and Garrison 1993; Thomas and Dieckmann 2010; Vancoppenolle et al. 2013). The most conspicuous fast ice-bound organisms are micro-algae (hereafter referred to as 'algae'; Arrigo et al. 2010) that form communities that are usually densest near the ice-water interface. These are referred to as bottom ice communities (Thomas and Dieckmann 2010), and are able to achieve high biomass due to their proximity to inorganic nutrients in the underlying water column (Kattner et al. 2004; McMinn et al. 1999). Consequently, chlorophyll *a* (chl *a*) concentrations in the bottom ice can exceed 300 mg chl *a* m^{-2} (Arrigo et al. 2010; Palmisano and Sullivan 1983; Trenerry et al. 2002).

High concentrations of chl *a* in sea ice are often correlated with copious extracellular organic carbon, which is exuded by sea ice algae and other microbes (e.g. Krembs et al. 2002; Meiners et al. 2004; Underwood et al. 2010, 2013; Figure 3.1). The ecological functions of the high extracellular organic carbon in sea ice remain unclear; it might aid in cell motility and attachment (Hoagland et al. 1993; Underwood and Paterson 2003), or alternatively, provide a protective coating, which may be a mechanism to cope with variable physicochemical conditions including low temperature, salinity, pH, or nutrient concentrations (Krembs and Deming 2008; Krembs et al. 2002, 2011; Ugalde et al. 2013).

Alternatively, the high degree of metabolic activity in ice-associated bacteria (Martin et al. 2008, 2009; Meiners et al. 2008) and tight seasonal coupling between the relative abundance of bacteria and algae is suggestive of an active microbial loop, similar to that of temperate oceanic systems (Azam et al. 1991; Christaki et al. 1998; Smith et al. 1995; Sullivan and Palmisano 1984). This relationship may develop when bacteria assimilate extracellular organic carbon exuded by algae, and in return, provide vitamins and/or recycled nutrients that are required for algal growth (Archer et al. 1996; Kottmeier et al. 1987; Taylor and Sullivan 2008). Finally, exuded organic carbon may also be an end-product of overflow metabolism, whereby cells release the carbon derived from primary production that is excessive to their growth requirements (Fogg 1983), as has been previously reported for planktonic and benthic diatoms (e.g. Bucciarelli and Sunda 2003; Myklestad et al. 1989; Staats et al. 2000).

The identification of specific mechanisms behind exudation of organic carbon by ice algae has been impeded by the complexity and confinement of the sea ice habitat. Laboratory-based studies of ice-associated diatoms have shown that both exudation rates and the molecular composition of organic carbon vary in response to physicochemical conditions, algal growth phase, and photosynthetic activity (Aslam et al. 2012; Ugalde et al. 2013). A significant component of sea ice dissolved organic carbon (DOC) contains carbohydrates (total carbohydrates [TCHO]) comprised of mono- (CHO_{Mono}) and polysaccharides (CHO_{Poly}; Herborg et al. 2001), which vary in complexity, from short-chain (less than 10 monomers) and long-chain (from 40 up to many 1000s monomers) molecules, to high

molecular weight compounds (Decho 2000; Bellinger et al. 2005; Underwood et al. 2010). The adhesive properties of exuded carbohydrates have the potential to coagulate into gels and to bind microbial aggregates, which, under natural conditions can be modified through biotic (e.g. microbial modification) and abiotic (e.g. hydrolysis, photolysis) catalysts (Underwood et al. 2010). The non-carbohydrate component of DOC may include an array of proteins, lipids, and free DNA (Abdullahi et al. 2006; Hoagland et al. 1993; Underwood and Paterson 2003).

Substantial concentrations of particulate organic carbon (POC) and DOC have been measured in most types of sea ice. Several studies have reported large variability in the distribution and composition of DOC, possibly due in part to strong spatial (vertical and horizontal) and temporal gradients in sea ice and brine physicochemistry (Aslam et al. 2012; Juhl et al. 2011; Krembs et al. 2011; Underwood et al. 2010). Contrary to earlier laboratory-based studies (e.g. Aslam et al. 2012; Krembs et al. 2011), the high spatial heterogeneity of extracellular organic carbon composition and distribution in Antarctic sea ice showed no correlation with temperature or salinity gradients (Underwood et al. 2010). However from data collated from both poles, heterogenic extracellular organic carbon concentrations showed robust relationships with algal biomass gradients (Underwood et al. 2013). The development of these gradients is dependent on the physical properties of the ice, which can restrict the exchange of liquid between brine channels and underlying seawater (Gleitz et al. 1995; Meiners et al. 2009; Papadimitriou et al. 2007). A theoretical threshold of 5 % brine volume fraction

(V_b/V; i.e. the relative contribution of brine volume to total ice volume) may inhibit brine percolation in columnar ice (Golden et al. 1998, 2007; Vancoppenolle et al. 2010). Early spring sea ice is generally characterised by strong vertical gradients in temperature, brine salinity, and overall lower brine volumes when compared to later in the season (Eicken 1992), and this affects sea ice permeability, biological activity and biogeochemistry (Gleitz et al. 1995; Meiners et al. 2009; Papadimitriou et al. 2007, 2009).

This study assesses the dynamics of extracellular organic carbon and algal photophysiology of an Antarctic bottom ice algal community. The concentration of DOC and the relative contribution of total carbohydrates (TCHO; sum of mono- [CHO_{Mono}] and polysaccharides [CHO_{Poly}]) are documented for discrete sections of sea ice over a period of two weeks during the spring-summer transition. The current study also provides a description of the microbial community (algal biomass and species composition, maximum quantum photosynthetic yield [F_v/F_m], bacterial abundance, particulate organic carbon [POC] and nitrogen [PON], particulate carbon isotopic composition [$\delta^{13}C$]) and brine physicochemistry (V_b/V, ice temperature, bulk ice and brine salinity). It was hypothesised that DOC concentrations and the relative contribution of TCHO would increase with a substantial rise in seasonal algal biomass and photosynthetic activity, influenced by changes in sea ice physical and chemical parameters.

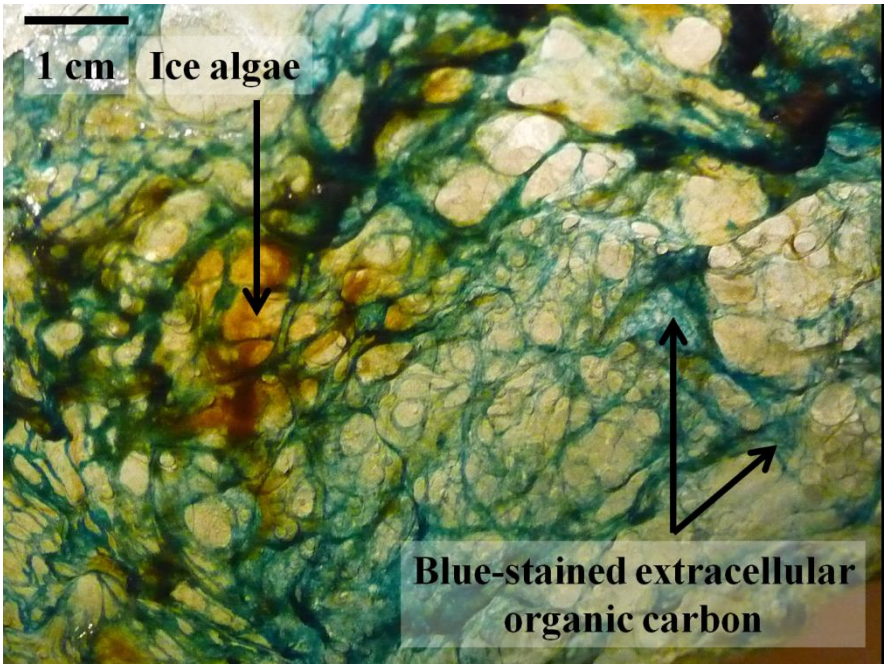

Figure 3.1: The bottom of a melting sea ice core at day 14 shows ice-associated algae (brown) and extracellular organic carbon (blue; Alcian Blue stained).

Image: Sarah C. Ugalde

3.4 METHODS

3.4.1 Site Description and Sampling Regime

Samples were collected in the vicinity of Turtle Rock (77° 44' S, 166° 46' E) in McMurdo Sound, Antarctica, between 16th November and 2nd December 2011. A 30 m^2 area was sampled three times over a period of two weeks. On each sampling day, three replicate parallel transects each constituting four bottom ice cores (12 cores total) were extracted using an Kovacs ice corer (13 cm internal diameter). To avoid light-shock, cores were stored in clean black plastic tubing for transport to the field camp. Two additional cores were collected for a

temperature/salinity profile and qualitative Alcian Blue imagery following a modified protocol of Juhl et al. (2011; Figure 3.1).

The transect ice cores were subsequently sliced into discrete sections in a dark room using a purpose-build support frame to allow for accurate and repeatable sectioning. Nine sections were taken from the base of each core; five 1 cm thick sections from 1 – 5 cm; three 2 cm thick sections from 5 – 11 cm; and one 5 cm thick section from 11 – 16 cm. Corresponding sections from the four ice cores of each replicate transect were combined and then melted over a 12 h period at 4 °C with the addition of 0.22 µm filtered seawater (0.2 l of filtered sea water added per cm of ice core section) in polypropylene containers, which had been rinsed thoroughly with Milli-Q water and autoclaved. The addition of filtered seawater was used to minimise changes in organic carbon exudation as a response to osmotic and temperature stress (Garrison and Buck 1986; Ryan et al. 2004). All particulate analyses were corrected for dilution factors. The dissolved carbon analyses were corrected for the added 0.22 µm filtered seawater, which was collected, filtered, and cooled prior to sampling each day (Riedel et al. 2006). Filtered sea water contained DOC (100 ± 10.14 [SE], 100.83 ± 9.51, and 102.50 ± 14.13 µmol C l^{-1} for initial, 7 d and 14 d, respectively), CHO_{Mono} (1.63 ± 0.23, 1.82 ± 0.47, and 2.75 ± 0.94 µmol C l^{-1} for initial, 7 d and 14 d, respectively), and CHO_{Poly} (5.73 ± 0.83, 5.21 ± 1.05, and 6.54 ± 0.94 µmol C l^{-1}) for initial, 7 d and 14 d, respectively).

3.4.2 Physicochemical Profiles and Ice Core Imagery

Two additional ice cores were extracted on each sampling day; a full-length core for ice temperature/salinity profiles, and a 30 cm bottom ice section for visualising extracellular organic carbon. Ice temperature was recorded immediately following core extraction. Holes to the centre of the core were produced with a battery-operated hand drill, and a thermometer probe (Hanna HI93510) was inserted into each hole and the temperature was recorded once stabilised. The temperature cores were then transported back to the field camp and sectioned for direct melting in polypropylene containers which had been rinsed thoroughly with Milli-Q water. Once melted, bulk ice salinity was measured with a digital seawater refractometer (Hanna HI96822). Brine salinity (S_b) was estimated from the *in situ* ice temperature measurements (t) as $S_b = 1000(1\text{-}54.11/t)^{-1}$ (Petrich and Eicken 2010). The brine-volume fraction, expressed as relative fraction of brine to ice volume (V_b/V), was calculated from the measured ice temperatures and bulk salinities using the equations in Cox and Weeks (1983) and Leppäranta and Manninen (1988).

For visualising extracellular organic carbon, the bottom 30 cm of the core was kept cool to prevent ice melt and placed in a light-protected container with Alcian Blue solution diluted with 0.22 µm filtered seawater for 12 h, following the protocol of Juhl et al. (2011). The stained core was then suspended from a horizontal beam and left to slowly melt at approximately 4 °C (Figure 3.1).

3.4.3 Maximum Quantum Yield (F_v/F_m)

Maximum quantum yield (F_v/F_m) was measured using a Pulse Amplitude Modulated fluorometer (WaterPAM, Waltz, Effeltrich). Ice shavings from the four cores of each replicate transect were collected during sectioning, and immediately measured with the addition of filtered sea water according to McMinn et al. (2010). Instrument gain settings were between 4 and 17.

3.4.4 Algal Biomass and Bacterial Abundance

For each core section, algal species composition, abundance and biovolume were determined from subsamples of 0.03 l, preserved with glutaraldehyde (0.2 % final concentration). For species counts, a subsample of 0.002 – 0.020 l was allowed to settle for > 6 h in a 37 mm diameter Utermöhl chamber, and counted at a magnification of 400 x using a Zeiss Axiovert inverted microscope at the Australian Antarctic Division (Tasmania). Both live and dead cells were counted (e.g. Oppenheim and Ellis-Evans 1989). Dead cells were those with no observable cell contents. Counts were conducted over random fields of view, until at least 400 (mean 742 ± 55 [standard error]) cells had been counted.

Subsamples of 0.01 l, used for measuring total brine biovolume, were pre-filtered through 50 µm mesh disks in a 47 mm filter holder, fixed to a sterile syringe. From each sample, the biovolume of particles measuring 3.74 to 60.00 µm in diameter was calculated from three 0.002 l subsamples using a Beckman Coulter Counter (Multisizer 3), and corrected for the ice dilution factor.

Samples for chl *a* analysis (0.03 – 0.05 l) were filtered onto 47 mm GF/F (Whatman) filters, and stored at - 20 °C. Chl *a* was extracted from each filter within 48 hrs of the initial freezing using HPLC-grade methanol (20 h in the dark at 4 °C). Chl *a* concentrations were determined fluorometrically using a Turner Design Model 10-AU digital fluorometer, calibrated against chl *a* standards (Sigma Chemicals Co., St Louis; Holm-Hansen and Riemann 1978).

Bacterial abundance samples (0.01 l) were preserved with glutaraldehyde (2 % final concentration) and stored at - 20 °C for later analysis at the Australian Antarctic Division (Tasmania). 500 µl of thawed samples were stained with Xul SYBR Green I nucleic acid gel (Molecular Probes, USA) and incubated in the dark at room temperate for 20 mins (Thomson et al. 2010) Cells were then counted using a Becton Dickinson FACScan flow cytometer, according to the protocol of Thomson et al. (2010). Green reference beads (Molecular Probes, USA) were added to each sample prior to staining. Manual gating was used to discriminate between bacterial cells of high and low nucleic acid content (HNA; LNA) according to Bouvier et al. (2007).

3.4.5 Particulate Organic Carbon/Nitrogen and Carbon Isotopes

Particulate organic carbon (POC) and nitrogen (PON) samples (15 – 400 ml) were filtered onto pre-combusted (12 h at 450 °C) 25 mm diameter quartz filters (Sartorius, Germany), and stored at - 80 °C. Thawed sample and blank filters were acidified with fuming 37 % HCl in a bell apparatus for 24 h, and dried in a clean oven (15 h at 60 °C). Filters were pressed into 5 x 9 mm pre-combusted

silver capsules (SerCon, United Kingdom), and analysed at the Central Science Laboratory (University of Tasmania) by combustion in oxygen-enriched helium atmosphere using a Haereus CHN-O-Rapid analyser.

Carbon isotopic composition of ^{13}C relative to ^{12}C ($\delta^{13}C$) samples (0.015 – 0.5 l) were filtered onto 25 mm diameter pre-combusted quartz filters (Sartorius), and prepared as above. Analysis was performed by continuous flow mass spectrometry with a Fisons 1500 elemental analyser coupled to a Finigan MAT Delta S mass spectrometer. Calibration was made by comparison with 15-µg aliquots of NBS22 oil ($\delta^{13}C$ = -29.7 NIST USA), which was run before and after the sea ice samples.

3.4.6 Extracellular Organic Carbon

DOC and CHO samples (0.1 – 0.6 l) were filtered through pre-combusted 45 mm GF/F filters (Whatman) under gentle vacuum pressure (< 200 mm Hg) and stored at - 20 °C for later analysis at the University of Tasmania and the Australian Antarctic Division (Tasmania). Samples were thawed, and DOC subsamples (0.02 – 0.03 l) were decanted into clean 0.04 l glass vials (Shimadzu, Japan; acid washed overnight and rinsed three times with Milli-Q water, followed by overnight pre-combustion at 500 °C). The concentration of DOC in each sample was measured using a Total Organic Carbon Analyser (Shimadzu, L-Series), as described by Qian and Mopper (1996).

Carbohydrate composition (CHO_{Mono} and CHO_{Poly}) was determined using the 2,4,6-tri pyridyl-*s*-triazine (TPTZ) spectroscopic method developed by Myklestad (1977) and modified by Hung and Santschi (2001). Prior to use, all glassware was acid washed overnight and rinsed three times with Milli-Q water, followed by pre-combustion (12 h at 500 °C). The carbohydrate concentration was measured against Milli-Q water using a Beckman spectrophotometer (DU640), and fitted to a D-glucose calibration curve. Due to the high light sensitivity of the analytical reagents, reactions were carried out either in the dark or with minimal red light (van Oijen et al. 2004). Total concentrations are expressed as µmol C l^{-1}, and have been normalised to chl *a* concentrations (mg C(mg chl *a*)$^{-1}$).

3.4.7 Statistical Analysis

All statistical analyses were performed using SAS (v.9.2). Only non-parametric statistics (Mann-Whitney U-test, p) were used to determine the statistical significance of vertical and temporal variations in extracellular organic and microbial physiological parameters, given the high variability and non-normal distribution of the data. Correlations were examined by Pearson's correlation analyses.

3.5 RESULTS

3.5.1 Physicochemical Profiles

Fast ice thickness was 1.90, 1.89, and 1.87 m for the initial, 7 d and 14 d sampling dates, respectively. The temperature at the ice-water interface was -1.7 °C, -1.1

°C, and -1.3 °C, for initial, 7 d, and 14 d, respectively (Figure 3.2A). Sea ice brine salinities ranged from 20 to 77 (mean: 37 ± 2) and showed profiles with the maxima towards the interior of the ice. Ice bulk salinities showed a reduction from the ice interior to the ice-water interface, with 14 d measurements beyond 4 cm from the ice-water interface not determined due to a sensor failure (Figure 3.2B). Calculated brine volume fraction (mean: 22 %; range: 9 to 52 %) decreased exponentially from the ice-water interface for all sampling dates by 38 %, 52 %, and 43 % for initial, 7 d, and 14 d, respectively (Figure 3.2C).

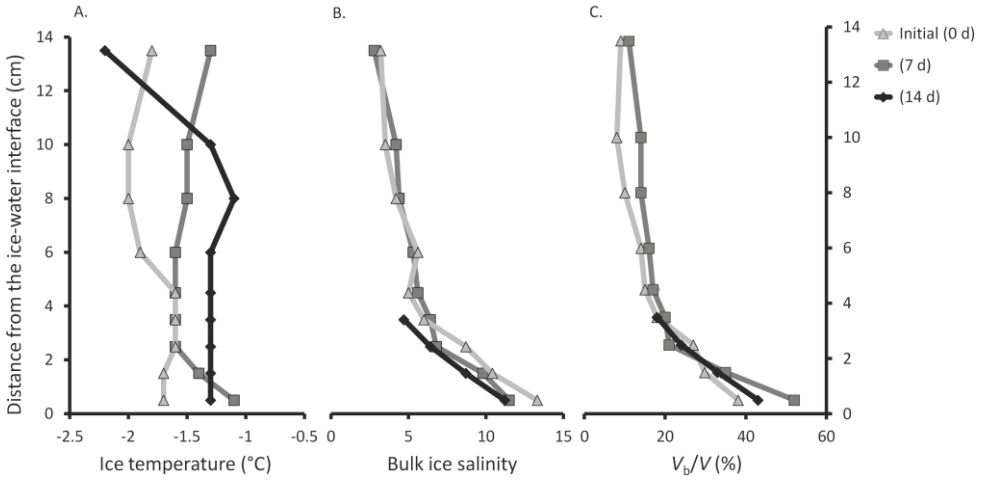

Figure 3.2: Vertical and temporal profiles of ice temperature (A), ice bulk salinity (B), and calculated brine volume percentage (V_b/V [%]; C). Error bars = ± SE.

3.5.2 Algal Biomass and Photophysiology

Profiles of chl *a* concentrations (mean: 97.99 µg l^{-1}; range: 0.26 to 635.16 µg l^{-1}) and F_v/F_m (mean: 0.16; range: 0.05 to 0.45) varied vertically and temporally ($p <$

0.001; Figure 3.3A, B). The vertical profiles of chl *a* concentrations showed an exponential decrease from the ice-water interface, although they did not significantly vary between 7 and 14 d. Initial chl *a* concentration at the ice-water interface was 211.80 ± 65.73 µg l^{-1}, reducing by 97 % within the first vertical 2 cm. At 7 d, chl *a* concentrations at the ice-water interface (635.16 ± 136.51 µg l^{-1}) reduced by 91 % within the first vertical 4 cm, thereafter remaining < 20 µg l^{-1}. At 14 d, chl *a* concentrations also reduced, declining by 92 % within 7 cm from the ice-water interface (Figure 3.3A). For each sampling date, F_v/F_m values showed an exponential decrease from the ice-water interface; with maximum values of 0.24 ± 0.01, 0.35 ± 0.05, and 0.45 ± 0.01, for initial, 7 d and 14 d, respectively (Figure 3.3B).

Molar POC to PON (C:N) ratios of melted ice cores are shown in Figure 3.3C. Means for the combined dataset were 8.40, 8.75, and 9.08 for initial, 7 d and 14 d, respectively (range: 6.89 to 12.08). The high standard errors between replicate cores resulted in no significant vertical or temporal variation.

The vertical profiles of initial $\delta^{13}C$ were relatively constant (range: -23.3 to -25.95), with one exception at 9 – 11 cm above the ice-water interface (Table 3.1). $\delta^{13}C$ values of 7 and 14 d increased from the ice-water interface towards the interior of the sea ice. $\delta^{13}C$ values at 7 d then declined from 2 – 3 cm above the ice-water interface to -21.0 at 11 – 16 cm above (Table 3.1). Similarly, 14 d $\delta^{13}C$ values declined between 2 – 7 cm above the ice-water interface, followed by a steady increase between 7 – 16 cm (Table 3.1). $\delta^{13}C$ values were positively

correlated with C:N ratios (Pearson Correlation Coefficient (r_p) = 0.559, significance level (p) = 0.002, sample size (n) = 81), and CHO_{Mono} (r_p = 0.522, p = 0.002, n = 81).

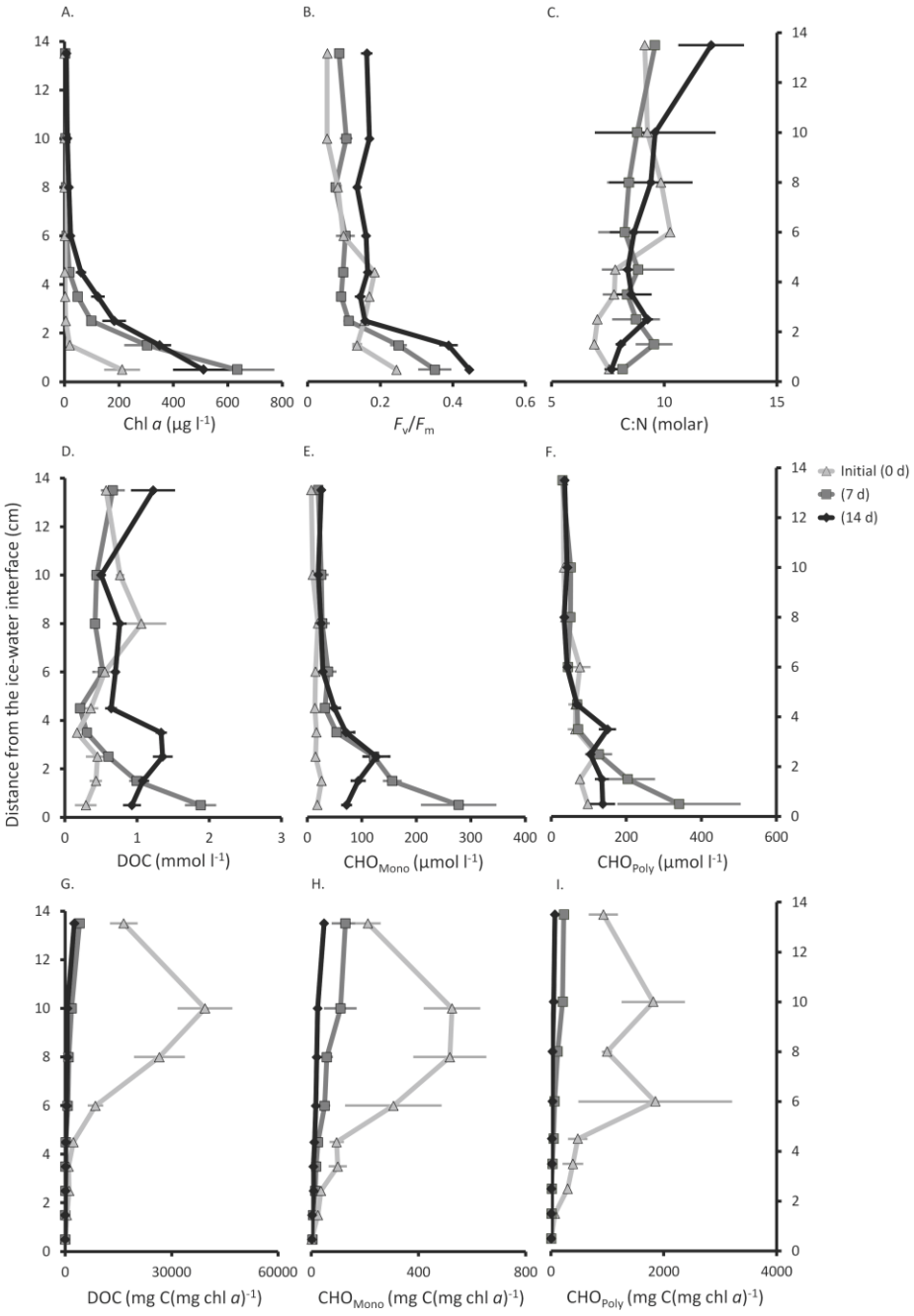

Figure 3.3: Vertical and temporal profiles of chlorophyll *a* (chl *a*; A), maximum photosynthetic yield (F_v/F_m; B), particulate organic carbon (POC): particulate organic nitrogen (PON) ratio (C:N; C), dissolved organic carbon (DOC; D), dissolved monosaccharides (CHO_{Mono}; E), dissolved polysaccharides (CHO_{Poly}: F), and extracellular carbon components normalised to chl *a* concentrations; DOC (G), CHO_{Mono} (H) and CHO_{Poly} (I). Error bars = ± SE.

Table 3.1: Temporal changes in $\delta^{13}C$, algal cell abundance, ratio of live:dead algal cells (live algal abundance %), total brine biovolume (3.74 to 60.00 µm diameter), and relative contribution of dominant algal groups to total cell abundance. Error bars = ± SE.

		Distance from ice-water interface (cm)								
	Time	0 - 1	1 - 2	2 - 3	3 - 4	4 - 5	5 - 7	7 - 9	9 - 11	11 - 15
δ13C	Initial	-23.4	-24.7	-24.7	-25.1	-25.6	-24.6	-26.0	-21.3	-24.4
	7 d	-20.6	-16.1	-14.5	-15.9	-17.9	-17.9	-19.3	-20.4	-21.0
	14 d	-24.7	-19.8	-15.9	-16.6	-17.4	-19.6	-24.4	-23.4	-19.0
Algal cell abundance (x 10^3 cells ml^{-1})	Initial	33.8	3.2	2.2	1.2	1.6	1.3	0.7	0.7	0.3
	7 d	91.9	19.9	15.9	9.6	3.9	3.3	2.2	1.6	1.0
	14 d	72.2	65.7	12.8	14.4	4.1	8.0	3.8	1.9	1.2
Live algal abundance (%)	Initial	98.0	97.1	76.2	90.0	94.2	89.0	93.0	69.3	83.4
	7 d	98.0	97.4	95.3	94.6	94.4	94.8	90.9	85.3	91.1
	14 d	94.1	95.1	98.3	98.1	97.8	87.7	94.3	94.9	90.4
Brine biovolume (x 10^4 μm^3 ml^{-1})	Initial	41.6	4.4	1.3	0.9	0.9	0.8	0.6	0.5	0.4
	7 d	113.3	33.4	26.5	18.0	2.6	4.6	3.1	2.9	9.2
	14 d	39.1	38.9	44.5	17.7	4.7	4.3	4.0	2.5	2.2
Entomoneis kjellmanni (%)	Initial	18.6	0.4	6.7	7.2	3.3	5.2	3.2	0.0	0.0
	7 d	46.4	4.3	4.0	3.5	1.4	0.6	0.7	1.2	1.4
	14 d	27.8	40.3	3.3	1.7	2.1	11.2	3.6	1.7	1.9
Nitzschia stellata (%)	Initial	37.8	6.5	7.2	10.2	1.9	10.7	4.8	4.2	0.6
	7 d	8.4	50.8	32.5	22.9	17.5	8.3	8.5	3.0	4.1
	14 d	2.2	5.4	45.0	47.8	22.4	24.0	6.5	17.6	17.4
Berkeleya adeliense (%)	Initial	6.1	0.7	5.4	2.2	1.3	1.4	12.3	2.8	1.1
	7 d	10.3	15.6	20.6	25.2	22.4	7.0	12.0	20.0	7.1
	14 d	1.7	3.4	25.5	21.9	14.5	24.3	7.2	56.4	12.1
Mangulinea spp. (%)	Initial	7.9	6.2	10.9	11.9	5.6	2.8	7.6	0.7	1.6
	7 d	2.8	8.0	7.4	6.1	10.7	11.2	8.4	6.6	2.4
	14 d	1.0	5.6	12.3	10.7	8.7	13.5	4.1	1.7	1.1
Fragilariopsis spp. (%)	Initial	11.5	7.6	5.9	5.4	4.1	6.8	2.5	0.0	0.8
	7 d	11.1	4.7	3.5	1.9	2.0	0.6	2.8	1.3	0.5
	14 d	9.8	0.4	0.7	0.8	3.7	2.0	0.6	2.0	1.7

3.5.3 Microalgal Taxa and Bacterial Abundance

Microscopic analysis showed the bottom ice algal community was dominated by *Entomoneis kjellmanni, Nitzschia stellata, Berkeleya adeliense, Mangulinea* spp., and *Fragilariopsis* spp. (Table 3.1), with other notable taxa including *Chaetoceros* spp., *Pleurosigma* spp., *Pinnularia quadreata,* and *Porosira glacialis.* Vertical and temporal cell abundance measurements varied significantly ($p < 0.001$) and decreased exponentially from the ice-water interface. Algal cell abundance decreased by ca. 99 % at 11 – 16 cm above the ice-water interface for all sampling dates (Table 3.1). The proportion of live algal cells relative to the total abundance (i.e. % live cells) ranged from 69.3 to 93.3 % ($p < 0.0001$; mean: 91.8 %; Table 3.1). For initial and 7 d, the % live cells were highest at the ice-water interface (98.0 %; Table 3.1), strongly declining with distance above this level. For 14 d, the % live cells showed a similar pattern to chl *a* concentrations, and was highest at 2 – 3 cm above the ice-water interface (98.3 %; Table 3.1).

Total brine biovolume is shown in Table 3.1, and ranged from 0.4 to 113.3 x 10^4 $\mu m^3\,ml^{-1}$ (mean: 15.7 x 10^4 $\mu m^3\,ml^{-1}$). Total brine biovolume measurements at the ice-water interface for initial (41.6 x 10^4 $\mu m^3\,ml^{-1}$) and 7 d (113.3 x 10^4 $\mu m^3\,ml^{-1}$) declined by 98 % and 76 % at 11 – 16 cm above, respectively. 14 d total brine biovolume measurements were highest at 2 – 3 cm above the ice-water interface (44.5 x 10^4 $\mu m^3\,ml^{-1}$), thereafter reducing by 91 % at 11 – 16 cm (Table 3.1). Total brine biovolume was significantly positively correlated with chl *a*, POC and maximum quantum yield (chl *a* [$r_p = 0.721$, $p < 0.001$, $n = 27$]; POC [$r_p = 0.834$, $p < 0.001$, $n = 27$]), F_v/F_v ($r_p = 0.750$, $p < 0.001$, $n = 27$), and extracellular organic

carbon concentrations (DOC [r_p = 0.811, p < 0.001, n = 27]; CHO_{Mono} [r_p = 0.745, p < 0.001, n = 27] and CHO_{Poly} [r_p = 0.627, p < 0.001, n = 27]).

Total bacterial abundance fractionated into high and low nucleic acid content (HNA; LNA) varied between sections and ranged from 0.54 to 28.90 x 10^5 cells ml^{-1} (mean = 6.05 x 10^5 cells ml^{-1}) and 0.49 to 48.47 x 10^5 cells ml^{-1} (mean: 16.22 x 10^5 cells ml^{-1}), respectively. Initial HNA and LNA bacterial abundance was highest at the ice-water interface (mean: 28.90 ± 28.73 and 20.56 ± 19.51 x 10^5 cells ml^{-1}, respectively) reducing by 94 and 91 % within 4 cm from the ice-water interface. HNA bacterial abundance for 7 d (mean: 6.20 ± 1.39 x 10^5 cells ml^{-1}) and 14 d (mean: 6.69 ± 0.96 x 10^5 cells ml-1) were reducing by 81 % and 36 % at 4 – 5 cm and 6 – 7 cm above the ice-water interface, respectively (Figure 3.4A). LNA bacterial abundance for 7 d (mean: 19.65 ± 16.01 x 10^5 cells ml^{-1}) and 14 d (25.19 ± 17.63 x 10^5 cells ml^{-1}) showed high standard errors, increasing by 72 % and 52 % at 3 – 4 cm above the ice-water interface, respectively (Figure 3.4B). HNA bacterial abundance was correlated with ice temperature (r_p = 0.503, p = 0.010, n = 27) and chl *a* concentration (r_p = 0.363, p = 0.001; n = 81). LNA bacterial abundance was positively correlated with C:N ratio (r_p = 0.293, p = 0.012, n = 81).

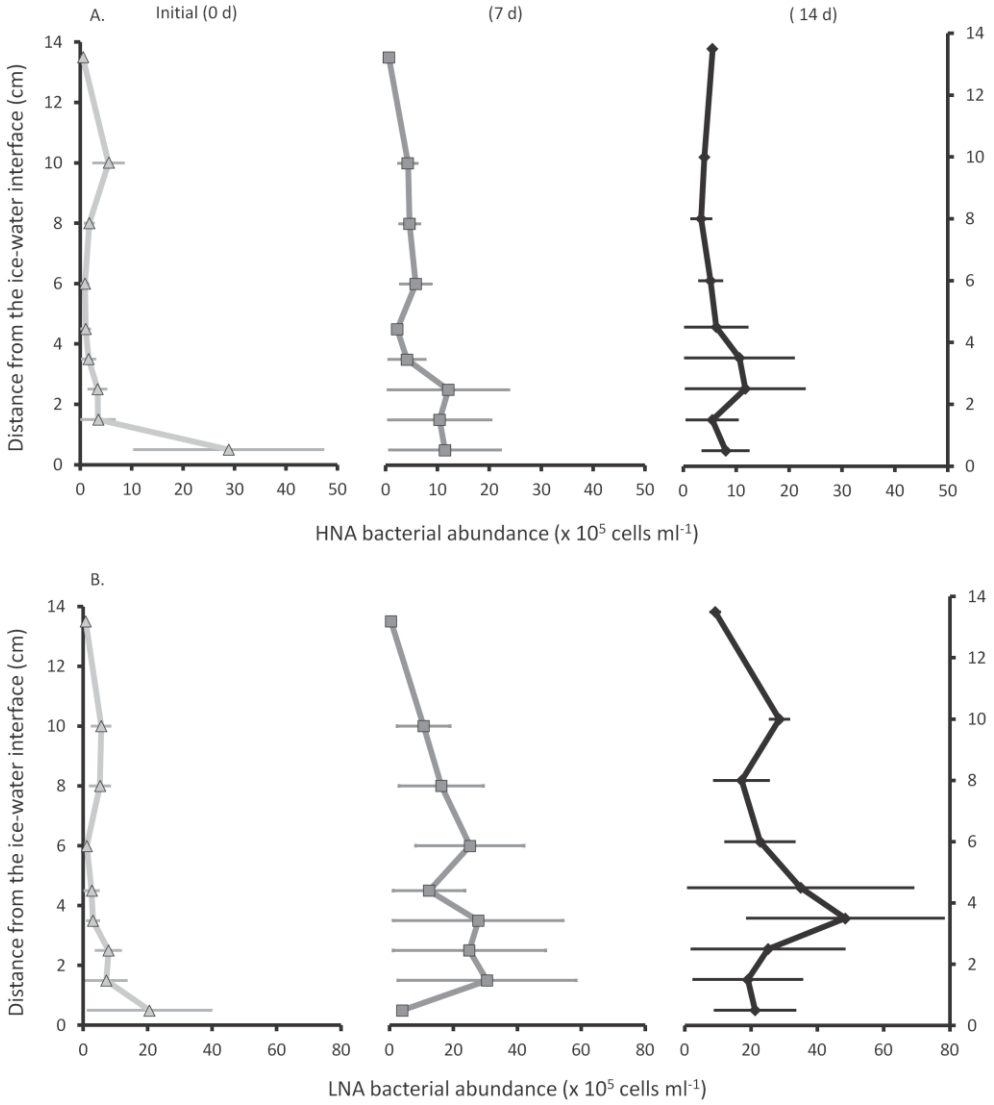

Figure 3.4: Vertical and temporal profiles of high nucleic acid bacterial cell abundance (A); low nucleic acid bacterial abundance (B). Error bars = ± SE

3.5.4 Extracellular Organic Carbon Components

Vertical and temporal measurements of DOC concentrations showed significant variation ($p < 0.005$; mean: 0.71 ± 0.08 mmol C l^{-1}), with each sampling date showing dissimilar vertical profiles (Figure 3.3D). Initial DOC concentrations ranged between 0.16 to 1.06 mmol C l^{-1} (mean: 0.51 ± 0.09 mmol C l^{-1}), and

showed no significant vertical variation. 7 d DOC concentrations showed significant decline, reducing by 89 % at 4 – 5 cm above the ice-water interface ($p < 0.005$; mean: 0.67 ± 0.17 mmol C l^{-1}; range: 0.21 to 1.88 mmol C l^{-1}). 14 d DOC concentrations reached 1.35 ± 0.14 mmol C l^{-1} at 2 – 3 cm above the ice-water interface ($p < 0.005$; mean: 0.94 ± 0.11 mmol C l^{-1}), thereafter declining by 79 % at 11 – 16 cm above (Figure 3.3D). DOC concentrations were correlated with chl *a* concentrations ($r_p = 0.649$, $p < 0.001$, $n = 81$), F_v/F_m ($r_p = 0.574$, $p < 0.001$, $n = 81$), and dissolved carbohydrates (CHO_{Mono} [$r_p = 0.766$, $p < 0.001$, $n = 81$]; CHO_{Poly} [$r_p = 0.738$, $p < 0.001$, $n = 81$]).

Values of CHO_{Mono} ranged between 7 to 278 µmol C l^{-1} (mean: 52 ± 11 µmol C l^{-1}), and CHO_{Poly} ranged between 30 to 341 µmol C l^{-1} (mean: 86 ± 13 µmol C l^{-1}; Figure 3.5). Initial CHO_{Mono} values were low (range: 7 to 26 µmol C l^{-1}; mean: 161 ± 2 µmol C l^{-1}) and were highest at 1 – 2 cm above the ice-water interface (Figure 3.3E). CHO_{Poly} initial values ranged between 31 to 120 µmol C l^{-1} (mean: 67 ± 10 µmol l^{-1}), and were highest at 2 – 3 cm above the ice-water interface (Figure 3.3F). At 7 d dissolved carbohydrates were highest at the ice-water interface; CHO_{Mono} (range: 20 to 278 µmol C l^{-1}; mean: 84 ± 29 µmol C l^{-1}) and CHO_{Poly} (range: 30 to 341 µmol C l^{-1}; mean: 110 ± 34 µmol C l^{-1}), reducing by 92 % and 91 % at 11 – 16 cm above, respectively. 14 d CHO_{Mono} values were highest at 2 – 3 cm above the ice-water interface (range: 20 to 127 µmol C l^{-1}; mean: 57 ± 12 µmol C l^{-1}), reducing by 91 % at 11 – 16 cm above (CHO_{Poly} range: 344 to 150 µmol C l^{-1}; mean: 83 ± 16 µmol C l^{-1}). Concentrations of CHO_{Mono} and CHO_{Poly} both showed correlations with ice temperature ($r_p = 0.408$, $p = 0.043$, $n = 27$), chl

a concentrations (r_p = 0.74 and 0.471, respectively, p < 0.001, n = 81) and F_v/F_m (r_p = 0.449 and 0.516, respectively, p < 0.001, n = 81).

3.5.5 Biomass-Normalised Extracellular Organic Carbon Components

Chl *a*-normalised DOC concentrations showed significant vertical and temporal variation (p < 0.005; mean: 4019 ± 1772 mg C(mg chl *a*)$^{-1}$; range: 23 to 39401 mg C(mg chl *a*)$^{-1}$; Figure 3.3G). Chl *a*-normalised DOC was lowest at the ice-water interface; 33 ± 27, 39 ± 9, and 23 ± 3 mg C(mg chl *a*)$^{-1}$, for initial, 7 d, and 14 d, respectively (Figure 3.3G). Initial chl *a*-normalised DOC concentrations vertically increased to reach a maxima of 44888 ± 13357 mg C(mg chl *a*)$^{-1}$ at 9 – 11 cm above the ice-water interface. 7 d and 14 d chl *a*-normalised DOC also strongly increased from the ice-water interface (p < 0.005), to reach 2809 ± 251 and 2539 ± 1796 mg C(mg chl *a*)$^{-1}$ at 11 – 16 cm above, respectively (Figure 3.3G).

Chl *a*-normalised CHO_{Mono} concentrations were low at the ice-water interface; 1.6 ± 1.0, 5.2 ± 0.2, and 2.0 ± 0.8 mg C(mg chl *a*)$^{-1}$ for initial, 7 d, and 14 d, respectively (Figure 3.3H). Initial chl *a*-normalised CHO_{Mono} concentrations (range: 1.6 to 525.5 mg C(mg chl *a*)$^{-1}$; mean: 202.1 ± 67.7 mg C(mg chl *a*)$^{-1}$) were highest at 7 – 9 cm above the ice-water interface, and CHO_{Poly} concentrations (range: 3.7 to 1849.0 mg C(mg chl *a*)$^{-1}$; mean: 287.9 ± 99.3 mg C(mg chl *a*)$^{-1}$) were highest at 5 – 7 cm above the ice water interface (Figure 3.3H, I). In comparison, chl *a*- normalised dissolved carbohydrates for both 7 d (CHO_{Mono} range: 5.2 to 128.0 mg C(mg chl *a*)$^{-1}$; mean: 46.2 ± 15.0 mg C(mg chl *a*)$^{-1}$, and CHO_{Poly} range: 7.7 to 208.3 mg C(mg chl *a*)$^{-1}$; mean: 80.7 ± 28.7 mg C(mg chl *a*)$^{-}$

^{1}) and 14 d (CHO_{Mono} range: 2.0 to 47.7 mg C(mg chl *a*)$^{-1}$; mean: 16.1 ± 4.7 mg C(mg chl *a*)$^{-1}$, and CHO_{Poly} range: 3.7 to 71.2 mg C(mg chl *a*)$^{-1}$; mean: 24.4 ± 7.5 mg C(mg chl *a*)$^{-1}$) were low (Figure 3.3H, L).

3.5.6 Dissolved Organic Carbon Composition

The relative contribution of TCHO to DOC had significant spatial and temporal variation ($p < 0.005$; mean: 24.9 % ± 3.4 %; range: 5.6 % to 76.3 %; Figure 3.5A). This portion of TCHO had high CHO_{Poly} contributions for initial measurements (mean: 78.8 % ± 2.2 %; range: 66.9 to 89.06 %; Figure 3.5B). At 7 d, the relative proportion of CHO_{Poly} to TCHO reached maxima at 9 – 11 cm above the ice-water interface, ranging between 49.3 % and 70.4 % (mean: 59.22 % ± 2.62 %; Figure 3.5B). At 14 d, the relative proportion of CHO_{Poly} to TCHO increased from the ice-water interface to reach 67.3 % ± 8.2 % at 2 – 3 cm above, ranging between 46.01 % and 67.3 % (mean: 59.6 % ± 3.0 %; Figure 3.5B).

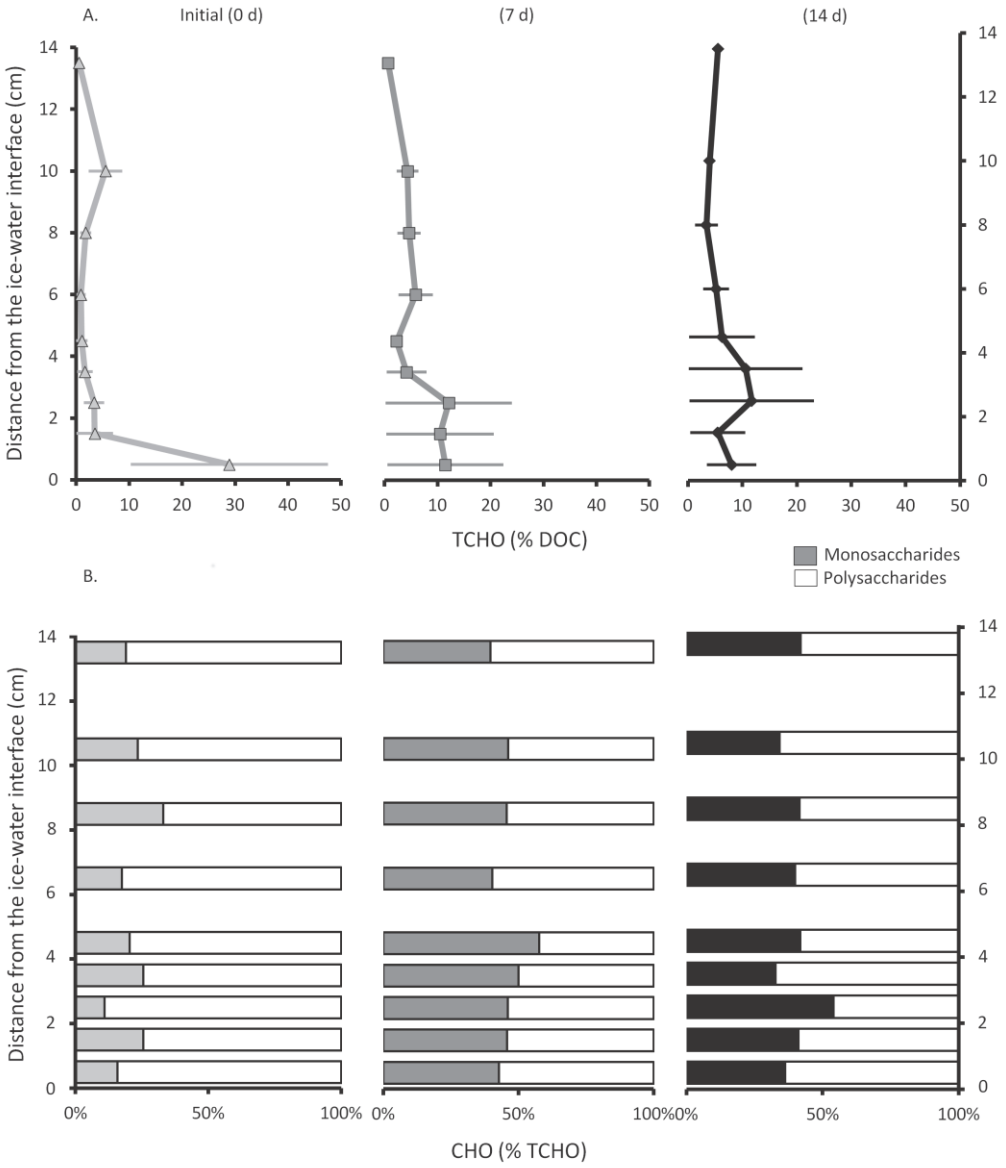

Figure 3.5: Temporal and vertical profiles of dissolved organic carbon (DOC) composition; relative contribution of total carbohydrates (TCHO) to DOC (A); and relative contribution of dissolved monosaccharides (CHO_{Mono}) and polysaccharides (CHO_{Poly}) to TCHO (B). Error bars = ± SE.

3.6 DISCUSSION

Seasonal changes in sea ice physical parameters create strong physicochemical gradients that affect biological activity and biogeochemistry (Fritsen et al. 1994; Gleitz et al. 1995; Papadimitriou et al. 2007, 2009; Vancoppenolle et al. 2010, 2013). At McMurdo Sound in November-December 2011, the calculated V_b/V fraction was well above the theoretical percolation threshold of 5 % (Golden et al. 1998, 2007; mean range: 28 % to 32 % at 0 – 4 cm above the ice-water interface for sampling dates), and is interpreted as an open brine channel network (i.e. ice melting), allowing for increased capacity for fluid transport across the ice-water interface by mixing nutrient-poor brine with comparatively fresh nutrient-rich seawater (Vancoppenolle et al. 2010). This fluid transport potential can be impeded by the development of brine salinity stratification caused by melting sea ice during warmer temperatures. Nonetheless, the observed increase in algal biomass (as indicated by chl *a* concentration and algal cell abundance) increased to within expected ranges for a bottom ice community at the ice-water interface (e.g. McMinn et al. 1999; Ryan et al. 2006). The taxonomic composition was comparable to previous studies in this area, although the relative abundance of the major taxa varied considerably over the period of two weeks. At Cape Evans over the spring-summer transition, McMinn et al. (2000) reported that *Nitzschia stellata* dominated the algal community (up to 94 % of cells), with *Berkeleya adeliensis*, *Pleurosigma antarctica*, *Entomoneis kjellmannii*, and *N. lecoitei* also present. Fiala et al. (2006) reported *Fragilariopsis*, *Nitzschia*, *Navicula* and *Pseudonitzschia* were dominant at Adélie Land during April to December, and was influenced by large spatial variability. In the current study, the bottom ice community was dominated by colony-forming diatoms; *N. stellata* (51 % max), *E.*

kjellmannii (46 % max), and *B. adeliensis* (56 % max). These particular species may exude organic carbon for the purpose of cell-attachment (Hoagland et al. 1993), and formation of colonies may partly account for the spatial heterogeneity within measured particulate (e.g. C:N, $\delta^{13}C$, chl *a*) and dissolved (e.g. DOC, $CHO_{mono/poly}$) parameters.

The photosynthetic parameter, F_v/F_m, was lower than expected (mean at the ice-water interface = 0.35), which for unstressed marine microalgae is typically 0.65 (Schreiber 2003). McMinn et al. (2003) reported F_v/F_m values of 0.45 ± 0.15 in over a hundred dark adapted samples from Antarctic fast ice. In the Arctic, McMinn and Hegseth (2004) have also reported similar values from apparently healthy sea ice communities. Therefore, the results herein are consistent with the suggestions that *in situ* ice algal communities have naturally low F_v/F_m values, possibly due to a temperature influence on photosynthetic performance (McMinn et al. 2010, Ralph and Gademann 2005). In the current study, the vertical reduction in F_v/F_m values demonstrated a clear coupling with algal biomass, and is interpreted as a consequence of increasing restrictive brine dynamics above the ice-water interface (i.e. V_b/V).

Fast ice algal communities exhibit a seasonal trend with respect to nutrient stress (Lizotte and Sullivan 1992). Typically, nitrogen limitation is evident when C:N ratios are greater than 7.7 (Redfield et al. 1963). For congelation ice, high ratios have been reported (e.g. Cota and Sullivan 1990; range = 8.8 to 16; and Lizotte and Sullivan 1992; range = 7.8 to 14.6). In the current study, although slightly elevated C:N ratios were measured (mean: 8.4, 8.7, and 9.1 for initial, 7 d, and 14

d, respectively), the high spatial heterogeneity suggests skewed abundances of colony-forming cells and/or cell associated- or colloidal extracellular organic carbon were captured on the filters during sampling. This may have resulted in an over-estimation of C:N ratios, and as such, the bottom ice community is considered to have experienced a reduced nutrient availability, but was not necessarily nutrient limited.

Along with nutrient drawdown, bottom ice assemblages may also be limited by the supply of CO_2 (Riebesell et al. 1993). Any reduction in aqueous CO_2 will be reflected in more positive $\delta^{13}C$ of the algae (Popp et al. 1999). In the current study, the $\delta^{13}C$ profiles showed an increase within 3 cm above the ice-water interface for 7 d and 14 d. This trend implies that demand for CO_2 exceeded supply (i.e. drawdown, Kennedy et al. 2002); either the demand for CO_2 is increased due to high algal growth, or alternatively, the supply of CO_2 across the ice-water interface is limited due to restrictive brine dynamics. In the current study, although a combination of both factors is likely, the latter maybe more important as algal growth rates need to be high to influence carbon isotopic composition (McMinn et al. 1999). For example, culture experiments with *Phaeodactylum tricornutum* revealed that growth rates in excess of 0.5 d^{-1} were needed to affect $\delta^{13}C$ values (Laws et al. 1995). This rate was not exceeded in the current study, with average ice algal *in situ* net cell growth rate estimates (calculated from changes in algal cell abundance) of 0.19 ± 0.02 (range: 0.12 to 0.30) and 0.05 ± 0.02 (range: -0.03 to 0.17) for initial to 7 d, and 7 to 14 d, respectively. These growth rates are comparable to typical values of 0.1 to 0.2 d^{-1}

previously observed in Antarctic fast ice (Palmisano and Sullivan 1983; Sullivan et al. 1985).

The ecological functions of bacterial communities are influenced by their phylogenetic composition, representing a wide range of DNA contents and cell sizes (Bouvier et al. 2007). HNA bacteria are generally larger, more metabolically active, and have higher growth rates than their LNA counterparts (Bouvier et al. 2007; Lebaron et al. 2002; Servais et al. 2003). In the current study, the HNA bacterial abundance was correlated with chl *a* concentrations (r_p = 0.363, p = 0.001, n = 81) and ice temperature (r_p = 0.503, p = 0.010, n = 27); LNA bacterial abundance had no such correlation. This may infer a direct association between the HNA bacteria and algal fractions of the community by means of a microbial loop, although this relationship is dependent on microbial composition (Martin et al. 2012, Taylor and Sullivan 2008), or alternatively, this association may be a consequence of warmer temperatures promoting general microbial growth. The lack of correlation between the bacterial community and exuded organic material is inconsistent with findings from other sea ice studies (e.g. Meiners et al. 2004), although a complete understanding of microbial and extracellular organic carbon dynamics within the sea ice ecosystems clearly requires information beyond the use of proxy measurements (Garrison et al. 2005).

The DOC concentrations in the current study are comparable to other sea ice studies from Antarctic and Arctic regions (Carlson et al. 2000; Herborg et al. 2001; Krembs et al. 2002; Thomas et al. 2001; Underwood et al. 2010). In

comparison to marine environments, DOC concentrations were more than ten-fold higher than those measured in surface oceanic water in the circumpolar Southern Ocean (Carlson et al. 2000; Doval et al. 2002; Kähler et al. 1997; Kirchman et al. 2001; Papadimitriou et al. 2007; Pakulski and Benner 1994; Wedborg et al. 1998). Given that the high DOC concentrations were present in the samples that had a high algal biomass ($r_p = 0.649$, $p < 0.001$, $n = 81$), there is clearly a strong link between algal activity and DOC accumulation in Antarctic sea ice, although this is not always the case in other studies (e.g. Herborg et al. 2001). Similarly carbohydrate accumulation, specifically high-molecular weight carbohydrates expressed as exopolymeric substances, in both sea ice (Krembs and Engel 2001; Riedel et al. 2006, 2008) and sediments (Underwood and Smith 1998) generally show a close correlation with algal biomass. Carbohydrate enrichment has been observed as sea ice ages, and this may be explained by changes in the brine environment, such as nutrients limitation, CO_2 drawdown, and elevated pH (Collins et al. 2008; Riedel et al. 2007; van der Merwe et al. 2009). In contrast, the high DOC concentration towards the ice interior at 14 d may be a due to the high V_b/V values at the ice-water interface, allowing for DOC to be released into the under-ice water prior to, or during, ice core extraction. Production studies have reported an increase in extracellular organic carbon exudation accompanying changes in physiology and growth phase in Antarctic sea ice algae (Aslam et al. 2012; Ugalde et al. 2013) as also observed in marine diatoms (e.g. Goto et al. 1999; Granum et al. 2002; Underwood et al. 2004). In the current study, chl *a*-normalised extracellular organic carbon concentrations showed a decrease over the sampling period, which coincided with increases in both F_v/F_m values and V_b/V, indicating an enhanced capacity for nutrient transport from the under-ice

realm into the bottom layers of the sea ice. This finding supports the notion that extracellular organic carbon plays an important role in the microbial response to physicochemical conditions (e.g. low temperature, nutrient availability), or possibly represents overflow metabolism.

Overflow metabolism is a well-established mechanism, although it has rarely been applied to polar environments (Myklestad et al. 1989; Waite et al. 1976). Fogg (1983) proposed that the exudation of organic carbon was an end-product of a process whereby photosynthesis takes place more rapidly than is necessary to supply the requirements for growth. Overflow metabolism has since been observed in planktonic and benthic diatoms, and can be stimulated by both nutrient limiting conditions (e.g. Bucciarelli and Sunda 2003; Myklestad et al. 1989; Staats et al. 2000) and low temperature (e.g. Wolfstein and Stal 2002). For ice-dwelling microbes, an increase in the exudation of organic carbon has been reported at reduced temperatures and nutrient limitation, possibly as a cellular survival mechanism (e.g. Aslam et al. 2012; Gleitz and Kirst 1991; Krembs and Deming 2008; Krembs et al. 2011; Underwood et al. 2013). However, as reduced growth rates can be associated with low temperatures, metabolic overflow may better explain this coupling (Aslam et al. 2012; Krell et al. 2007; Mock and Valentin 2004). Gleitz and Kirst (1991) suggested the prominent observation of allocation to carbohydrates may indicate nutrient depletion in ice algal assemblages from Weddell Sea pack ice in spring. In the current study, the microbial community was exposed to both reduced, but not limiting, nutrient availability (based on C:N ratios of > 7.7) and low temperatures. Therefore, overflow metabolism cannot be excluded as a possible explanation for the

observed spatial and temporal trends of chl *a*-normalised extracellular organic carbon.

The proportion of DOC as TCHO was generally < 20 %, and this is comparable to previous reported values in Arctic and Antarctic seawater (Engbrode and Kattner 2005; Herborg et al. 2001; Kirchman et al. 2001; Myklestad and Børsheim 2007; Pakulski and Benner 1994; Wang et al. 2006). In Antarctic sea ice, the mean proportion of TCHO to DOC is < 35 %; however it ranges from 1 to 99 % (Herborg et al. 2001; Thomas et al. 2001). In contrast, Underwood et al. (2010) reported values from melted ice cores of between 30 % and 50 %, and they considered that this variation may be due, in part, to differing methods used to isolate and measure carbohydrate concentrations between seawater and ice. For example, the methods used by Underwood et al. (2010) required dialysis to exclude salts from the samples. This resulted in low-molecular weight materials, including carbohydrates < 8 KDa, being lost prior to TCHO analysis. In the current study, the methods applied did not require dialysis, but this alone does not explain the difference in TCHO values reported. Rather, the current study suggests that either the carbohydrate fraction of DOC may have been rapidly modified through abiotic (e.g. hydrolysis, photolysis) or biotic (e.g. microbial loop) processes. Alternatively, the bottom ice microbial assemblages may have invested heavily into non-carbohydrate DOC, consisting of proteins, lipids, and free DNA, possibly also including organic nitrogen-containing carbohydrates (e.g. proteoglycans and amino-sugars; Underwood et al. 2010). The current study supports the need for further research and comparison of methods for the isolation

and quantification of extracellular organic carbon components, particularly in the sea ice habitat.

The current study demonstrates that CHO_{Poly} contributes substantially to TCHO in late spring (mean = 79 %), and this contribution rapidly decreases over time (mean = 59 %). If extracellular organic carbon provides protection against challenging abiotic conditions (Krembs et al. 2011), then a shift towards molecules with greater structural potential (i.e. polysaccharides) might be expected in addition to any increase in abundance (Krembs and Deming 2008; Krembs and Engel 2001; Underwood et al. 2010). Gleitz and Kirst (1991) reported interior pack ice algal assemblages allocate approximately five times higher into extracellular polysaccharides, compared with infiltration assemblages (8 and 44 % of total ^{14}C uptake, respectively), possibly due to nutrient limitation in the interior of the ice. In the current study, the high relative contribution of CHO_{Poly} to TCHO in early season ice indicates that the cells were experiencing adverse abiotic conditions, as was reflected by relatively low F_v/F_m values. This, coupled with lower calculated brine volume in early season ice, suggests a limited capacity for fluid exchange between brine channels and the underlying seawater.

3.7 CONCLUSION

The current study provides a detailed description of microalgal physiology and exuded organic carbon dynamics in an Antarctic bottom ice community, and is the first attempt to describe their successive changes during the spring-summer transition. It was hypothesised that sea ice algal would increase carbon allocation

to extracellular organic components with an increase in algal biomass. This hypothesis was supported with total concentrations of extracellular organic carbon components (DOC and TCHO [sum of CHO_{Mono} and CHO_{Poly}]) increasing during the sampling period. However, extracellular organic carbon concentrations normalised to chl *a* showed a substantial decrease during the sampling period. This change was associated with improved algal physiology and brine conditions, initiated by an increase in brine volume allowing transport across the ice-water interface. These findings support the theory that exudation of organic carbon by sea ice algae is associated with adverse brine conditions, either as a direct (in response to reduced temperatures or nutrient availability) or indirect (overflow metabolism or microbial loop) mechanism.

3.8 ACKNOWLEDGEMENTS

We are most grateful for the expert help and logistical support of Antarctic New Zealand and our colleagues working with us in the field and in the lead-up to the expedition, particularly C. Thorn and N. Higgison (Victoria University of Wellington, New Zealand). We thank the Australian Antarctic Division (AAD) for their ongoing support and access to infrastructure. This work was made possible by the support of the Australian Government's Cooperative Research Centre Program through the Antarctic Climate and Ecosystems Cooperative Research Centre (ACE CRC), the Trans-Antarctic Association and the Australian Antarctic Division (AAS 4008).

CHAPTER 4

Characteristics and primary productivity of East Antarctic pack ice during the winter-spring transition

Citation: Ugalde SC, Westwood KJ, van den Enden R, McMinn A, Meiners KM. Characteristics and primary productivity of East Antarctic pack ice during the winter-spring transition. Deep Sea Research II. Submitted (special edition).

4.1 ABSTRACT

Microbial communities have evolved mechanisms to allow them to survive within the challenging and changing pack ice environment. One such mechanism may be the exudation of photosynthetically-derived organic carbon into various extracellular pools. During the 2nd Sea Ice Physics and Ecosystem eXperiment (SIPEX-2), East Antarctic pack ice productivity and subsequent carbon allocation were quantified, together with physico-biogeochemical characteristics (29 September – 28 October, 2012). Mean ice thickness ranged between 0.87 and 2.24 m, and typically exhibited a warm ice interior with weak temperature gradients. All stations, with one exception, were layered with granular (mean: 78%), columnar (mean: 15%), and mixed granular/columnar (mean: 4%) ice. Highest ice brine-volume fractions were at the ice-water interface, but all ice had high brine-volume fractions conducive for brine percolation (mean: 15 %). Dissolved inorganic nutrient concentrations in the brine were scattered around theoretical dilution lines (TDLs), with some values of nitrate and nitrite,

ammonium and silicic acid falling below TDLs, indicating nutrient depletion. Bulk ice dissolved organic carbon was low (mean: 64 µmol kg^{-1}), but most samples showed enrichment in relation to TDLs. Microbial biomass (bacterial and algal) was low, and generally showed maxima in the sea-ice interior. Bottom ice algal communities were dominated by pennate diatom species (mean: 86 % of total cell abundance). ^{14}C-total primary productivity (^{14}C-TPP) ranged from < 0.01 to 2.29 mg C (mg chl *a*)$^{-1}$ d^{-1} (< 0.01 to 5.65 mg C m^{-2} d^{-1}). The relative contribution of ^{14}C-total extracellular organic carbon (^{14}C-TEOC) to ^{14}C-TPP decreased over the observational period (range: 43% to 21%), with the remaining proportion being ^{14}C-particulate organic carbon. ^{14}C-TEOC composition was dominated by low molecular weight ^{14}C-extracellular dissolved organic carbon (mean: 62%), with the remaining proportion allocated to ^{14}C-colloidal organic carbon. Production of ^{14}C-extracellular polymeric substances was not detected at any station.

4.2 KEY WORDS

Biomass

Carbon

Extracellular polymeric substances

Microalgae

Primary production

Sea ice

4.3 INTRODUCTION

Sea ice annually extends over an area of 15 – 22 x 10^6 km^2 of the polar oceans (Arrigo et al., 2014). As a result, sea ice is one of the most expansive, yet ephemeral, biomes on Earth. In the Southern Ocean, sea ice reaches its maximum coverage in September at ~19 x 10^6 km^2, reducing to 4 x 10^6 km^2 in February (Comiso, 2010). Of this ice mass, approximately 90 % constitutes pack ice (Lizotte and Sullivan, 1992).

Sea ice is comprised of two phases; solid ice and liquid brine (Weeks and Ackley, 1986). The fraction of each phase is mostly determined by temperature and sea-ice bulk salinity (Frankenstein and Garner, 1967; Light et al., 2003). During sea-ice formation, salt is actively excluded, leaving a lattice of solid ice crystals that are essentially salt- and nutrient-free. Liquid brine inclusions result from the remaining salt being concentrated into channels. The brine channel system is semi-isolated from the underlying water column (Papadimitriou et al., 2007; Petrich and Eicken, 2010; Vancoppenolle et al., 2013), the extent to which is dependent on the brine-volume fraction (V_b/V). Theoretically, V_b/V of < 5 % is considered sufficient to inhibit brine percolation in columnar ice, but a higher fraction is required for granular ice due to the more random orientation of crystals and brine channels (Golden et al., 1998). During winter and early spring the ice is generally characterised by low V_b/V and strong vertical gradients in temperature, brine salinity, and nutrients (Eicken, 1992; Reeburgh, 1984). As ice warms during spring and early summer, the V_b/V increases and enables more fluid to be exchanged between the brine channel system and the underlying seawater.

Brine channel systems contain a complex biological community, comprising microalgae (hereafter referred to as algae), bacteria, viruses, heterotrophic protists, and metazoans (Horner et al., 1992; Mock and Thomas, 2005; Thomas and Dieckmann, 2010). In pack ice, algal communities are generally dominated by diatoms, and the highest biomass can be concentrated at the ice-water interface (Becquevort et al., 2009; Grose and McMinn, 2003; McMinn et al., 2007). In older sea ice, which has been subject to surface melt and refreezing and/or surface-flooding due to heavy snow-loading, surface or interior assemblages can dominate (Ackley et al., 2008; Fritsen et al., 1994; Kattner et al., 2004; Meiners et al., 2012).

The primary production rate of algal assemblages varies throughout the season. Primary production and cell metabolism can be high during autumn ice formation, and then slow with the onset of winter in response to altering light and brine physicochemical conditions (e.g. increasing salinity, nutrient limitation; Gleitz and Thomas, 1992; Krell et al., 2008; McMinn and Martin, 2013). In spring, light levels increase and primary production resumes (McMinn et al., 2010, Petrou and Ralph, 2011).

Sea-ice algae have a low photosynthetic capacity and are highly shade adapted compared to pelagic phytoplankton (Cota, 1985; McMinn et al., 2000; Palmisano et al., 1985; Trenerry et al., 2002). However, their contribution to total primary production in the Antarctic seasonal sea ice zone has been estimated to range between 6.1 – 35.0 % in October and 1.1 – 2.1 % in January, and comprise 12 % of total annual primary production (Arrigo et al., 1997,1998b; Saenz and Arrigo,

2014). Saenz and Arrigo (2014) estimated sea-ice algal primary production to be 23.7 Tg C a^{-1}, with 80 % of production in the bottom 0.2 m of ice. The bottom ice algal layer, which is considered an important food resource for krill and other invertebrates, can have a low biomass or be absent in pack ice, when internal or surface assemblages dominate (Arrigo et al., 1997; Jia et al., this issue; Legendre et al., 1992).

Microalgae allocate photosynthetically-derived carbon into two general pools; particulate organic carbon (POC; biomass) and total extracellular organic carbon (TEOC; Aslam et al., 2012; Juhl et al., 2011; Krembs et al., 2011; Underwood et al., 2010). The chemical composition of TEOC is largely uncharacterised, but it is known to range from simple molecules (such as glucose) to highly complex molecules comprising 1000s of monomers. It includes compounds such as carbohydrates, proteins, lipids, and free DNA (Bellinger et al., 2005; Decho, 2000; Underwood et al., 2010). TEOC has the potential to bind together to form colloidal material that can be modified through biotic (e.g. microbial activity) and/or abiotic (e.g. hydrolysis, photolysis) catalysts (Underwood et al., 2010). Typically, precipitation of TEOC, usually in 70 % ethanol, isolates particularly heavy molecules, referred to extracellular polymeric substances (EPS; Mancuso Nichols et al., 2005; McConville et al., 1985, 1999). EPS is often tightly bound to the producer organism (Decho, 2000), and is considered to have high ecological significance, given its molecular complexity and diversity. Research to date has not attempted to directly quantify algal allocation to TEOC within the sea-ice habitat.

Improved understanding of sea-ice primary productivity, subsequent carbon allocation, and driving factors within the diverse pack ice habitat is critical to determine the response of the sea ice–covered ecosystem to future environmental changes. TEOC, or an isolated fraction, has been suggested to provide benefits directly to the producer organism, such as aiding in cellular motility and attachment (either through binding cells together or attachment to ice crystals), as well as acting as a layer/buffer to protect against adverse, and potentially harmful, physicochemical conditions; e.g. temperature, salinity, pH, and nutrients (Apoya-Horton et al., 2006; Ewert and Deming, 2013; Krembs and Deming, 2008; Krembs et al., 2002, 2011; Mishra and Jha, 2009; Smith and Underwood, 2000; Underwood and Paterson, 2003; Underwood et al., 2004). Its exudation may also influence brine channel microstructure, improving sea-icehabitability for the producer organism (Krembs et al., 2011). The high degree of bacterial metabolic activity and seasonal coupling between the relative abundance of bacteria and algae has also led to the suggestion that TEOC is the primary substrate for an active microbial loop, similar to that of temperate oceanic systems (Azam et al., 1991; Sullivan and Palmisano, 1984; Martin et al., 2008, 2009). In addition, extracellular material may be an end-product of overflow metabolism, in which the producer organism releases carbon derived from excessive primary production, and uses it to manage growth and abiotic requirements, similar to that of marine and benthic diatoms (Bucciarelli and Sunda, 2003; Fogg, 1983; Myklestad, 1989; Staats et al., 2000).

The purpose of the current study was to determine the relationships between ecological, physical, and biogeochemical parameters of East Antarctic pack ice

during the winter-spring transition. The study quantifies bottom ice ^{14}C-primary production, and the subsequent allocation into carbon fractions; ^{14}C-POC and ^{14}C-TEOC (sum of colloidal organic carbon [^{14}C-COLLOC], extracellular dissolved organic carbon [^{14}C-EDOC], and extracellular polymeric substances [^{14}C-EPS]) and ice algal species abundance. It also provides vertical profiles of microbial biomass (chlorophyll *a* [chl *a*] concentrations, bacterial abundance, particulate organic carbon [POC] and nitrogen [PON]), sea-ice physical parameters (ice temperature, bulk salinity, brine-volume fraction, sea-ice texture), and biogeochemistry (dissolved organic carbon [DOC], dissolved inorganic nutrients). These are discussed in relation to carbon dynamics during this important transitional period for sea-ice microbial community development.

4.4 METHODS

4.4.1 Site and Sampling

Data were collected during the 2nd Sea Ice Physics and Ecosystem Experiment (SIPEX-2) voyage onboard the RSV *Aurora Australis* between September and October 2012. Samples were taken within a sector ranging from 64.42 °S to 65.27 °S and 116 °E to 121 °E off East Antarctica, and floes were selected according to accessibility and physical characteristics. Six ice floes were sampled (stations # 2 – 4 and 6 – 8), and on each floe, a ~ 2 m^2 site, free from deformation, was selected. At each station, snow thickness was recorded (n = 5) and between 10 and 19 ice cores (A – T) were extracted using a powered Kovacs Mark II ice corer (0.09 m internal diameter). Sea-ice thickness and freeboard measurements (n = 5) were recorded from the resulting ice core holes.

Four ice cores (C – F) were sectioned into six discrete sections measured from the ice-water interface; 0–0.02 m; 0.02–0.10 m; the remainder of each core was quartered. Ice core sections were placed in polyethylene containers, which had been rinsed thoroughly with Milli-Q water, and the ice melted in the dark at 4 °C. Sections from two ice cores (E – F) were melted as per above, with the addition of 0.22 µm filtered seawater (0.2 l filtered seawater added per 0.01 m of ice core) to avoid cellular osmotic stress (Garrison and Buck, 1986). Seawater used to melt cores was collected at the same site using a seawater line on the ship (5 m below the surface), filtered at 0.22 µm, and cooled to 4 °C prior to use.

4.4.2 Temperature Profiles

Sea-ice temperature was determined on a further ice core (A). Immediately after sampling, holes were drilled into the centre of the core at 0.1 m intervals using a manual hand drill, and temperature measured using an electronic thermometer (Hanna HI93510). Thereafter, the core was discarded.

4.4.3 Ice Texture and Stable Oxygen Isotopes

A further ice core (B) was sealed in clean plastic tubing and transported to an onboard freezer laboratory (- 24 °C) for analysis of ice texture and stable oxygen isotopic composition. Ice texture was determined by thin-section analysis using cross-polarised light (e.g. Lange, 1988; Meiners et al., 2011). Stratigraphic units were determined by crystal size and orientation (Eicken and Lange, 1989). The remaining core material was cut into sections based on the stratigraphic units, and melted without the addition of seawater in sealed plastic containers at 4 °C.

Subsamples were taken for stable oxygen isotopes ($\delta^{18}O$) and stored in sealed glass vials for later analysis with a VG Isogas SIRA mass spectrometer (for details see Meiners et al., 2011). Ratios of oxygen isotopes were expressed relative to the Vienna Standard Mean Oceanic Water (V-SMOW) standard, with standard deviations for repeated measurements < 0.07 ‰. Based on isotopic characteristics, ice sections with granular stratigraphy were classified as either granular ice ($\delta^{18}O > 0$ ‰) or snow ice ($\delta^{18}O < 0$ ‰; Lange et al., 1990). Hence, four ice types were identified: snow ice, granular ice, columnar ice, and granular/columnar (g/c) ice.

4.4.4 Chemical Parameters

Subsamples (0.01 l) of the six melted sections from ice core C were filtered through 0.22 µm syringe filters (Acrodisk, Pall Corp.) attached to a sterile syringe. The subsamples were stored frozen at - 18 °C in sterile polypropylene vials for subsequent determination of dissolved phosphorus (PO_4^{3-}), silicic acid ($Si(OH)_4$), nitrate and nitrite (NO_x), and ammonium (NH_4^+). PO_4^{3-}, NO_x and NH_4^+ analyses were performed using a Lachat Flow Injection analyser based on American Public Health Association (APHA) Standard methods (APHA 2005; minimum reporting limit: PO_4^{3-} 0.0646 µmol l^{-1}, NO_x and NH_4^+ 0.1427 µmol l^{-1}). $Si(OH)_4$ concentrations were determined using an Aquakem 250 and ammonium molybdite with tin (II) chloride reduction (APHA 2005; minimum reporting limit: $Si(OH)_4$ 1.6647 µmol l^{-1}). All nutrient analyses were performed within 4 months of sampling. Ice bulk salinity was measured from the remaining melted sample using a conductivity meter (WTW-Tetraconn 325).

4.4.5 Particulate and Dissolved Organic Carbon

Subsamples from the six melted sections of ice core D were used to quantify particulate organic carbon (POC), particulate organic nitrogen (PON), and dissolved organic carbon (DOC). POC:PON subsamples (0.050 to 2.5 l) were filtered onto 25 mm diameter pre-combusted (overnight at 450 °C) quartz filters (Sartorius), and kept frozen at - 20 °C for later processing. To dissolve the inorganic carbon, thawed filters (sample and blank filters) were acidified for 24 h by fuming with 37 % HCl in a bell apparatus, and dried in a clean oven (15 h at 60 °C). Filters were pressed into 5 x 9 mm pre-combusted silver capsules (SerCon, United Kingdom) and analysed at the Central Science Laboratory, Hobart, by combustion in oxygen-enriched helium atmosphere using a Haereus CHN-O-Rapid analyser.

The POC:PON filtrate was captured for DOC determination, and stored frozen (-20 °C) in 40 ml glass vials with rubber septa caps (Shimadzu, Japan). Vials had been acid washed and rinsed three times with Milli-Q water, followed by overnight pre-combustion at 500 °C. Concentrations of DOC were measured using a catalytic oxidation combustion Total Organic Carbon Analyser (Shimadzu, L-Series), according to Qian and Mopper (1996).

4.4.6 Microbial Biomass

Corresponding melted sections from ice cores E – F were combined and subsampled for determination of chl *a* by high performance liquid chromography (HPLC). Chl *a* subsamples (0.07 to 1.68 l) were filtered onto 13 mm GF/F (Whatman) filters and stored in liquid nitrogen until analysis. Sample and blank

filters were thawed and extracted by sonication in 1 – 1.5 ml 100 % HPLC-grade methanol, using 130 ng apo-8'-carotenal (Fluka) as an internal standard, and detected using a Waters996 photodiode array and a Hitachi FT1000 fluorescence detector (Wright et al., 2010).

Additional subsamples from the same ice cores (0.25 l) were fixed with acid Lugol's solution and stored at 4 °C in the dark. Sea-ice algae were subsequently counted at the Australian Antarctic Division, Tasmania. Samples were concentrated and allowed to settle for at least 6 h in a 37 mm diameter Utermöhl chamber, and counted at a magnification of 600 x using a Zeiss Axiovert inverted microscope. Counts were conducted over random fields of view, until at least 400 cells had been counted.

Further subsamples (0.002 l) from melted cores E – F were preserved with glutaraldehyde (2 % final concentration) and stored at - 20 °C. Bacterial abundances were subsequently determined at the Australian Antarctic Division, Tasmania. Samples were thawed at room temperature and 500 µl were stained with SYBR Green I nucleic acid gel (Molecular Probes, USA) and incubated in the dark for 20 min. Cells were then counted using a Becton Dickinson FACScan flow cytometer, according to the protocol of Thomson et al. (2010). Manual gating was used to discriminate between nucleic acid content, according to Bouvier et al. (2007); Y-Geo mean $Bact_{Gate1}$ = 278; $Bact_{Gate2}$ = 114; $Bact_{Gate3}$ = 49; $Bact_{Gate4}$ = 12. Total bacterial abundance ($Bact_{Total}$) was expressed as the sum of all gates.

4.4.7 Bottom Ice Algal Primary Production and Carbon Allocation

Up to 14 ice cores (G – T) were sampled for bottom ice algal ^{14}C-photosynthesis-irradiance (P-E) curves and ^{14}C-carbon allocation. From the resulting core holes, water samples were taken for determination of dissolved inorganic carbon (n = 3) near the ice-water interface. Air contact was avoided during collection and the samples placed in acid washed glass bottles (250 ml). Samples were preserved using 100 µl saturated mercuric chloride solution and later analysed according to Ugalde et al. (2013).

The lowermost 0.02 m from each core was finely shaved off using a stainless steel saw and ice core support frame. The loose ice crystals were evenly divided into clean opaque polyethylene screw cap containers (n = 3). Containers were kept cool and protected from the light, and immediately transported back to an onboard laboratory. To avoid osmotic stress to algal cells, between 1.5 and 2.0 l of 2 ± 1 °C, 0.22 µm pre-filtered sea water was added to each container (Kaartokallio 2004; Kudoh et al., 2003). To isolate algal biomass from the ice crystals, each container was agitated for 5 min at 4 °C and subsequently passed through course mesh to separate the intact ice crystals and free-floating biomass. The volume of the filtrate was measured (mean: 105.9 % ± 0.8 % of initial added volume), and subsamples were taken to determine ^{14}C-photosynthesis-irradiance (P-E) curves and ^{14}C-carbon allocation.

4.4.8 P-E Curves and Under Ice Irradiance

P-E incubations were conducted according to the method of Westwood et al. (2011), with 1 h incubations under 21 intensities ranging from 0 to 1300 µmol m^{-2}

s^{-1}. Carbon uptake rates were corrected for chl *a* concentrations and for total dissolved inorganic carbon availability. Curves were plotted and analysed using SYSTAT (Version 13). The equation of Platt et al. (1980) was used to fit curves to the data using least squares non-linear regression:

$$P = P_{\max}\left(1 - \left(e^{\frac{-\propto *E}{P_{\max}}} * e^{\frac{-\beta *E}{P_{\max}}}\right)\right) + c$$

Where *P* was the rate of primary productivity (mg C (mg chl a) $^{-1}$ h^{-1}), P_{max} was the light-saturated photosynthetic rate (mg C (mg chl *a*)$^{-1}$ h^{-1}), α was the initial slope of the light-limited section of the P-E curve (mg C (mg chl *a*)$^{-1}$ h^{-1} (mmol m^{-2} s^{-1}) $^{-1}$), E was the light intensity at which carbon-uptake became maximal (calculated as P_{max} / α = E_k, mmol m^{-2} s^{-1}), β was the rate of photoinhibition where applicable (mg C (mg chl *a*)$^{-1}$ h^{-1} (mmol m^{-2} s^{-1})$^{-1}$), and *c* was the intercept of the P-E curve with the carbon uptake axis (mg C (mg chl *a*) $^{-1}$ h^{-1}).

At each station, incoming surface PAR was recorded from two onboard sensors (2 pi; accuracy ± 3 %). The sensor with the highest PAR recording was used for subsequent calculations. PAR at the bottom of the sea ice (i.e. lowermost 0.02 m) was calculated for ca. 5 min intervals over a 24 h period using the modified equation from Smith et al. (1988):

$$I_z = I_o\,(1 - A)\,e^{(-k_s * z_s * - k_i * z_i)}$$

where I_z was the irradiance incident at given depth (i.e. at the bottom of the ice), I_o was the maximum incoming irradiance measured from ship-board sensors, *A* was the surface albedo constant (0.8; Maykut, 1985), k_s was the snow attenuation coefficient (10.095 m^{-1}; Smith et al., 1988), z_s was the snow depth (m), k_i was the ice attenuation coefficient (1.82 m^{-1}; Michael and Higgins, 2014), and z_i was the midpoint ice section depth (i.e. the lowermost 0.01 m).

For each PAR time interval, the rate of primary productivity was calculated using the above P-E equation (*2*). The sum of which expressed the primary productivity across the 24 h period (i.e. mg C (mg chl a)$^{-1}$ d^{-1}). Integrated chl *a* values determined from the bottom of the sea ice was used to normalise sea ice primary productivity, to give sea ice production (i.e. mg C m^{-2} d^{-1}).

4.4.9 Definition of ^{14}C-Carbon Pools

^{14}C-total primary productivity (^{14}C-TPP) was determined from P-E curves, and defined as the sum of ^{14}C-particulate organic carbon (^{14}C-POC; intercellular) and ^{14}C-total extracellular organic carbon (^{14}C-TEOC; extracellular). ^{14}C-TEOC is defined as the sum of ^{14}C-extracellular dissolved organic carbon (^{14}C-EDOC) and ^{14}C-colloidal organic carbon (^{14}C-COLLOC). ^{14}C-COLLOC incorporates both colloidal and cell-associated carbon that is unable to pass through a GF/F filter. The subtracted proportion of ^{14}C-EDOC and ^{14}C-COLLOC was defined as ^{14}C-extracellular polymeric substances (^{14}C-EPS) and was precipitated using 70 % ethanol (Decho, 1990; Underwood et al., 1995).

4.4.10 ^{14}C-Carbon Allocation

Carbon fractions were isolated according to Ugalde et al. (2013), modified from Goto et al. (1999). Three replicates of four 0.02 l subsamples were used to isolate carbon fractions; ^{14}C-POC and ^{14}C-TEOC (sum of ^{14}C-EDOC, ^{14}C-COLLOC, and ^{14}C-EPS).

Subsamples were transferred into clear scintillation vials and inoculated with an aqueous antibiotic cocktail of penicillin (benzylpenicillin potassium, CSL Ltd, final concentration 75 µg ml^{-1}) and streptomycin (strepromycin sulfate, Sigma USA, final concentration 125 µg ml^{-1}). After 1 h, 200 µl ^{14}C-$NaHCO_3$ (activity = 148 kBq ml^{-1}) was added to each vial and further incubated for a given time depending on algal biomass (24 h ± 3 h). At the end of the incubation period, samples were filtered under low pressure (< 0.13 bar). 200 µl 32 % HCl was immediately added to the filtrate (0.005 l). This fraction was defined as ^{14}C-EDOC, and subsequently agitated for 3 h in a custom-built shaker box. The material trapped on the remaining filter was submerged in 4 nmol l^{-1} EDTA (Decho 1993), and centrifuged according to Ugalde et al. (2013).

This material was subsequently filtered again, and the filtrate, defined as ^{14}C-COLLOC, was immediately acidified with 300 µl of 32 % HCl prior to agitation in the shaker box. The intact filter was acidified with 50 ml of 2 % HCl, and defined as ^{14}C-POC.

Three ml of the acidified filtrate of ^{14}C-EDOC and ^{14}C-COLLOC was transferred to capped 15 ml falcon tubes and precipitated following Goto et al. (1999) using

cold ethanol (70 % final concentration, - 20 °C) and centrifuged (400 x *g* for 10 min) after an incubation of 10 h. The precipitated material was washed with cold 70 % ethanol and resuspended in distilled water, repeated twice. The precipitate obtained was defined as ^{14}C-EPS, and was undetectable (i.e. < $DPM_{T=0}$) at all stations.

For radioactive counts of aqueous ^{14}C-EDOC and ^{14}C-COLLOC fractions, 0.015 l of Aquassure (Amersham) liquid scintillation cocktail were added to each vial. For radioactive counts of ^{14}C-POC filters, 0.002 l acetone were added according to Ugalde et al. (2013), with 0.001 l Aquassure later added. All samples were briefly mixed and protected from the light prior to measurement, and counted using a scintillation counter. Rates of production used the following equation:

$$P = \frac{\frac{\mathrm{DPM} - \mathrm{DPM_{T=0}}}{\mathrm{DPM_{100\,\%}}} * \mathrm{DIC} * k_1 * k_2}{T}$$

Where *P* was the rate of production, DPM was the disintegrations per minute of the sample, $DPM_{T=0}$ was the background count, DIC was the under ice dissolved inorganic carbon (µg l^{-1}), k_1 was the correction factor (1.05) for the 5 % metabolic discrimination for the uptake of ^{14}C relative to ^{12}C (Ærtebjerg-Nielsen and Bresta, 1984), k_2 was the correction factor for subsampling given that only part of the incubated sample was utilised, *T* was the incubation time factor, and $DPM_{100\%}$ was the total radioactivity added to each vial.

From the above equation (*3*), the relative contribution of each carbon fraction (%) was applied to calculated bottom ice primary productivity rates over a 24 h period, derived from P-E curves and estimates of under-ice irradiance. Rate of carbon allocation is expressed as productivity (i.e. mg C (mg chl *a*) $^{-1}$ d^{-1}).

4.4.11 Statistical Analysis

All statistical analyses were performed using SPSS (IBM SPSS Statistics, 22.0). Non-parametric Spearman-Rank tests were applied to explore correlations between response variables. The non-parametric Kruskal-Wallis test was used to test for significant differences between median values of non-normal distributed data.

4.5 RESULTS

4.5.1 Physical Properties

Ice thickness at the sampled sites ranged between 0.80 and 2.16 m (mean: 1.34 m; Table 1). Snow cover ranged between 0.06 and 0.66 m. With the exception of two stations (stations 2 and 7), sea-ice freeboard was positive (range: - 0.09 to 0.05 m). The sea ice was generally warm with weak temperature gradients. Mean ice temperatures were high, with measurements ranging between - 6.7 and - 1.2 °C (Table 1). Minimum temperatures mostly occurred scattered throughout the profiles. However, stations 2 and 3 had minimum temperatures occurring in the upper ice layers, and station 2 had a generally linear temperature increase with ice depth (Figure 1A). With the exception of station 1, sea-ice salinities showed L-shaped profiles with maxima at the ice-water interface (Figure 2A).

V_b/V ranged between 7.6 and 36.1 %, with maxima always occurring at the ice-water interface (Figure 2B). V_b/V was correlated with ice depth (r_s = -0.339, p = 0.043, n = 36), nutrient concentrations in brine ($Si(OH)_4$ r_s = 0.605, p < 0.001, n = 36; NO_x r_s = 0.562, p < 0.001, n = 36; PO_4^{3-} r_s = 0.583, p < 0.001, n = 35; NH_4^+ r_s = 0.705, p < 0.001, n = 35), and brine DOC (r_s = -0.336, p = 0.028, n = 36). Most of the sea ice showed V_b/V above the theoretical threshold for brine percolation of 5 % for columnar ice (Golden et al. 1998; Table 1). Sea-ice sections with V_b/V of ≤ 10 % contributed 25 % of total ice core lengths, and sections with V_b/V of > 10 % to ≤ 20 % contributed 50 %. Sections with V_b/V of > 20 % contributed 25 % of the total core lengths for all stations.

All stations, with the exception of station 7, showed layering of granular, columnar, and mixed granular/columnar (g/c) ice (Figure 3). Granular ice was the dominant ice type, contributing 44 % to 97 % of the total core length (mean: 78 %). Columnar and g/c ice contributed 0 to 48 % (mean: 15 %) and 0 to 14 % (mean: 4 %), respectively. Snow ice was observed at all stations, with the exception of station 3, contributing 0 to 5 % of total core length (mean: 2 %).

Table 4.1: Station number (#), sampling date (2015), station latitude (mean), station longitude (mean), ice thickness (mean and range (m)), snow depth (mean (m)), freeboard (FB; mean (m)), ice bulk salinity (range), ice temperature (mean and range (°C)), brine-volume fraction (V_b/V; mean and range *(%)*), integrated (over entire ice thickness) chlorophyll *a* (chl *a*) concentrations (mg chl *a* m^{-2}) and particulate organic carbon (POC) concentrations (mg POC m^{-2}) for the sea-ice stations sampled during SIPEX-2. nd = not determined.

#	Date	Lat. (S)	Long. (E)	Ice thickness	Snow	FB	Salinity	Temperature	V_b/V	Chl *a*	POC
2	29 Sep.	64.42	120.09	0.80 (0.62 - 0.88)	0.06	-0.09	3.8 - 7.4	-4.3 (-6.7 - -2.3)	7.8 (5.8 - 12.5)	6.15	321
3	3 Oct.	64.92	120.96	1.93 (1.79 - 1.99)	0.66	nd	4.3 - 9.7	-2.1 (-3.5 - -1.6)	14.9 (10.3 - 21.1)	2.68	402
4	8 Oct.	65.11	121.15	0.94 (0.94 - 0.95)	0.63	0.04	4.0 - 8.0	-2.2 (-2.9 - -1.6)	13.8 (9.5 - 22.9)	10.47	692
6	14 Oct.	65.27	120.00	1.29 (1.20 - 1.38)	0.14	0.05	4.0 - 12.5	-1.9 (-2.1 - -1.6)	18.7 (10.8 - 33.7)	19.75	766
7	21 Oct.	65.20	118.66	0.90 (0.87 - 0.95)	0.36	-0.07	3.4 - 11.1	-2.0 (-2.2 - -1.6)	15.4 (8.2 - 31.8)	29.90	716
8	28 Oct.	64.78	116.27	2.16 (2.04 - 2.24)	0.51	0.02	3.5 - 13.4	-1.8 (-2.3 - -1.2)	19.1 (10.0 - 36.1)	3.27	1083

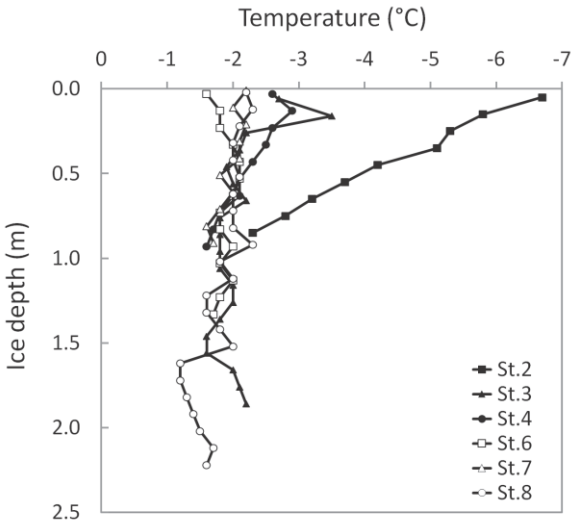

Figure 4.1: Vertical profiles of ice core temperature (°C) measured from each station

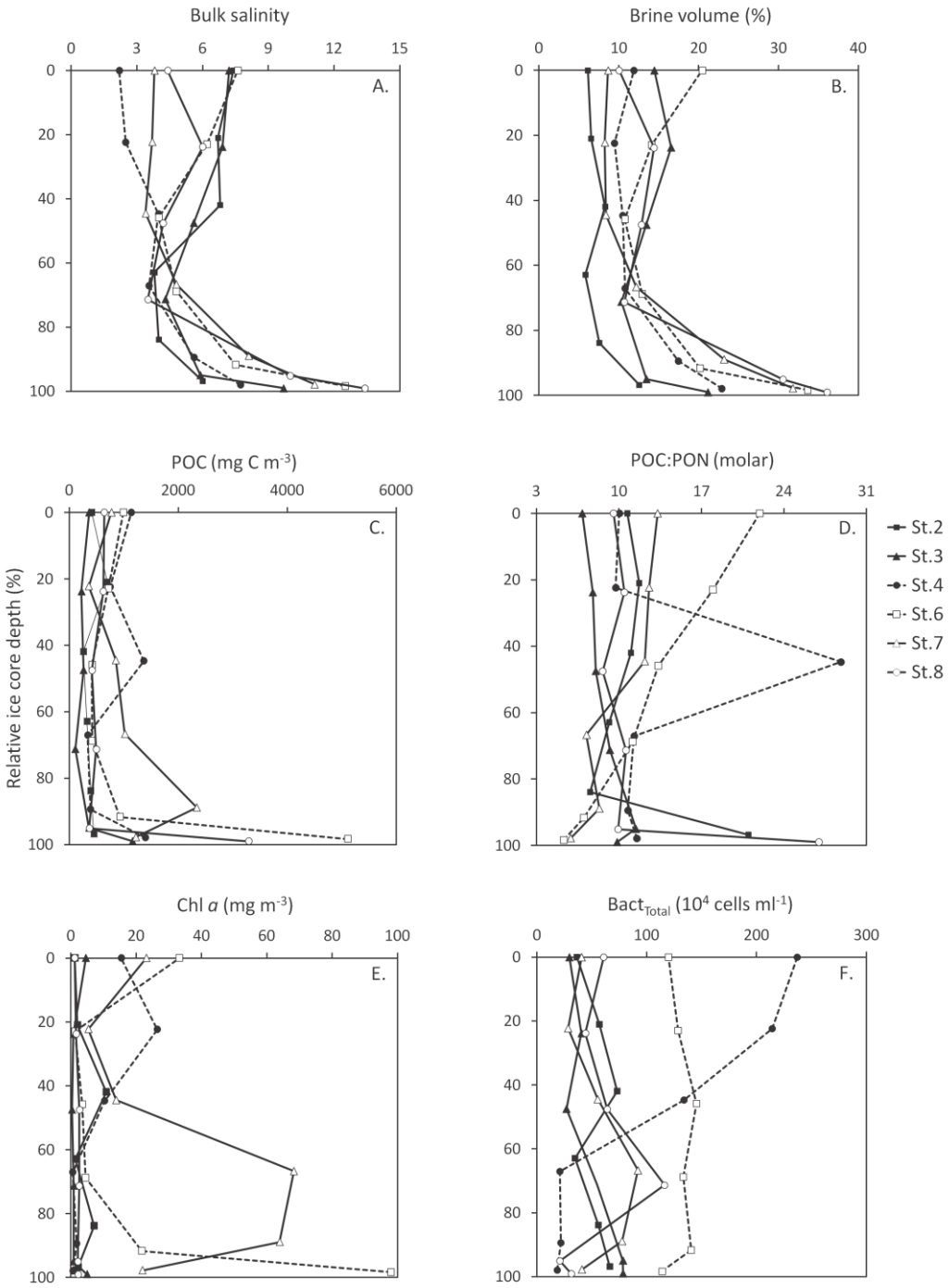

Figure 4.2: Concentrations of bulk salinity (A), brine-volume (B), particulate organic carbon (POC, C), molar ratio of POC to particulate organic nitrogen (POC:PON; D), chlorophyll *a* (chl *a*; E), and total bacterial abundance ($Bact_{Total}$; F) for the relative ice core depths at each station.

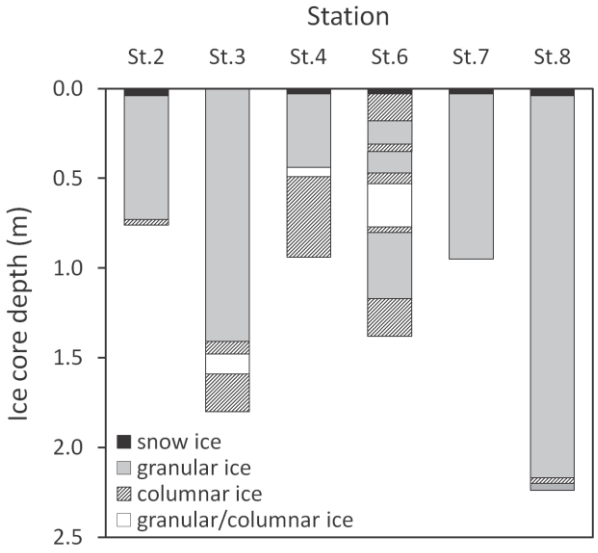

Figure 4.3: Vertical distribution of ice types determined from each station.

4.5.2 Biogeochemical Parameters

Bulk ice macro-nutrient concentrations of $Si(OH)_4$, NO_x, and PO_4^{3-} varied between ice stations, and ranged from 1.66 to 21.46 µmol kg^{-1} ($p = 0.002$; mean: 8.12 ± 0.77 [standard error] µmol kg^{-1}), 0.14 to 13.10 µmol kg^{-1} ($p = 0.002$; mean: 4.16 ± 0.54 µmol kg^{-1}), and 0.10 to 1.22 µmol kg^{-1} ($p = 0.027$; mean: 0.45 ± 0.04 µmol kg^{-1}), respectively (Figure 4). NH_4^+ concentrations ranged from 0.21 to 3.67 µmol kg^{-1} (mean: 0.89 ± 0.12 µmol kg^{-1}). One sample from the ice-water interface at station 6 was uncharacteristically high for all analyses; 21.37, 24.74, 27.74, and 3.67 µmol kg^{-1} for $Si(OH)_4$, NO_x, PO_4^{3-} and NH_4^+, respectively. It was assumed to be contaminated and therefore excluded. Maximum NO_x, NH_4^+ and $Si(OH)_4$ concentrations occurred at the ice-water interface, with two exceptions (NH_4^+ at station 2 and $Si(OH)_4$ at station 1).

Theoretical dilution lines (TDLs) for $Si(OH)_4$, NO_x, and PO_4^{3-} were calculated from under ice seawater measurements at each station (data from Lannuzel et al., this issue). A number of brine nutrient values fell below the TDLs, indicating biological uptake of nutrients (Figure 5A.C.D). NH_4^+ values showed scatter above the TDL, indicating enrichment when compared to pure conservative behaviour with salinity. (Figure 5B).

The molar ratios of total nitrogen (TN; sum of NH_4^+ and NO_x):$Si(OH)_4$ and TN:PO_4^{3-} ranged between 0.12 to 4.04 (mean: 0.72 ± 0.11) and 2.09 to 28.68 (mean: 12.13 ± 1.03), respectively. All bottom ice samples (i.e. 0.00 to 0.02 m above the ice-water interface) were above nutrient ratios calculated for sea-ice diatoms (e.g., Günther et al., 1999), indicating TN was limiting over $Si(OH)_4$ or PO_4^{3-} (Figure 6A-B).

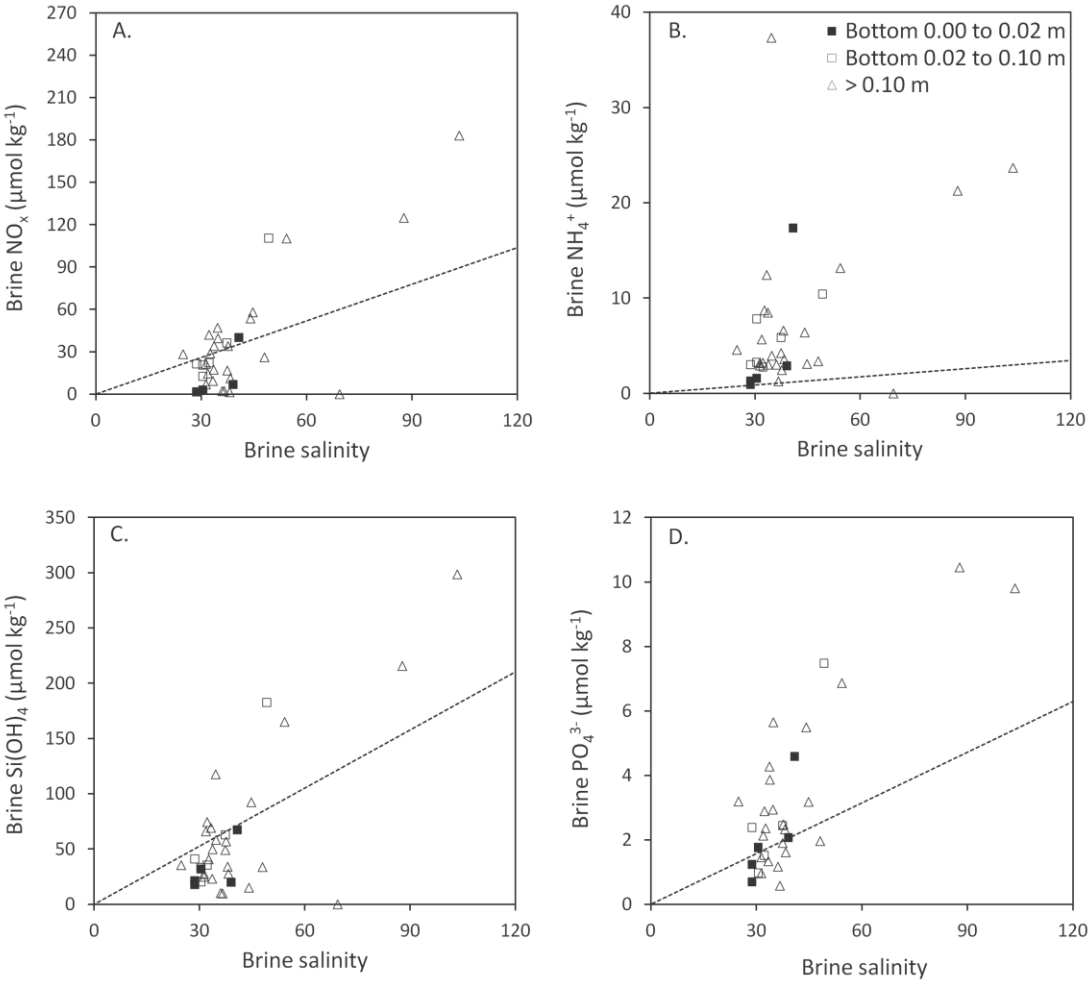

Figure 4.4: Concentrations of calculated dissolved inorganic nutrients within sea-ice brines against brine salinity; NO_x (sum of NO_2^- and NO_3^-; A), NH_4^+ (B), $Si(OH)_4^+$ (C), and dissolved inorganic phosphorous (PO_4^{3-}; D). Solid squares denote samples from 0.00 to 0.02 m above the ice-water interface, transparent squares denote samples from 0.02 to 0.10 m above the ice-water interface, and triangles indicate samples from above 0.10 m the ice-water interface. Dashed lines indicate theoretical dilution lines (TDL), based on seawater nutrient concentrations measured from each station.

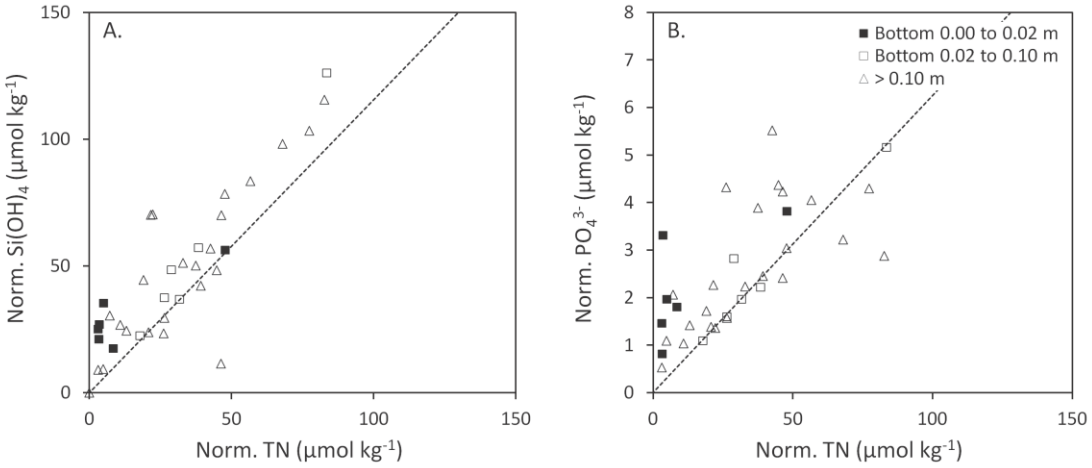

Figure 4.5: Ratios of salinity-normalised total nitrogen (TN; sum of NO_x and NH_4^+) to salinity-normalised $Si(OH)_4^+$ (A), and salinity-normalised TN to salinity-normalised PO_4^{3-} (B). Solid squares denote samples from 0.00 to 0.02 m above the ice-water interface, transparent squares denote samples from 0.02 to 0.10 m above the ice-water interface, and triangles indicate samples from above 0.10 m the ice-water interface. Dashed lines indicate the calculated nutrient ratios, based on N:Si ratio of 16:18.5 and N:P ratio of 16:1 for sea-ice diatoms (e.g. Günther et al., 1999)

4.5.3 Microbial Biomass

Integrated ice core POC and PON concentrations (integrated over the entire ice thickness; n = 6) showed high variation, with POC ranging between 321 and 1083 mg C m^2 (mean: 663 ± 112 mg C m^2) and PON ranging between 35 and 120 mg m^2 (mean: 74 ± 5 mg m^2; Table 1). Median bulk POC concentrations (Figure 2C) varied between stations (Kruskal-Wallis test: p = 0.39), and were significantly correlated with V_b/V (r_s = 0.420, p = 0.011, n = 36), bacterial abundance ($Bact_{Total}$ r_s = 0.398, p = 0.016, n = 36), and chl *a* concentrations (r_s = 0.572, p < 0.001, n = 36). The molar POC:PON ratio (range: 5.3 to 28.8; mean 11.64 ± 0.9) in the

lower most 0.02 m of sea-ice cores averaged 13.4 ± 3.5 (range: 5.3 to 27.0; Figure 2D).

Chl *a* concentrations varied between stations (p = 0.012), and profiles showed maximum concentrations in the sea-ice interior, with two exceptions (station 3 and 6; Figure 2E). Concentrations of chl *a* (range: 0.34 to 195.79 mg m^{-3}, mean: 18.90 ± 6.52 mg m^{-3}) were significantly correlated with bacterial abundance ($Bact_{Total}$ r_s = 0.529, p = 0.001, n = 36). Total algal cell abundance for the lowermost 0.02 m of cores was correlated with chl *a* concentrations (r_s = 0.886, p = 0.019, n = 6), and was dominated by pennate diatoms (Table 2). Dominant species were *Fragilariopsis spp*., *Nitzschia longissima*, and *Entomoneis kjellmanni* (Table 3). *Berkeleya adeliensis* was the dominant species at station 6 and only found at this site (Table 3).

Mean POC:chl *a* ratios were 290 ± 71, ranging between 15 and 2147 (Figure 7A). POC:chl *a* ratios were negatively correlated with bacterial cell abundance ($Bact_{Total}$ r_s = -0.447, p = 0.006, n = 36).

Total bacterial cell abundances varied between 19 and 237 x 10^4 cells ml^{-1} (mean: 76 ± 9 x 10^4 cells ml^{-1}), and profiles of total bacterial cell abundances generally showed lowest concentrations in the sea-ice interior (Figure 2F). Bacterial biomass was dominated by $bact_{Gate3}$ cells (range 44 and 75 %; mean 59 ± 1 %; Figure 8A-D).

Table 4.2: Descriptive statistics of biogeochemical and biological characteristics of bottom ice algal communities sampled from the lowermost 0.02 m of the ice cores. Algal cell counts; total, pennate, centric and flagellate cell counts, chlorophyll *a* (chl *a*), particulate organic carbon (POC), ratios of POC and particulate organic nitrogen (PON; POC:PON), dissolved organic carbon (DOC), ratios of DOC:chl *a* concentrations, total bacterial cell counts ($Bact_{Total}$), and brine-volume fraction (V_b/V).

Variable	Min	Max	Mean	SDERR	n
Total algal counts (x 10^3 l^{-1})	17	1393	310	219	6
Pennate algal counts (x 10^3 l^{-1})	13	1365	294	216	6
Centric algal counts (x 10^3 l^{-1})	2.2	20.8	9.4	3.0	6
Flagellate algal counts (x 10^3 l^{-1})	1.2	21.0	5.9	3.1	6
Chl *a* (mg m^{-3})	0.6	97.9	21.6	15.6	6
POC (mg m^{-3})	449	5109	2101	716	6
POC:PON (molar)	5.3	26.9	13.4	3.5	6
DOC (µmol kg^{-1})	7.5	184.2	84.3	31.2	6
DOC:Chl *a* (mg C[mg chl *a*]$^{-1}$)	22.7	912.7	218.6	140.1	6
$Bact_{Total}$ (x 10^4 cells ml^{-1})	18.6	113.1	35.1	14.3	6
V_b/V (%)	12.5	36.1	26.3	3.7	6

Table 4.3: Relative contribution of dominant algal taxa groups to total algal cell abundance (%) from the lowermost 0.02 m of the ice cores at each station.

	Station #					
Taxa	2	3	4	6	7	8
Fragilariopsis spp.	60.6	66.5	57.0	40.2	80.7	61.9
Berkeleya adeliense	0.0	0.0	0.0	41.7	0.0	0.0
Centric spp.	2.9	1.3	6.0	0.5	3.1	10.7
Flagellate spp.	3.3	2.7	7.3	1.5	1.9	6.7
Nitzschia longissima	12.6	5.4	2.6	0.0	1.9	0.4
Entonomeis kjellmanni	1.3	1.3	2.6	7.7	4.5	1.2
Chaetoceros spp.	1.3	4.9	6.0	0.0	3.0	2.8
Nitzschia stellata	2.9	2.7	4.0	1.0	0.7	2.0
Other taxa	15.1	15.2	14.6	7.4	4.2	14.3

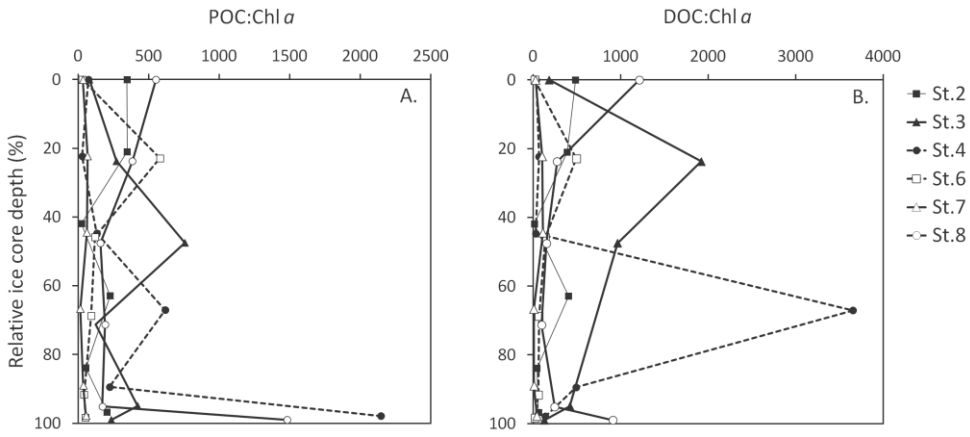

Figure 4.6: Chlorophyll *a* (chl *a*)-normalised particulate organic carbon (POC; A) and chl a-normalised dissolved organic carbon (DOC; B) for the relative ice core depths at each station.

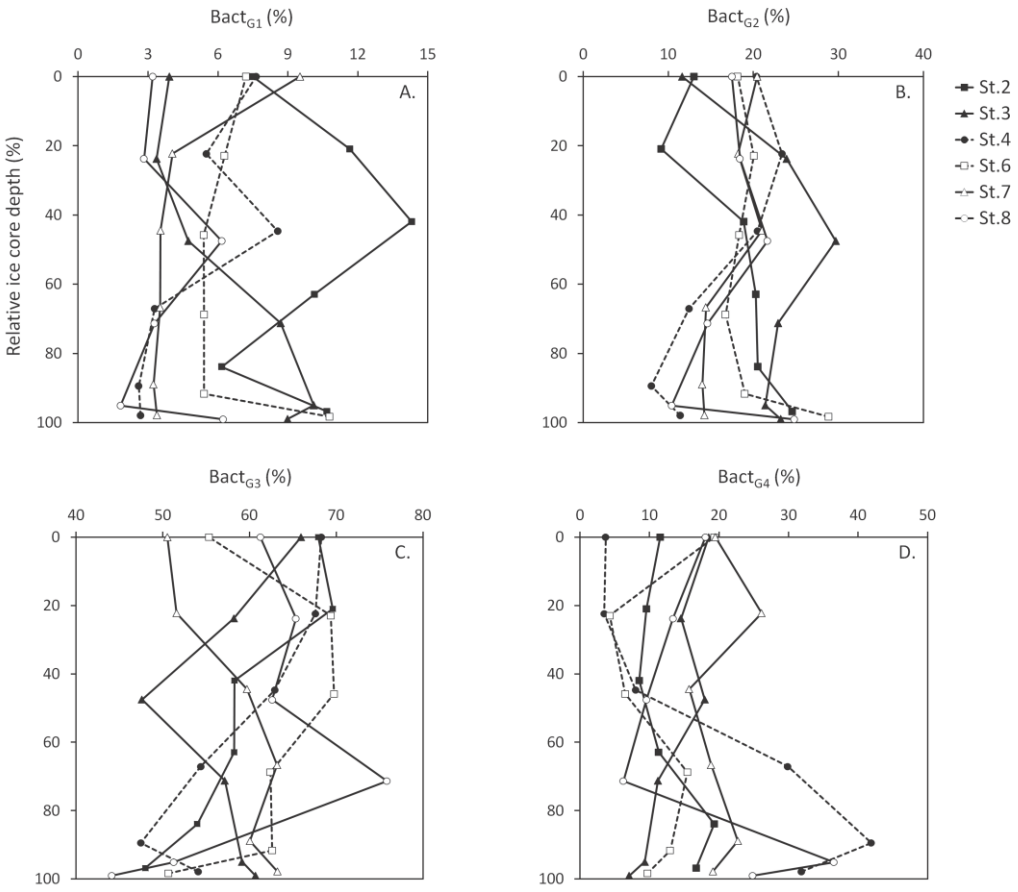

Figure 4.7: Total bacterial abundance and the relative contribution of bacterial abundance in gate 1 ($Bact_{G1}$; A), gate 2 ($Bact_{G2}$; B), gate 3 ($Bact_{G3}$; C), and gate 4 ($Bact_{G4}$; D) for the relative ice core depths at each station.

4.5.4 Dissolved Organic Carbon

DOC concentrations ranged between 7.5 and 184.8 µmol kg^{-1} (mean: 64.4 ± 7.9 µmol kg^{-1}; Figure 9A). One internal ice sample at station 3 was uncharacteristically high and was presumed an outlier (597.2 µmol kg^{-1}). It was therefore excluded.

Brine DOC:POC ratios ranged between 0.06 and 7.02 (mean: 1.34 ± 0.23; Figure 9B). The overall contribution of bulk DOC to total carbon (TC = DOC / DOC +

POC) was 49 ± 3 % (range: 6 to 88 %; Figure 9C). The lowermost 0.02 m of the ice had a mean relative contribution of DOC to TC of 30 ± 9 % (range: 6 to 45 %), with all stations showing a decrease at the ice-water interface, with one exception (station 7).

A TDL for DOC was determined from under-ice water measurements recorded during SIPEX (Norman et al., 2011). Sea-ice DOC values fell above the TDL, indicating enrichment within brine channels (Figure 10).

Bulk DOC:chl *a* ratios varied between stations ($p = 0.022$; range: 10 to 3654; mean: 393 ± 115; Figure 7B), and were negatively correlated with bacterial abundance ($r_s = -0.552$, $p = 0.001$, $n = 36$).

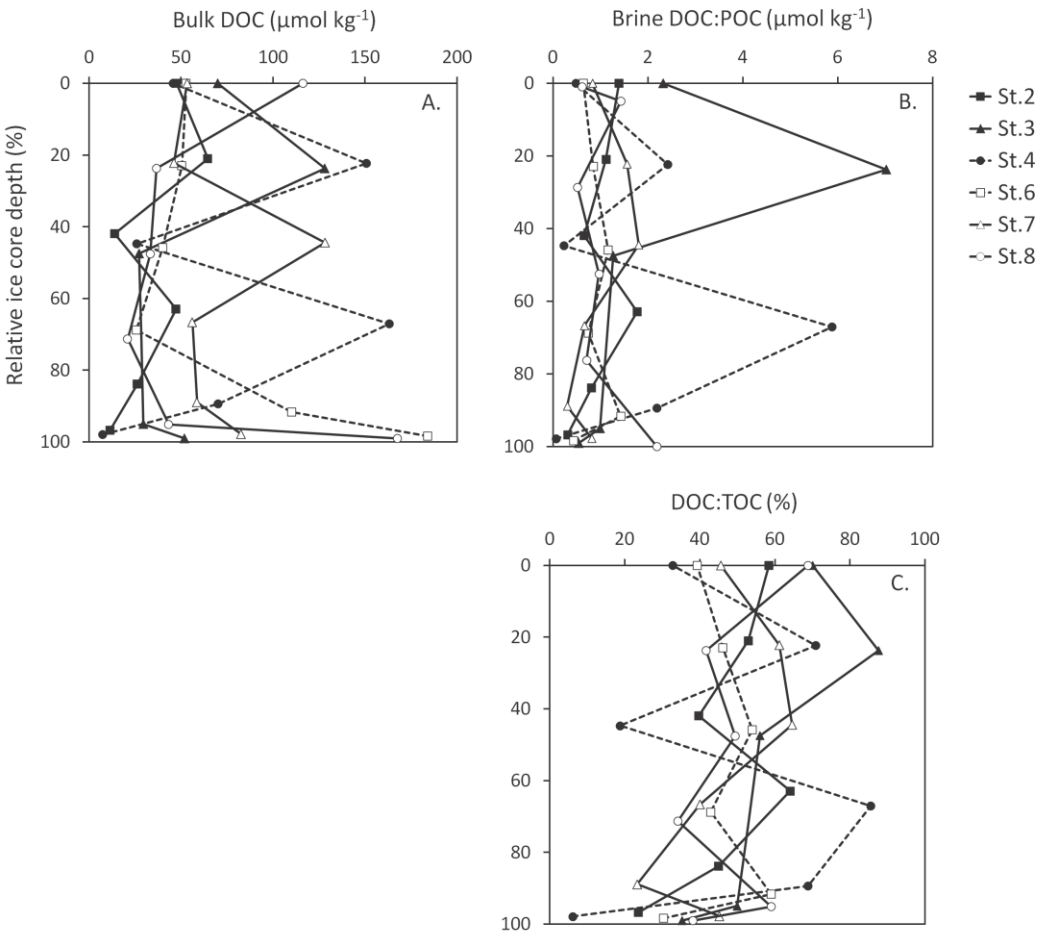

Figure 4.8: Concentrations of dissolved organic carbon (DOC, A), ratios of DOC to particulate organic carbon (POC; DOC:POC), and the relative contribution of DOC to total carbon (TC = DOC / DOC + POC) for the relative ice core depths at each station.

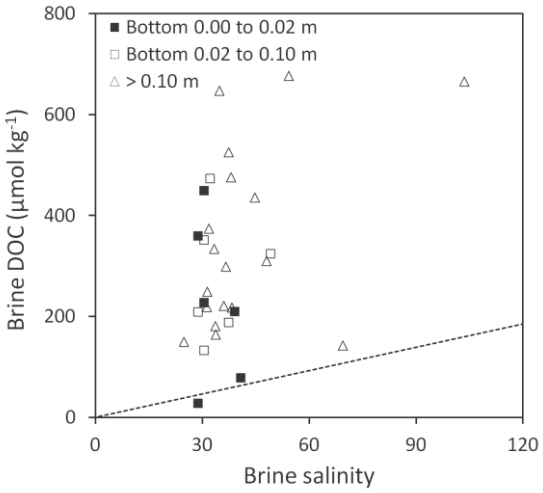

Figure 4.9: Calculated DOC within sea-ice brine against brine salinity. Solid squares denote samples from 0.00 to 0.02 m above the ice-water interface, transparent squares denote samples from 0.02 to 0.10 m above the ice-water interface, and triangles inidcate samples from above 0.10 m the ice-water interface. Dashed line indicates the theoretical dilution line (TDL), based on seawater DOC concentrations measured during SIPEX voyage (2007; Norman et al., 2011).

4.5.5 Bottom Ice Algal Primary Production and Carbon Allocation

Ice algal production (mg C m^{-2} d^{-1}) and productivity (mg C (mg chl *a*)$^{-1}$ d^{-1}), and subsequent carbon allocation, were determined from bottom sections of ice cores sampled at all stations (< 0.02 m of ice floes). A summary of bottom ice biogeochemical/biological descriptive statistics at the ice-water interface is given in Table 2. Tables 4 and 5 give model outputs and primary production/carbon allocation, respectively. Ice algal production ranged from << 0.01 to 3.03 mg C m^{-2} d^{-1} (mean: 0.78 ± 0.58 mg C m^{-2} d^{-1}), excluding a negative production value recorded at station 4. ^{14}C-TPP ranged from < 0.001 to 2.218 mg C (mg chl *a*)$^{-1}$ d^{-1} (mean: 0.892 ± 0.489 mg C (mg chl *a*)$^{-1}$ d^{-1}), excluding station 4. The relative contribution of ^{14}C-TEOC to ^{14}C-TPP decreased over the observational period,

ranging from 44 % (station 1) to 21 % (station 8; mean: 38 ± 4 %). The remaining contribution to ^{14}C-TPP constituted an increase in ^{14}C-POC over the observational period (Table 5; Figure 11A).

^{14}C-TEOC constituted carbon fractions of ^{14}C-COLLOC and ^{14}C-EDOC only, with ^{14}C-EPS not detected at any station (Table 5; Figure 11B). The relative contribution of ^{14}C-EDOC varied between stations, ranging from 2 to 99 % of ^{14}C-TEOC (mean: 55 ± 18%). Carbon isotope fractionation did not show any correlations with other measured parameters.

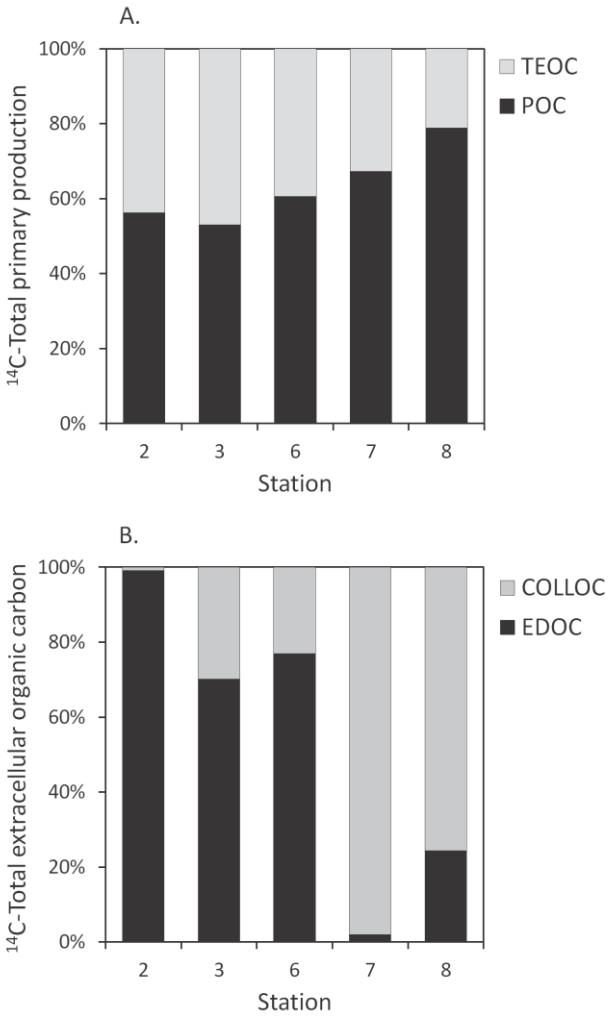

Figure 4.10: ^{14}C-total primary production fractions of ^{14}C-total extracellular organic carbon (TEOC) and ^{14}C-particulate organic carbon (POC, A), and ^{14}C-TEOC fractions of ^{14}C- colloidal organic carbon (COLLOC) and ^{14}C- extracellular dissolved organic carbon (EDOC, B) at each station, exluding station 4.

Table 4.4: Bottom ice (lowermost 0.02 m) photosynthesis-irradiance (P-E) modelling outputs. Station number (#), snow depth (z_s), ice depth (z_i), maximum incoming irradiance measured from onboard sensors (I_o), calculated irradiance incident at the bottom of the ice (I_z; mean and maximum), the sea-ice algal photosynthetic modelling outputs of maximum photosynthetic rates (Pmax), initial slope of the light-limited section of the P-E curve (α), rates of photoinhibition (β), intercept of the P-E curve with the carbon uptake axis (c), light intensity at which carbon-uptake became saturated (E_k), and R^2 value.

#	z_s	z_i	I_o	$I_{z\,(mean)}$	$I_{z\,(max)}$	Pmax	α	β	C	Ek	R^2
	m		µmol m^{-2} s^{-1}			mg C(mg chl *a*)$^{-1}$ h^{-1}				µmol m^{-2} s^{-1}	
2	0.062	0.612	50.406	8.832	35.074	0.178	0.0245	0.0089	0.009	7.26	0.98
3	0.664	1.975	68.699	0.002	0.008	0.022	0.0012	0.0000	0.001	17.88	0.69
4	0.630	0.935	55.147	0.017	0.056	0.131	0.0033	0.0005	-0.038	40.16	0.70
6	0.137	1.190	58.169	1.673	7.244	0.033	0.0039	0.0002	0.000	8.49	0.93
7	0.364	0.890	73.091	0.367	1.206	2.174	0.2683	0.0027	-0.001	8.10	0.94
8	0.512	2.030	100.953	0.014	0.047	0.168	0.0110	0.0001	0.007	15.32	0.69

Table 4.5: Bottom ice (lowermost 0.02 m) production and carbon allocation into various fractions. Station number (#), bottom ice ^{14}C-total primary productivity (^{14}C-TPP), integrated chlorophyll *a* (chl *a*) concentrations measured using HPLC, rates of ^{14}C-production, and carbon allocation fractions of total extracellular organic carbon [^{14}C-TEOC; mean ± STDERR (% of ^{14}C-TPP)], particulate organic carbon [^{14}C-POC; mean ± STDERR (% of ^{14}C-TPP)], extracellular organic carbon [^{14}C-EDOC; mean ± STDERR (% of ^{14}C-TPP)], and colloidal organic carbon [^{14}C-COLLOC; mean ± STDERR (% of ^{14}C-TPP)]. bd = below detection.

#	^{14}C-Productivity	Chl *a*	^{14}C-Production	^{14}C-TEOC		^{14}C-POC		^{14}C-EDOC		^{14}C-COLLOC	
	mg C(mg chl *a*)$^{-1}$ d^{-1}	mg chl *a* m^{-2}	mg C m^{-2} d^{-1}	mg C(mg chl *a*)$^{-1}$ d^{-1}							
2	1.949	0.069	0.135	0.854 ± 0.068	(44 %)	1.095 ± 0.068	(56 %)	0.846 ± 0.075	(43 %)	0.008 ± 0.008	(< 1 %)
3	5.561 x 10^{-5}	0.099	0.524 x 10^{-5}	2.616 ± 0.559 x 10^{-5}	(47 %)	2.946 ± 0.559 x 10^{-5}	(53 %)	1.835 ± 0.378 x 10^{-5}	(33 %)	0.781 ± 0.182 x 10^{-5}	(14 %)
4	-0.912	0.043	-0.040	bd		bd		bd		bd	
6	0.130	5.647	0.732	0.051 ± 0.003	(39 %)	0.079 ± 0.003	(61 %)	0.039 ± 0.005	(30 %)	0.012 ± 0.003	(9 %)
7	2.218	1.368	3.034	0.725 ± 0.040	(33 %)	1.492 ± 0.040	(67 %)	0.014 ± 0.007	(1 %)	0.711 ± 0.039	(32 %)
8	0.165	0.045	0.007	0.035 ± 0.004	(21 %)	0.130 ± 0.004	(79 %)	0.008 ± 0.003	(5 %)	0.026 ± 0.004	(16 %)

4.6 DISCUSSION

The aim of the current study was to determine the relationships between physical, biogeochemical, and photophysiological parameters of East Antarctic pack ice during the winter-spring transition. It quantified bottom ice ^{14}C-total primary productivity (^{14}C-TPP), and subsequent allocation into carbon fractions (particulate organic carbon [^{14}C-POC], colloidal organic carbon [^{14}C-COLLOC], extracellular dissolved organic carbon [^{14}C-EDOC], and extracellular polymeric substances [^{14}C-EPS]).

4.6.1 Ice Characteristics

Physical ice floe characteristics reflected the regionally variable conditions (Table 1). Sea-ice thickness (range: 0.80 to 2.16 m) and snow depth (range: 0.06 to 0.66 m) were high compared to other research programs; e.g. East Antarctic pack ice during September - October (ice thickness range: 0.59 to 2.22 m; snow depth mean: 0.02 to 0.22 m; Worby et al., 2011), and Antarctic sea-ice generally (ice thickness range: 0.59 to 0.78 m; snow depth range: 0.12 to 0.13 m; Worby et al., 2008). Extremes in pack ice thickness are rarely sampled as thinner ice (ca. 0.5 m) can be unsafe to gain sampling access and thick ice ridges prevent ship access and are difficult to sample (Worby et al., 2011). Therefore, current average values of sea-ice parameters are not necessarily representative of overall pack ice characteristics (e.g. Meiners et al., 2012).

Sea ice typically consists of two horizontally stratified layers; granular and columnar ice (e.g. Eicken and Lange, 1989). Granular ice formation is a result of dynamic ice growth, consisting of randomly oriented, fine-grained crystals which

are formed by turbulent mixing of surface waters, capable of scavenging high concentrations of particulate organic matter during formation (Garrison et al., 1990). This contrasts with columnar ice which forms under calm conditions, and may reject particles during initial growth (Weissenberger and Grossmann, 1998). This suggests that ice type is an important factor determining biological assemblages (Scott et al., 199). In the current study there was no statistical difference in chl *a* and POC concentrations between granular and columnar ice (Figure 3), which is consistent with other pack ice studies off East Antarctica (e.g. Becquevort et al., 2009; Meiners et al., 2011). This may indicate that phytoplankton and POC concentrations of the surrounding water, during ice formation and growth, were low.

In the current study, heavy snow loading was identified as a key factor affecting sea ice physical properties, in particular temperature profiles. Station 2, which had the lowest snow loading (mean snow depth: 0.06 m), was the only station to exhibit a strong linear profile with temperatures increasing with depth. (Figure 1). All other stations had heavy snow loading (mean snow depth: 0.46 m) and warm ice interiors with weak temperature profiles. At thermal equilibrium, the temperature profiles were linear, with temperatures at the ice-water interface at freezing point and the upper ice surface near atmospheric temperature (Maykut, 1986). The ice interior can be warmed and temperature profiles minimalised through conductive heat fluxes from the relatively warm seawater in comparison to the cool atmosphere. A warm interior may also reflect a thermal adjustment to a previous surface temperature. This influence can be exaggerated by the addition of heavy snow loading, capable of providing an insulative layer between the ice

surface and the atmosphere. Heavy snow loading can also depress ice, causing surface flooding and increasing the ice surface temperature with warm seawater (Fritsen et al., 1994; Massom et al., 2001). Snow-covered sea ice rarely exhibits a simple linear vertical temperature gradient (Arrigo et al., 2014).

Brine volumes across all sea-ice stations were highest at the ice-water interface (mean: 26 %) compared with values > 0.1 m above the ice-water interface (mean: 11 %; Figure 2B). While sea-ice temperature and brine salinity are co-dependent, V_b/V is a function of temperature and bulk-ice salinity. At a bulk salinity of 5 and a temperature of - 5 °C, sea ice has a theoretical V_b/V of only 5 % and this is considered to be the threshold for brine percolation in columnar ice (Golden et al., 1998). In the current study, 78 % of ice sampled was granular ice, which has a higher theoretical percolation threshold than columnar ice due to a more random distribution of brine inclusions (Golden et al., 1998, 2007). The very high brine-volume fraction of most of the ice sampled indicates that the sea-ice algal community had access to resupplied nutrients from under-ice seawater (Tison et al., 2008; Vancoppenolle et al., 2010).

4.6.2 Chemical Parameters

Inorganic nutrient concentrations in the brine showed wide variations, although they were within expected concentrations for East Antarctic pack ice (Becquevort et al., 2009; Meiners et al., 2011; Figure 5A–D). Concentrations within brine channels are a function of initial concentrations trapped within the sea ice during formation, brine percolation, autotrophic drawdown, and heterotrophic remineralisation (Gleitz et al., 1995; Lannuzel et al., 2008; Meiners et al., 2009;

Papadimitriou et al., 2007; Thomas and Dieckman, 2010; Vancoppenolle et al., 2010). Molar POC:PON ratios are indicative of a response to nutrient availability, with values over 7.7 generally considered to reflect nitrogen limitation (Redfield et al., 1963). Measured values in the current study (mean: 11.6 ± 0.9; range: 5.3 to 28.9) exceeded this threshold, and may indicate that the algal community was experiencing nitrogen limitation at the time of sampling (Figure 2D). POC:PON ratios were comparable to previous studies; McMinn et al. (1999; 6.5 to 8.5), Cota and Sullivan (1990; 8.8 to 16), and Lizotte and Sullivan (1992; 7.8 to 14.6). Roukaerts et al. (this issue) also reported high POC:PON values for the sea-ice interior recorded during SIPEX-2. Unlike other studies (e.g. McMinn et al., 1999), the POC:PON ratios showed significant vertical trends. The high POC:PON ratios observed, may also be the result of colloidal or cell-associated extracellular organic carbon trapped on the filters during sampling, heterotrophic biomass, and detrital material accumulated in the sea ice.

When physical processes alone control nutrient concentrations, they behave predictably and should follow theoretical dilution lines (TDLs, Gleitz et al., 1995; Granskog et al., 2003). Dissolved NO_x, NH_4^+, $Si(OH)_4$ and PO_4^{3-} showed positive (indicating remineralisation) and negative (indicating nutrient uptake) values in relation to TDLs, with more negative values for ice sections < 0.10 m above the ice-water interface. This indicated nutrient drawdown through biological uptake in the bottom sections of the sea ice. In comparison to the TDL, NH_4^+ was predominantly enriched in ice core sections. Elevated NH_4^+ in sea-ice brines has been associated with heterotrophic nitrogen remineralisation and grazing activity (Schnack-Schiel et al., 2004). In conclusion, nutrient concentrations within the

brine channel system were driven by a combination of physical nutrient replenishment, ice algal uptake and heterotrophic remineralisation.

Comparison of dissolved nutrient ratios and elemental ratios reported for sea-ice diatoms (Günther et al., 1999) showed some scatter. Total nitrogen (TN; sum of NO_x and NH_4^+) was generally depleted, though modestly in comparison to $Si(OH)_4$ and PO_4^{3-} (Figure 6A–B). However, values generally aligned with elemental ratios, indicating that the brine microbial community was mostly experiencing balanced nutrient growth, and was not heavily nitrogen limited at the time of sampling. This observation was further supported by sea-ice brine concentrations with TN (range: 3.1 to 83.5; mean: 31.3) being higher than the average nitrogen half-saturation constant reported for oceanic phytoplankton ($K_s(N)$ = 1.6 ± 1.9 µmol kg^{-1}; Sarthou et al., 2005).

4.6.3 Microbial Biomass

Integrated sea-ice algal biomass varied between 3 and 30 mg chl *a* m^{-2} (mean: 13 ± 2 mg chl *a* m^{-2}) and was within ranges reported by other studies; 2 – 23 mg chl *a* m^{-2} along the Western Antarctic Peninsula (August/September; Kottmeier and Sullivan, 1987), and 1 – 14 mg chl *a* m^{-2} in East Antarctica (September/October, Meiners et al., 2011). Collations of large biological datasets provide further comparisons. Ice algal biomass values measured in this study were consistent with values reported in Dieckmann et al. (1998), McMinn et al. (2007) and Meiners et al., 2012.

Highest algal biomass was generally located at the surface or interior of ice cores. The large ice thickness (range: 0.80 to 2.16 m) indicated that the ice was relatively old and deformed, which presumably would have allowed sufficient time for a bottom ice community to accumulate. This also meant that there was more time for a heavy snow load to develop (snow thickness range: 0.06 to 0.66 m) which was capable of depressing the surface of the ice. Subsequent flooding enabled the development of surface algal communities. High ice thickness, snow cover, and the development of surface algal communities caused significant attenuation of down welling light to the bottom ice algal community, thus restricting their growth. This finding is important as the distribution of algae within ice is critical for zooplankton grazers and other invertebrates that rely on this food resource. While some crustaceans and protozoa are able to graze on biomass within the brine channels, most of the algal biomass is only available to higher trophic levels if it is present on the bottom of the ice or once the ice melts. However, some studies have shown that bottom ice communities may be absent, or insignificant. Therefore, the bottom ice algal community may be inconsequential to total chl *a* standing stocks (Arrigo et al., 1998b; Legendre et al., 1992). In contrast, Grose and McMinn (2003) showed that bottom communities dominated in East Antarctica, contributing an average of 76 % of total production. This was supported by McMinn et al. (2007) who reported that 44 % of total algal biomass was located in the bottom 0.01 m of ice. In the current study, 21 % of total algal biomass was located in the bottom 0.01 m of ice (7 % in the bottom 0.002 m). This infers that during SIPEX-2, the lower pack ice layers harboured ecologically significant microbial concentrations, despite being clearly dominated by internal and surface communities.

The bottom ice algal community in the current study was dominated by pennate diatoms, such as *Fragilariopsis* spp.. Dominant diatoms species observed were consistent with previous studies on East Antarctic pack ice (e.g. Scott et al., 1994; McMinn et al., 2007; Meiners et al., 2011). The POC:chl *a* ratio (mean: 212 ± 46; Figure 7A) was comparable to other studies in the Amundsen Sea (mean: 214 ± 191; Arrigo et al., 2014) and the Weddell Sea (mean: 284 ± 351; Kennedy et al., 2002). However, values were lower than previously recorded in East Antarctic pack ice (mean: 400 ± 113; Meiners et al., 2011).

Bulk ice DOC concentrations (range: 8 to 184 µmol kg^{-1}; mean: 64 µmol kg^{-1}; Figure 9A) were considerably lower than other surveys; in East Antarctica (range: 17 – 812 µmol kg^{-1}; mean: 105 µmol kg^{-1}; Norman et al., 2011), in the Weddell Sea during winter (range: 1500 – 1950 µmol kg^{-1}; mean: 110 µmol kg^{-1}; Lemke, 2009) and in the Western Weddell Sea during spring (range: 50 to 393 µmol kg^{-1}; mean: 118 µmol kg^{-1}; Hellmer et al., 2008). However, based on the TDL (calculated from mean under ice DOC concentrations; Norman et al., 2011), brine channel DOC concentrations were enriched (Figure 10). The overall relative contribution of DOC to total carbon (TC = DOC / DOC + POC; 48 %, Figure 10C) was comparable to previous observations; 50 % for bulk ice (56 % for seawater) in East Antarctica (Norman et al., 2011), 27 % for bulk ice (93 % for seawater) in Weddell Sea during spring (Hellmer et al., 2008), and 36 % in Weddell Sea during winter (Lemke, 2009). In the current study in the lowermost 0.02 m of the ice, 33 % of the TC was DOC compared with 29 % ^{14}C-EDOC to ^{14}C-TPP (i.e. productivity). This implies that algal-exudation of DOC may be

equivalent to DOC loss, either through loss to the underlying seawater through brine drainage or carbon remineralisation by heterotrophs. Both are evident in the current study, but the latter may be the more dominant process given that both DOC and NH_4^+ showed positive deviations from TDLs, suggesting heterotrophic activity.

In the current study, there was no correlation between DOC and POC or PON (overall mean ratio: 1.3; Figure 9B) and this was also observed by Lannuzel et al. (this issue). In East Antarctica during SIPEX, a correlation between DOC and POC was reported, and this may have indicated algal exudation of DOC (van der Merwe et al., 2009). The lack of correlation in the current study may have been the result of low biomass and exudate concentrations.

Interest in sea-ice DOC has highlighted a potential microbial loop between bacteria and algal-derived exudates (e.g. Giesenhagen et al., 1999; Martin et al., 2009, 2011). That is, the bacterial assimilation of exudates may provide the algal community with a source of remineralised vitamins and/or nutrients, similar to that observed in temperate oceanic systems (Azam et al., 1991; Smith et al., 1995). In the current study, a positive correlation between algal biomass and bacteria ($p < 0.001$) implied the presence of an active microbial loop at the time of sampling. However, there was no association between DOC and bacterial abundance. This observation is consistent with other findings (e.g. Meiners et al., 2004; Ugalde et al., 2014) and may be due to the low microbial biomass measured in the current study, or bacteria utilising particulate (e.g. colloidal organic carbon

or transparent exopolymer particles; Meiners et al., 2008), rather than dissolved material.

The separation of bacterial populations based on DNA content has been used to describe communities based on phylogentics (Bouvier et al., 2007; $Bact_{Gate\ 1}$ = high nucleic acid (HNA) content, $Bact_{Gate\ 4}$ = low nucleic acid (LNA) content; Figure 8A–D). In the current study, the bacterial gating was not correlated with any measured parameters, leaving the factors influencing bacterial community composition undetermined.

4.6.4 Bottom Ice Primary Production

There have been limited direct measurements of primary production in Antarctic pack ice. In the current study, bottom ice ^{14}C-production (mean: 0.78 ± 0.58 mg C m^{-2} d^{-1}; Table 5) was broadly comparable to other pack ice studies; Mock (2002) reported autumn production rates of 0.27 mg C m^{-2} d^{-1} in young (< 0.4 m ice thickness) sea ice. McMinn and Hegseth (2003) reported much higher values for Prydz Bay bottom ice during spring. In Eastern Antarctica over three years (2002 – 2004), McMinn et al. (2007) reported considerably higher daily spring production rates for bottom ice communities (mean: 51 mg C m^{-2} d^{-1}), although this was associated with high chl *a* concentrations (mean: 2.20 mg m^{-2} for 2004) and thin ice (0.63 m for 2004). Ice algal primary production in the early season is influenced by low algal biomass and irradiance. In the current study, light availability at the ice-water interface was low due to thick ice coupled with heavy snow loading. Importantly, there would have been attenuation of light from internal and surface microbial communities (93 % of algal biomass > 0.02 m

above the ice-water interface) and temperature-driven optical backscattering (Buckley and Trodahl, 1987) not accounted for in the calculated irradiance incident at the bottom of the ice, possibly resulting in an overestimation of reported production rates

In the current study, station 4 exhibited negative production (-0.04 mg C m^{-2} d^{-1}). Low chl *a* values (0.03 mg m^{-2}) likely reduced the accuracy and precision of the modelling output (R^2 = 0.70; Figure 5). In addition, a considerable proportion of ^{14}C that was incorporated into the photosynthetic cells was exuded as organic material, and bacteria were able to utilise this carbon source. While no antibiotic treatment was applied during the P-E incubations, antibiotics were used during the ^{14}C incubations in the carbon allocation experiments (e.g. Goto et al., 1999; Ugalde et al., 2013).

^{14}C-TPP values determined in the current study (mean: 0.89 ± 0.49 mg C (mg chl *a*)$^{-1}$ d^{-1}; Table 5) were significantly lower than previous studies; 0.03 and 0.73 mg C (mg chl *a*)$^{-1}$ h^{-1} in Eastern Antarctica for the lowermost 0.05 m of ice (McMinn and Hegseth, 2003), and 0.02 and 1.2 mg C (mg chl *a*)$^{-1}$ h^{-1} in the Weddell Sea for the lowermost 0.30 m of ice (Mock, 2002). This suggested that the photosynthetic cells were predominantly restricted by light availability (e.g. McMinn et al., 2007), and the high variations between stations reflected the patchy and dynamic pack ice environment.

Modelled E_k values may be an indicator of photoacclimation (Sakshaug et al., 1997). Therefore, the incident irradiance available to cells should theoretically be

reflected in the calculated E_k values. However, since irradiance fluctuates and acclimation takes some time, E_k is constantly changing and rarely matches the instantaneous irradiance (Sakshaug et al., 1997). In the current study, calculated E_k values (mean: 16.20 µmol m^{-2} s^{-1}; Table 4) were much higher than irradiances available to bottom ice communities (maximum mean: 7.27 µmol m^{-2} s^{-1}; mean: 1.82 µmol m^{-2} s^{-1}). High E_k values have been previously observed in other studies (e.g. Meiners et al., 2009; McMinn et al., 1999), and indicate that the algal communities were capable of photosynthesising at much higher rates than those experienced by the cells during the time of sampling.

4.6.5 Bottom Ice Carbon Allocation

Bottom ice photosynthetic communities (i.e. lowermost 0.02 m of the ice) contributed a significant proportion of their fixed carbon to extracellular organic products (range: 21 to 47 % of ^{14}C-TPP; mean 38 ± 4 %; Figure 11A; Table 5). Values were within the expected range, despite a considerable increase over the sampling period. Ugalde et al. (2013) reported an allocation of 36 % of ^{14}C-TPP into ^{14}C-TEOC during the lag phase for a common sea-ice diatom (*Fragilariopsis cylindrus*), increasing to 72 % in the stationary phase. Goto et al. (1999) reported a mean allocation of 22 % of ^{14}C-TPP into ^{14}C-TEOC during the exponential phase for microphytobenthos, increasing to 51 % in the stationary phase. This infers that the growth status of a photosynthetic community is a primary driver in determining carbon allocation to extracellular material.

The composition of ^{14}C-TEOC indicated that there were two low molecular weight (LMW) carbon pools present; extracellular dissolved organic carbon (^{14}C-

EDOC) and colloidal or cell-associated organic carbon (^{14}C-COLLOC; Figure 11B; Table 5). Neither pool contained high-molecular weight (HMW) material, defined as extracellular polymeric substances (^{14}C-EPS). When compared with ^{14}C-EPS, LMW material may have less biochemical potential due to lower structural complexity of exuded molecules. In the current study, allocation to ^{14}C-EDOC may reflect the seasonal microbial growth cycle, in which the algal community limits growth during winter by varying their contribution to intra- (i.e. particulate organic carbon) and extracellular organic material. Specifically, the photosynthetic cells pass simple carbohydrates (or possibly other molecules, such as proteins) across their cell walls, and therefore, are able to effectively lag their growth rate during the colder months. This is described as 'overflow metabolism', a well-established mechanism which has rarely been applied to the sea-ice habitat (Myklestad et al., 1989; Staats et al., 2000).

In the current study, increased allocation to bottom ice ^{14}C-COLLOC towards the end of the sampling period (stations 7 and 8; Figure 11B; Table 5) may indicate pre-bloom conditions, in which the photosynthetic community prepares for elevated spring growth. Photosynthesis within the confines of a brine channel can induce adverse physicochemical changes, such as depleted CO_2, elevated pH and nutrient limitation (Gleitz et al., 1995; Krembs and Deming, 2008; Krembs et al., 2002, 2011; Underwood et al., 2004). Extracellular cell-associated organic carbon may act as a buffer against such changes. The COLLOC fraction is typically caught on a GF/F filter during sampling, and hence is quantified as a contribution to POC. This suggests that previous studies may have underestimated the contribution of sea-ice algae to extracellular material.

Attempts to isolate ^{14}C-EPS (HMW material) from both ^{14}C-EDOC and ^{14}C-COLLOC by precipitating in 70 % ethanol produced negligible quantities. However, other studies have identified large quantities of HMW material in Antarctic sea ice during the spring-summer transition; Underwood et al. (2010) reported that high molecular weight EPS (precipitated in 70 % ethanol) contributed 23 % of EDOC in Antarctic ice brine, and Ugalde et al. (2014) reported polysaccharides contributed 68 % of EDOC in Antarctic bottom ice. The lack of ^{14}C-EPS was not unexpected, as exudation is known to increase with adverse physicochemical conditions, such as nutrient drawdown, CO_2 limitation, low temperatures, and salinity (Decho, 1990; Smith and Underwood, 2000; Staats et al., 2000; Ugalde et al., 2013). In the current study, there was limited indication of these physicochemical limitations capable of inducing significant cellular stress. Negligible EPS production indicated either that the photosynthetic community was not exuding EPS (e.g. exudation may be species-specific, or only occurs during particular circumstances), or that the rate of exudation was below detection limits for the applied methods. A similar observation was also reported by Ugalde et al. (2013), where ^{14}C-EPS exudation was undetectable for *Fragilariopsis cylindrus* during the lag phase, increasing to 5.7 % of ^{14}C-TEOC during the senescent phase.

4.7 CONCLUSION

The data collected in the current study over a one month period showed high spatiotemporal variation which is characteristic of pack ice. The sea-ice interior

was generally warm with weak temperature gradients, due predominantly to heavy snow loading, which provided an insulating surface layer and depressed floes. The ice texture was stratified and dominated by granular ice. Brine-volume fractions (V_b/V) were above the theoretical threshold of 5 % (Golden et al., 1998) allowing brine percolation and the resupply of nutrients from the underlying seawater, particularly close to the ice-water interface. There was partial evidence for brine nutrient limitation (NO_x, $Si(OH)_4$ and PO_4^{3-}), however NH_4^+ was enriched. Overall algal biomass was low, and highest concentrations were located in the ice interior or surface which was supported by warm temperatures and increased light. Rates of bottom ice (lowermost 0.02 m) primary productivity were broadly comparable to other studies, although low biomass resulted in extremely low production. The microbial community allocated considerable amounts of photosynthetically-derived organic carbon to extracellular organic carbon components, constituting low molecular weight material, either dissolved or cell-associated/colloidal. Exudation of high molecular weight material (i.e. extracellular polymeric substances) was not detected. The observed patterns in organic carbon allocation inferred that the photosynthetic community was effectively lagging their growth prior to the onset of spring, supportive of pre-bloom conditions.

4.8 ACKNOWLEDGEMENTS

We are thankful to Captain M. Doyle, and the officers and crew of *RSV Aurora Australis* for their outstanding support during the SIPEX-2 voyage (2012/13 VMS). We are grateful to the assistance provided by the voyage leader (A. Cianchi) and deputy voyage leader (B. Free) in the lead-up and during the voyage. We acknowledge the expert help of the AAD Science Technical Support team and colleagues working with us in the field or laboratories. This work was supported by the Australian Government's Cooperative Research Centre Program through the Antarctic Climate and Ecosystems Cooperative Research Centre (ACE CRC) and through the Australian Antarctic Science grant #4073.

CHAPTER 5

Consolidation

The aim of the thesis was to examine and quantify primary production and subsequent carbon allocation of Antarctic sea ice algae. This was achieved by integrating three independent studies; *in vitro* study (Chapter 2), *in vivo* study (Chapter 3), and ecosystem study (Chapter 4). Each chapter described alternative approaches to the thesis aim, and the key findings of each can be found at the conclusion section at the end of each chapter. This final chapter consolidates the studies to provide new information and understandings of sea ice algal allocation of carbon into specified intra- and extracellular organic carbon pools, and how this relates to microbial growth dynamics and responses to physicochemical change.

Microbes, predominantly photosynthetic algae, existing within the sea ice brine channel system can reach high standing stocks (Arrigo et al. 2010). But prolonged photosynthetic activity within the confines of brine channels can alter the biogeochemical properties of the liquid inclusions; depletion of CO_2, increased pH, reduced nutrient availability, high ammonia concentrations, and high concentrations of dissolved organic matter (Gleitz et al. 1995; Thomas and

Dieckman 2010). These alterations have the potential to adversely affect primary production and cell metabolism. Therefore, microbial survival and functioning would require a complex suite of physiological and metabolic adaptations which would not only allow them to survive, but thrive, within such biogeochemical extremes.

The thesis demonstrated that exudation of photosynthetically-derived carbon is an adaptive mechanism employed by sea ice algae to allow them to manage adverse conditions. Four key findings are discussed in turn:

1. Sea ice algae adjust allocation between intra- and extracellular organic carbon,
2. Exuded carbon composition varies in response to adverse conditions,
3. Exuded carbon composition has varying benefits to the producer organism, and
4. Current research underestimates ecological significance of extracellular carbon.

Key Finding 1: Sea ice algae adjust allocation between intra- and extracellular organic carbon

Within the thesis, two approaches were used to quantify sea ice algal carbon allocation into intra- (i.e. biomass) and extracellular pools; quantifying *concentration* and *production*. The majority of research endeavours to quantify the *concentration* of microbial biomass (e.g. particulate organic carbon, chlorophyll *a* concentrations) and dissolved organic carbon, and these are used as

proxies of intra- and extracellular organic carbon, respectively (Chapter 3). The thesis also quantified *production* by applying ^{14}C-methods to provide, for the first time, insight into real-time carbon allocation and functional responses to the surrounding physico-biogeochemical conditions (Chapter 2, 4).

The modified ^{14}C-methods showed that photosynthetic algae purposely vary allocation between intra- and extracellular organic carbon pools (range: 33 – 69 % of photosynthetically-derived carbon exuded, Chapter 2). Allocation into exuded organic carbon was highest during times of adverse conditions, such as challenging biochemical (Chapter 2; e.g. carbonate chemistry) and physicochemical conditions (Chapter 4; e.g. snow and ice thickness). With the onset of improved conditions in spring, photosynthetic algae may reduce exudation of organic carbon, thereby allowing for increased capacity and resources for microbial growth and cell maintenance (Chapter 4).

Key finding 2: Exuded carbon composition varies in response to adverse conditions

The thesis isolated three extracellular organic carbon pools; extracellular dissolved organic carbon (EDOC or DOC), colloidal organic carbon (COLLOC), and extracellular polymeric substances (EPS; Figure 5.1). These pools were isolated by a series of filtration and dissolution/precipitation steps, making isolation simple and accurate to reproduce (standard error between replicates typically < 5 %, Chapter 4).

The thesis clearly demonstrated through the use of isolates, that sea ice alga varies the composition of extracellular organic carbon in response to surrounding conditions (Chapter 2, 3, 4). The observed magnitude of changes in extracellular allocation indicated that each isolate imparts different ecological roles and/or benefits to the producer organism. While this in itself is an important finding, major questions still remain relating to the molecular composition and physiological triggers that induce the different synthetic pathways within the producer organisms.

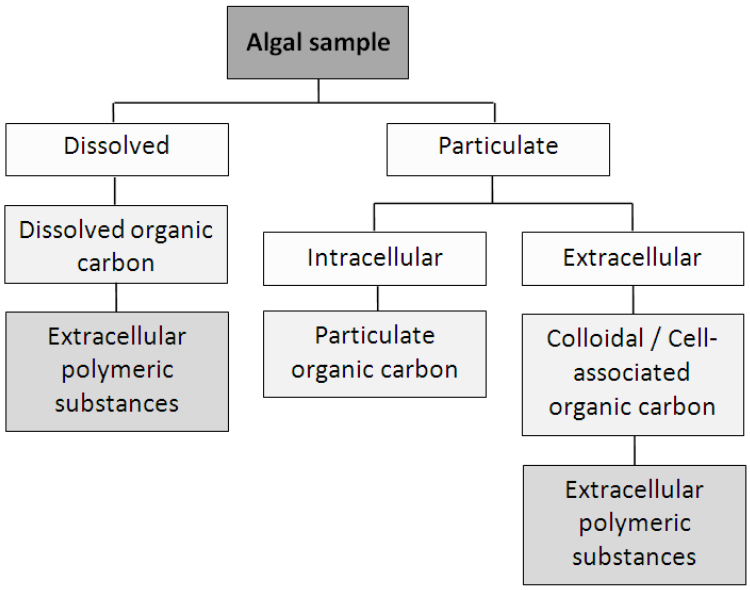

Figure 5.1: Isolated carbon pools

Key finding 3: Exuded carbon composition has varying benefits to the producer organism

The distinct patterns in carbon allocation observed in this thesis undoubtedly reflect benefits to the producer organism. However, discussing these benefits requires some speculation, due to the complex nature and limited knowledge of the topic. The following considers each extracellular isolate defined above, its likely ecological role, and how it directly benefits the producer organism within the sea ice habitat.

Extracellular dissolved organic carbon (EDOC or DOC) is commonly quantified within the sea ice habitat, but its specific ecological role has remained obscure. This is partly due to its all-inclusive molecular assay, grouping carbohydrates (constituting up to 30 % of DOC, Chapter 3), proteins, lipids, and a range of other long and short chain carbon-based molecules. Predominantly containing low molecular weight material (i.e. EPS was not detected; Chapter 2, 4; Figure 5.1), DOC dominated early in the winter-spring transition (Chapter 4). But with the onset of spring/summer and improved conditions suitable for microbial growth, allocation to this carbon isolate decreased (Chapter 3, 4). The most suitable explanation for this observation is *overflow metabolism*; a 'starvation' response during adverse conditions whereby the microbial photosynthetic community allocated carbon to extracellular material, thereby reducing their growth rate and cellular requirements (Chapter 2, 4). Overflow metabolism has been identified predominantly in non-photosynthetic microbes (e.g. yeasts, bacteria), but has not previously been found in the sea ice habitat. This new and exciting observation of

sea ice microbial ecology raises many additional questions relating to sea ice algal adaptive strategies, and consequential ecosystem impacts and carbon flux dynamics.

Colloidal organic carbon (COLLOC) is a collective term for organic carbon that is either (1) colloidal or (2) cell-associated, and is below the size fraction of EPS (i.e. cannot be precipitated in 70 % ethanol; Figure 5.1). Due to the particulate nature of this isolate, the methods applied within this thesis could not separate these two carbon groups. The relative contribution of each group to overall COLLOC remains unclear, and this is important as each is likely to have different benefits to the producer organism.

(1) Colloidal materials are carbon-based aggregates that contribute to carbon cycling, particle/trace metal scavenging, and may act as a substrate for bacteria contributing to an active microbial loop (Chapter 3, 4). But by this definition, some colloidal material may also be present in isolated DOC. The presence of a microbial loop would be particularly important during times when nutrient availability is low. This thesis does not provide direct evidence to support (or otherwise) the presence of a microbial loop associated with either COLLOC or DOC isolates. Granted, no direct correlations were present between the bacterial community and extracellular organic carbon, other parameters (such as NH_4^+ concentrations and algal biomass) may have indicated the presence of a microbial loop within the sea ice habitat.

On the other hand, (2) cell-associated material directly interacts with the producer organism, and its associated benefits may be simpler to describe. A minimum quantity of cell-associated material is required by some producer organisms, and this is important for aiding in cell attachment (e.g. chain forming cells and adhering to ice crystals) and motility. However, this material may become increasingly significant during times of adverse physicochemical conditions, where the producer organism becomes wrapped in extracellular material in an attempt to protect or buffer against potentially harmful conditions. This may be particularly important within the sea ice habitat, where increased photosynthetic activity within the confines of brine channels, triggered by improved seasonal changes, induces rapid changes in biogeochemical properties (e.g. carbonate chemistry, nutrient availability, salinity). This thesis provided evidence to support this concept, with an increase in COLLOC observed with the onset of spring (Chapter 4). This suggests the producer organisms were preconditioning themselves for increased photosynthetic activity (Chapter 4).

Extracellular polymeric substances (EPS) have received recent scientific attention, and are described as high-molecular weight material (dissolved or colloidal) that can be precipitated in 70 % ethanol (Figure 5.1). This thesis has demonstrated that, although the relative contribution of EPS to total primary production is low (up to 6%, Chapter 2), it is likely to have high ecological significance since it is only exuded in detectable quantities during times of severe adverse physicochemical conditions (Chapter 2, 3, 4). As such, the lack of EPS detected does not provide any evidence to support (or otherwise) its exudation as a means to manipulate the micro-morphology of brine channels, or alternatively, as a

potential energy source during times of low primary production due to light limitation (Chapter 4). This infers that the specific benefits to the producer organism may be diverse, particularly given the complexity of the molecules and the energy required to manufacture and exude that material.

Regardless, this thesis demonstrated that the sea ice algal community varies their carbon allocation between three extracellular isolates, with each isolate likely to have varying benefits to the producer organism (Chapter 2, 3, 4).

Key finding 4: Current research underestimates ecological significance of extracellular carbon

The thesis has clearly demonstrated that Antarctic sea ice algae are capable of exuding high quantities of photosynthetically-derived organic carbon (Chaper 2, 3, 4). The work reported here is the first attempt to directly quantify exudation into isolated carbon pools within the Antarctic sea ice habitat.

Importantly, this thesis has highlighted the complexities of organic carbon exudation. Generally in other studies, only the dissolved fraction of organic carbon is routinely quantified within the sea ice and underlying seawater. The estimates of extracellular organic carbon allocation reported (Chapters 2, 3, 4) shows that limiting quantification to dissolved material is likely to substantially underestimate the significance of extracellular organic carbon (^{14}C-EDOC < 10 % of ^{14}C-TPP, Chapter 2, 4).

The thesis, a collation of three peer-reviewed papers/manuscripts, has provided a sound foundation in this under-studied topic. With an increased ability to quantify exudation of organic carbon, large scale estimates of the contribution of sea ice algae to total primary production and carbon flux dynamics within ice covered areas could be achieved (e.g. Saenz and Arrigo 2014; Underwood et al. 2013). Furthermore, the methods presented herein can be used to develop and test new, and more efficient, technologies, such as microsensors and fluorometry analysis. It is my sincere wish that the work reported here can help to provide the rationale for this future research.

CHAPTER 6

Literature Cited

Abdullahi AS, Underwood GJC, Gretz MR (2006) Extracellular matrix assembly in diatoms (Bacillariophyceae). V. Environmental effects on polysaccharide synthesis in the model diatom, *Phaeodactylum tricornutum*. J Phycol 42:363–378

Ackley SF, Lewis MJ, Fritsen CH, Xie H (2008) Internal melting in Antarctic sea ice: Development of ''gap layers''. Geophys Res Lett 35(L11503) doi:10.1029/2008GL033644.

Ærtebjerg-Nielsen G, A-M Bresta (1984) Guidelines for the measurement of phytoplankton primary production. Baltic Marine Biologists (2nd edn). Marine Pollution Laboratory, Charlottenlund.

Alldredge AL (2000) Interstitial dissolved organic carbon (DOC) concentrations within sinking marine aggregates and their potential contribution to carbon flux. Limnol. Oceanogr. 45(6):1245–1253.

Antoine D, Morel A (1996) Oceanic primary production – adaptation of a spectral light-photosynthesis model in view of application to satellite chlorophyll observation. Global Biogeochem Cycles, doi: 10.1029/95GB02831.

Apoya-Horton MD, Yin L, Underwood GJC, Gretz MR (2006) Movement modalities and responses to environmental changes of the mudglat diatom *Cylindrotheca closterium* (Bacillariophyceae). J Phycol 42:379–390.

Archer SD, Leakey RJG, Burkill PH, Sleigh MA, Appleby CJ (1996) Microbial ecology of sea ice at a coastal Antarctic site: community composition, biomass and temporal change. Mar Ecol Prog Ser 135:179–195.

Arrigo KR, Brown ZW, Mills MM (2014) Sea ice algal biomass and physiology in the Amundsen Sea, Antarctica. Elementa (Washington, DC) 2(1) doi:10.12952/journal.elementa.000028.

Arrigo KR, Mock T, Lizotte MP (2010) Primary producers and sea ice. In: *Sea ice*, 2nd edition (eds DN Thomas, GS Dieckmann), Wiley-Blackwell, Oxford, 283–326.

Arrigo KR, van Dijken G, Long M (2008) Coastal Southern Ocean: a strong anthropogenic carbon dioxide sink. Geophys Res Lett 35 L21602, doi:10.1029/2008GL035624.

Arrigo KR, Weiss AM, Smith Jr WO (1998a) Physical forcing of phytoplankton dynamics in the southwestern Ross Sea. J Geophys Res 103:1007–1021.

Arrigo KR, Worthen DL, A Schnell, Lizotte MP (1998b) Primary production in Southern Ocean waters. J Geophys Res 103:15587–15600.

Arrigo KR, Worthen DL, Lizotte MP, Dixon P, Dieckmann G (1997) Primary production in Antarctic sea ice. Science 276(5311):394–397.

Aslam SN, Cresswell-Maynard T, Thomas DN, Underwood JC (2012) Production and characterization of the intra- and extracellular carbohydrates and polymeric substances (EPS) of three sea-ice diatom species, and evidence for a cryoprotective role for EPS. J Phycol 48:1494–1509.

Aslam SN, Underwood GJC, Kaartokallio H, Norman L, Autio R, Fischer M, Kuosa H, Dieckmann GS, Thomas DN (2012b) Dissolved extracellular polymeric substances (dEPS) dynamics and bacterial growth during sea ice formation in an ice tank study. Polar Biol 35:661 – 676.

Azam F, Smith DC, Hollibaugh JT (1991) The role of the microbial loop in Antarctic pelagic ecosystems. Pol Res 10:239–243.

Becquevort S, Dumont I, Tison J-L, Lannuzel D, Sauve´e M-L, Chou L, Schoemann V (2009) Biogeochemistry and microbial community composition in sea ice and underlying seawater off East Antarctica during early spring. Polar Biol 32(6):879–895.

Bellinger BJ, Abdullahi AS, Gretz MR, Underwood GJC (2005) Biofilm polymers: relationship between carbohydrate biopolymers from estuarine mudflats and unialgal cultures of benthic diatoms. Aquat Microb Ecol 38:169–180.

Blain S, Quéguiner B, Armand L, Belviso S, Bombled B, Bopp L, Bowie A, Brunet C, Brussaard C, Carlotti F, Christaki U, Corbière A, Durand I, Ebersbach F, Fuda J-L, Garcia N, Gerringa L, Griffiths B, Guigue C, Guillerm C, Jacquet S, Jeandel C, Laan P, Lefèvre D, Lo Monaco C, Malits A, Mosseri J, Obernosterer I, Park Y-H, Picheral M, Pondaven P, Remenyi T, Sandroni V, Sarthou G, Savoye N, Scouarnec L, Souhaut M, Thuiller D, Timmermans K, Trull T, Uitz J, van Beek P, Veldhuis M, Vincent D, Viollier E, Vong L, Wagener T (2007) Effect of

natural iron fertilization on carbon sequestration in the Southern Ocean. Nature 446:1070–1074.

Bluhm BA, Gradinger RR, Schnack-Schiel SB (2010) Sea ice meio- and macrofauna. In: Thomas, D.N., Dieckmann, G. (eds.), Sea ice, 2nd Edition. Blackwell, Oxford, UK. 357–394.

Bouvier T, Del Giorgio PA (2007) Key role of selective viral-induced mortality in determining marine bacterial community composition. Environ Microbiol 9:287–297.

Bouvier T, Del Giorgio PA, Gasol JM (2007) A comparative study of the cytometric characteristics of high and low nucleic-acid bacterioplankton cells from different aquatic ecosystems. Environ Microbiol 9:2050−2066.

Bowman JP, McCammon SA, Brown MV, Nichols DS, McMeekin TA (1997) Diversity and association of psychrophilic bacteria in Antarctic sea ice. Appl Environ Microbiol 63(8):3068–3078.

Braissant O, Decho AW, Dupraz C, Glunk C, Przekop KM, Visscher PT (2007) Exopolymeric substances of sulfate-reducing bacteria: Interaction with calcium at alkaline pH and implication for formation of carbonate minerals. Geobio 5:401–411.

Brown MV, Bowman JP (2001) A molecular phylogenetic survey of sea-ice microbial community (SIMCO). Microbiol Ecol 35(3):267–275.

Bucciarelli E, Sunda WG (2003) Influence of CO_2, nitrate, phosphate, and silicate limitation on intracellular dimethylsulfoniopropionate in batch cultures of the coastal diatom *Thalassiosira pseudonana*. Limnol Oceanogr 48(6):2256–2265.

Carlson CA, Hansell DA, Peltzer ET, Smith WO (2000) Stocks and dynamics of dissolved and particulate organic matter in the southern Ross Sea, Antarctica. Deep-Sea Res II 47:3201–3326.

Chen CY, Durbin EG (1994) Effects of pH on the growth and carbon uptake on marine phytoplankton. Mar Ecol Prog Ser 109:83–94.

Christaki U, Dolan JR, Pelegri S, Rassoulzadegan F (1998) Consumption of picoplankton-size particles by marine ciliates: effects of physiological state of the ciliate and particle quality. Limnol Oceanogr 43:458–464.

Collins RE, Carpenter SD, Deming JW (2008) Spatial heterogeneity and temporal dynamics of particles, bacteria and pEPS in Arctic winter sea ice. J Mar Syst 74:902–917.

Collins RE, Rocap G, Deming JW (2010) Persistence of bacterial and archaeal communities in sea ice through an Arctic winter. App Environ Microbiol 12:1828–1841.

Comiso JC (2010) Variability and trends of the global sea ice cover. In: Thomas DN, Dieckmann G (eds.), Sea ice, 2nd Edition. Wiley-Blackwell, Oxford, UK. 205–246.

Cooksey KE, Wigglesworth-Cooksey B (1995) Adhesion of bacteria and diatoms to surface in the sea: A review. Aquat Microb Ecol 9:87–96.

Cota GF (1985) Photoadaptation of high Arctic ice algae. Nature 315:219–222.

Cota GF, Sullivan CW (1990) Photoadaptation, growth and production of bottom ice algae in the Antarctic. J. Phycol 26(3):399–411.

Cox GFN, Weeks WF (1983) Equations for determining the gas and brine volume in sea ice samples. J Glaciol 29(102):306–31.

Cunningham SD, Munns DN (1984) The correlation between extracellular polysaccharide production and acid tolerance in rhizobium. Soil Sci Am J 48(6):1273–1276.

De Brouwer JFC, Stal LJ (2002) Daily fluctuations of exopolymers in cultures on the benthic diatoms *Cylindrotheca closterium* and *Nitzschia sp.* (Bacillariophyceae). J Phycol 38:464–472.

Decho AW (1990) Microbial exopolymer secretions in ocean environments: their roles in food webs and marine processes. In: Barnes M (eds) Oceanography and Marine Biology Annual Review. Aberdeen University Press 28:73–153.

Decho AW (1993) Methods for the observation and use in feeding experiments of microbial exopolymers. In: Kemp PF, Sherr BF, Cole JJ (Eds.) Handbook of methods in aquatic microbial ecology. Lewis Publishers, Boca Raton 685–694.

Decho AW (2000) Microbial biofilms in intertidal systems: an overview. Cont Shelf Res 20:1257–1273.

Delille D, Fiala M, Kuparinen J,Kuosa H, Plessis C (2002) Seasonal changes in microbial biomass in the first-year ice of Terra Adélie area (Antarctica). Aquat Microb Ecol 28:257–265.

Dickson AG (1981) An exact definition of total alkalinity and a procedure of the estimation of alkalinity and total inorganic carbon from titration date. Deep-Sea Res I 28:609–623.

Dieckmann GS, Eicken H, Haas C, Garrison DL, Gleitz M, Lange M, Nothig EM, Spindler M, Sullivan CW, Thomas DN, Weissenberger J (1998) A compilation of data on sea ice algal

standing crop from the Bellingshausen, Amundsen and Weddell Seas from 1983 to 1994. In: Lizotte MP, Arrigo KR (Eds.) Antarctic sea ice: biological processes, interactions and variability. Antarctic Research Series 73. American Geophysical Union, Washington, 85–92.

Doval MD, Alvarez-Salgado XA, Castro CG, Perez FF (2002) Dissolved organic carbon distributions in the Bransfield and Gerlache Straits, Antarctica. Deep-Sea Res II 49:663–674.

Dubischar CD, Bathmann UV (1997) Grazing impact of copepods and salps on phytoplankton in the Atlantic section of the Southern Ocean. Deep Sea Re II 44(1-2):415-433.

Eicken H (1992) The role of sea ice in structuring Antarctic ecosystems. Polar Biol 12(1):3–13.

Eicken H, Lange MA (1989) Development and properties of sea ice in the coastal regime of the south-eastern Weddell Sea. J Geophys Res 94(C6):8193–8206.

El-Sayed SZ, Weber LH (1982) Spatial and temporal variations in phytoplankton biomass and primary productivity in the Southwest Atlantic and the Scotia Sea. Polar Biol 1:83–90.

Engbrodt R, Kattner G (2005) On the biogeochemistry of dissolved carbohydrate in the Greenland Sea (Arctic). Org Geochem 36:937–948.

Eriksen R (1997) A practical manual for the determination of salinity, dissolved oxygen and nutrients in seawater. Antarctic CRC Res. Rep. II, Univ. of Tasmania, Hobart.

Ewert M, Deming JW (2013) Sea ice microorganisms: environmental constraints and extracellular responses. Biol 2:603–628.

Fiala M, Kuosa H, Kopczynska EE, Oriol L, Delille D (2006) Spatial and seasonal heterogeneity of sea ice microbial communities in the first-year ice of Terre Adélie area (Antarctica). Aquat Microb Ecol 43:95–106.

Fogg GE (1983) The ecological significance of extracellular products of phytoplankton photosynthesis. Bot Mar 26:3–14.

Frankenstein G, Garner R (1967) Equations for determining the brine-volume of sea ice from – 0.5 ° to – 22.9 °C. J Glaciol 6(48):943 – 944.

Frazer TK, Quetin LB, Ross RM (1997) Abundance and distribution of larval krill, Euphausia superba, associated with annual sea ice in winter. In: Battaglia B, Valencia J, Walton DWH (Eds.), Antarctic Communities: Species, Structure and Survival, Cambridge University Press, 107-111.

Fritsen CH, Lytle VI, Ackley SF, Sullivan CW (1994) Autumn Bloom of Antarctic Pack-Ice Algae. Science 266(5186):782–784.

Froneman PW, Laubscher RK, McQuaid CD (2001) Size-fractionated primary production in the south Atlantic and Atlantic sectors of the Southern Ocean. J Plankton Res 23(6):611–622.

Garrison DL, Buck KR (1986) Organism losses during ice melting: A serious bias in sea ice community studies. Polar Biol 6:237–239.

Garrison DL, Close AR, Reimnitz E (1990) Microorganisms concentrated by frazil ice. CRREL Monogr 90(1):92–96.

Garrison DL, Gibson A, Coale SL, Gowing MM, Okolodkov YB, Fritsen HF, Jefferies MO 2005 Sea ice microbial communities in the Ross Sea: autumn and summer biota. Mar Ecol Prog Ser 300:39 – 52.

Giesenhagen HC, Detmer AE, de Wall J, Weber A, Gradinger RR, Jochem FJ (1999) How are Antarctic planktonic microbial food webs and algal blooms affected by melting of sea ice? Microcosm simulations. Aquat Microb Ecol 20:183–201.

Giordano M, Beardall J, Raven JA (2005) Mechanisms in algae: mechanisms, environmental, modulation, and evolution. Annu Rev Plant Biol 56:99–131.

Gleitz M, Kirst GO (1991) Photosynthetic-irradiance relationships and carbon metabolism of difference ice algal assemblages collected from Weddell Sea pack ice during austral spring (EPOS 1). Polar Biol 11:385–392.

Gleitz M, Rutgers vd Loeff M, Thomas DN, Dieckmann GS, Millero FJ (1995) Comparison of summer and winter inorganic carbon, oxygen and nutrient concentrations in Antarctic sea ice brine. Mar Chem 51(2):81–91.

Gleitz M, Thomas DN (1992) Physiological responses of a small Antarctic diatom (Chaetoceros sp.) to simulated environmental constraints associated with sea-ice formation. Mar Ecol Prog Ser 88:271–278.

Gleitz M, Van der Loeff MR, Thomas DN, Dieckmann GS, Millero FJ (1995) Comparison of summer and winter inorganic carbon, oxygen and nutrient concentrations in Antarctic sea ice brine. Mar Chem 51:81–91.

Golden KM, Ackley SF, Lytle VI (1998) The percolation phase transition in sea ice. Science 282(5397):2238–2241.

Golden KM, Eicken H, Heaton AL, Miner J, Pringle DJ, Zhu J (2007) Thermal evolution of permeability and microstructure in sea ice. Geophys Res Lett 34 L16501.

Goto N, Kawamura T, Mitamura O, Terai H (1999) Importance of extracellular organic carbon production in the total primary production by tidal-flat diatoms in comparison to phytoplankton. Mar Ecol Prog Ser 190:289–295.

Granskog MA, Kaartokallio H, Shirasawa K (2003) Nutrient status of Baltic Sea ice: evidence for control by snow-ice formation, ice permeability, and ice algae. J Geophys Res 108(C8) doi: 10.1029/2002JC001386.

Granum E, Kirkvold S, Myklestad S (2002) Cellular and extracellular production of carbohydrates and amino acids by the marine diatom *Skeletonema costatum*: diel variations and the effects of N depletion. Mar Ecol Prog Ser 242:83 – 94.

Granum E, Stale K, Myklestad SM (2002) Cellular and extracellular production of carbohydrates and amino acids by the marine diatom *Skeletonema costatum*: diel variations and effects on N depletion. Mar Ecol Prog Ser 242:83–94.

Griffiths FB, Bates TS, Quinn PK, Clementson LA, Parslow JS (1999) Oceanographic context of the First Aerosol Characterisation Experiment (ACE-1): A physical, chemical and biological overview. J Geophys Res Atmos 104:21649–21671.

Grose M, McMinn A (2003) Algal biomass in east Antarctic pack ice: how much is in the east? In: Huiskes AHL, Gieskes WWC, Rozema J, Schorno RML, van der Vies SM, Wolff WJ (Eds.) Antarctic biology in a global context. Proceedings of the VIIIth SCAR.

Grossart H-P, Kiørboe T, Tang K, Ploug H (2003) Bacterial colonization of particles: Growth and interactions. App Environ Microbiol 69:3500–3509.

Guillard RRL, Ryther JH (1962) Studies of marine planktonic diatoms. 1. *Cyclotella nana* Hustedt and *Detonula confervacea* (Cleve) Gran Can J Microbiol 8:229–239.

Günther M, Gleitz M, Dieckmann GS (1999) Biogeochemistry of Antarctic sea ice: a case study on platelet ice layers at Drescher Inlet, Weddell Sea. Mar Ecol Prog Ser 177:1–13.

Healey FP (1975) Physiological indicators of nutrient deficiency in algae. Fisheries and Marine Service Research and Development Technical Report. 585.

Hellmer HH, Schröder M, Hass C, Dieckmann GS, Spindler M (2008) The ISPOL drift experiment. Deep Sea Res II 55(8–9):913–817.

Herborg LM, Thomas DN, Kennedy H, Haas C, Dieckmann GS (2001) Dissolved carbohydrates in Antarctic sea ice. Ant Sci 13(2):119–125.

Hoagland KD, Rosowski JR, Gretz MR, Roemer SC (1993) Diatom extracellular polymeric substances: Functions, fine structure, chemistry, and physiology. J Phycol 29(5):537–566.

Holm-Hansen O, Hewes CD (2004) Deep chlorophyll-*a* maxima (DCMs) in Antarctic waters. Polar Biol 27:699–710.

Holm-Hansen O, Riemann B (1978) Chlorophyll a determination: Improvements in methodology. Oikos 30(3):438–447.

Horner R, Ackley SF, Dieckmann GS, Gulliksen B, Hoshiai T, Legendre L, Melnikov IA, Reeburgh WS, Spindler M, Sullivan CW (1992) Ecology of sea ice biota. 1. Habitat, terminology, and methodology. Polar Biol 12:417–427.

Hung CC, Santschi PH (2001) Spectrophotometric determination of total uronic acids using cation-exchange separation and pre-concentration by lyophilisation. Anal Chim Acta 427:111–117.

Huntley ME, Karl DM, Niiler P, Holm-Hansen O (1991) Research on Antarctic Coastal Ecosystem Rates (RACER): an interdisciplinary field experiment. Deep Sea Res 38:911–941.

Jia Z, Swadling KM, Meiners KM, Kawaguchi S, Virtue P (submitted) The zooplankton food web under East Antarctic pack ice – a stable isotope study. Deep Sea Res II.

Juhl AR, Krembs C, Meiners KM (2011) Seasonal development and differential retention of ice algae and other organic fractions in first-year Arctic sea ice. Mar Ecol Prog Ser 436:1–16.

Junge K, Eicken H, Deming JW (2004) Bacterial activity at – 2 and – 20 °C in Arctic wintertime sea ice. Appl Environ Microbiol 70(1):550–557.

Junge K, Imhoff F, Staley T, Deming JW (2002) Phylogenetic diversity of numerically important Arctic sea-ice bacteria at subzero temperature. Microb Ecol 43:315–328.

Kaartokallio H (2004) Food web components and physical and chemical properties of Baltic Sea ice. Mar Ecol Prog Ser 273:49–63.

Kähler P, Bjørnsen PK, Lochte K, Anita A (1997) Dissolved organic matter and its utilization by bacteria during spring in the Southern Ocean. Deep-Sea Res II 44:341–353.

Kang S-H, Fryxel GA (1992) Fragilariopsis cylindrus (Grunow) Krieger: The most abundant diatom in water column assemblages of Antarctic marginal ice-edge zones. Polar Biol 12(6-7):609–627.

Kattner G, Thomas DN, Haas C, Kennedy H, Dieckmann GS (2004) Surface ice and gap layers in Antarctic sea ice: highly productive habitats. Mar Ecol Prog Ser 277:1–12.

Kennedy H, Thomas DN, Kattner G, Haas C, Dieckmann GS (2002) Particulate organic matter in Antarctic summer sea ice: concentration and stable isotopic composition. Mar Ecol Prog Ser 238:1–13.

Kirchman DL, Meon B, Ducklow HW, Carlson CA, Hansell DA, Steward GF (2001) Glucose fluxes and concentrations of dissolved combined neutral sugars (polysacchardies) in the Ross Sea and polar Front Zone, Antarctica. Deep-Sea Res II 48:4179–4197.

Kottmeier ST, McGrath Grossi S, Sullivan CW (1987) Sea ice microbial communities. VIII. Bacterial production in annual sea ice of McMurdo Sound, Antarctic marginal ice-edge zones. Deep Sea Res I 37:1311–1330.

Kottmeier ST, Sullivan CW (1987) Late winter primary production and bacterial production in sea ice and seawater west of the Antarctic Peninsula. Mar Ecol Prog Ser 36:287–298.

Krell A, Beszteri B, Dieckmann G, Glockner G, Calentine K, Mock T (2008) A new class of ice-binding proteins discovered in a salt-stress-induced cDNA library of the psychrophilic diatom *Fragilariopsis cylindrus* (Bacillariophyceae). Eur J Phycol 43:423–433.

Krell A, Funck D, Plettner I, John U, Dieckmann G (2007) Regulation of proline metabolism under salt stress in the psychrophilic diatom *Fragilariopsis cylindrus* (Bacillariophyceae). J Phycol 43:753–762.

Krembs C, Deming JW (2008) The role of exopolymers in microbial adaptation to sea ice. *Psychrophiles: From Biodiversity to Biotechnology*, eds Margesin R, Schinner F, Marx J-C, Gerday C (Springer, Heidelberg) 247–264.

Krembs C, Eicken H, Deming JW (2011) Exopolymer alteration of physical properties of sea ice and implications for ice habitability and biogeochemistry in a warmer Arctic. Proc Natl Acad Sci 108(9):3653–3658.

Krembs C, Eicken H, Junge K, Deming JW (2002) High concentrations of exopolymeric substances in Arctic winter sea ice: Implications for the polar ocean carbon cycle and cryoprotections of diatoms. Deep Sea Res I 49:2163–2181.

Krembs C, Engel A (2001) Abundance and variability of microorganisms and transparent exopolymer particles across the ice-water interface of melting first-year sea ice in the Laptev Sea (Arctic). Mar Biol 138:173–185.

Kudoh S, Imura S, Kashino Y (2003) Xanthophyll-cycle of ice algae on the sea ice bottom in Saroma Ko lagoon, Hokkaido, Japan. Polar Biosci 16:86–97.

Lange MA (1988) Basic properties of Antarctic sea ice as revealed by textural analysis of ice cores. Ann Glaciol 10:95–101.

Lange MA, Schlosser P, Ackley SF, Wadhams P, Dieckmann GS (1990) 18O concentrations in sea ice of the Weddell Sea, Antarctica. J Glaciol 36(124):315–323.

Lannuzel D, Chever F, van der Merwe P, Janssens J, Roukaerts A, Cavagna A-J, Townsend A, Bowie A, Meiners K (submitted) Iron biogeochemistry in Antarctic pack ice during SIPEX-2. Deep Sea Res II.

Lannuzel D, Schoemann V, de Jong J, Chou L, Delille B, Becquevort S, Tison J-L (2008) Iron study during a time series in the western Weddell pack ice. Mar Chem 108:85–95.

Laundry MR, Hassett RP (1982) Estimating the grazing impact of marine micro-zooplankton. Mar Biol 67:283–288.

Laws EA, Bidigare RR, Popp BN (1995) Effect of growth rate and CO2 concentration on carbon isotopic fractionation by the marine diatom *Phaeodactylum tricornutum*. Limnol Oceanogr 42(7):1552–1560.

Lebaron P, Servais P, Baudoux A-C, Bourrain M, Courties C, Parthuisot N (2002) Variations of bacterial-specific activity with cell size and nucleic acid content assessed by flow cytometry. Aquat Micro Ecol 28:131–140.

Legendre L, Ackley SF, Dieckmann GS, Gulliksen B, Horner R, Hoshiai T, Melnikov IA, Reeburgh WS, Spindler M, Sullivan CW (1992) Ecology of sea ice biota. Polar Biol 12:429–444.

Lemke P (2009) Itinerary and Summary. Cruise Report Winter Weddell Outflow Study (WWOS)-ANT XXIII/7. Reports in Polar Research 586:10–11.

Leppäranta M, Manninen T (1988) The brine and gas content of sea ice with attention to low salinities and high temperatures. Finnish Institute Marine Research Internal Report 88-2, Helsinki.

Lewis E, Wallace DW (1998) Program Developed for CO2 System Calculations. ORNL/CDIAC-105. Carbon Dioxide Information Analysis Center, Oak Ridge National Laboratory, U.S. Department of Energy, Oak Ridge, Tennessee.

Lewis MR, Smith JC (1983) A small volume, short-incubation-time method for measurement of photosynthesis as a function of incident irradiance. Mar Eco Prog Ser 13:99–10.

Light B, Maykut GA, Grenfell TC (2003) Effects of temperature on the microstructure of first-year Arctic sea ice. J Geophys Res-OC 108(C2) doi:10.1029/2001JC000887.

Lizotte MP (2001) The contributions of sea ice algae to Antarctic marine primary production. Amer Zoo 41(1):57–73.

Lizotte MP, Sullivan CW (1992) Photosynthetic capacity in microalgae associated with Antarctic pack ice. Polar Biol 12:497–502.

Loeb V, Siegel V, Holm-Hansen O (1997) Effects of sea-ice extent and salp or krill dominance on the Antarctic food web. Nature 387:897–900.

Mancuso Nichols C, Guezennec J, Bowman J (2005) Bacterial expolysaccharides from extreme environments with special consideration of the Southern Ocean, sea ice, and deep sea hydrothermal vents: a review. Mar Biotechnol 7:253–271.

Martin A, Anderson MJ, Thorn C, Davy SK, Ryan KG (2011) Response of sea ice microbial communities to environmental change: an *in situ* experiment in the Antarctic. Mar Ecol Prog Ser 424:25–37.

Martin A, Hall JA, O'Toole R, Davy SK, Ryan KG (2008) High single-cell metabolic activity in Antarctic sea ice bacteria. Aquat Micro Ecol 52:25–31.

Martin A, Hall JA, Ryan KG (2009) Low salinity and high-level UV-B radiation reduce single-cell activity in Antarctic sea ice bacteria. Appl Environ Microbiol 75:7570–7573.

Martin A, McMinn A, Davy SK, Anderson MJ, Miller HC, Hall JA, Ryan KG (2012) Preliminary evidence for the microbial loop in Antarctic sea ice using microcosm simulations. Ant Sci 24(6):547–553.

Martin JH, Gordon RM, Fitzwater SE (1990) Iron in Antarctic waters. Nature 345:156–158.

Massom RA, Eicken H, Haas C, Jeffries MO, Drinkwater MR, Sturm M, Worby AP, Wu X, Lytle VI, Ushio S, Morris K, Reid PA, Warren S, Allison I (2001) Snow on Antarctic sea ice. Rev Geophys 39(3):413–445.

Maykut GA (1985) The ice environment. In: Horner R (Eds.) Sea ice biota. CRC Press, Boca Raton, 21–28.

Maykut GA (1986) The surface heat and mass balance, in The Geophysics of Sea Ice, NATO ASI Ser, Ser B, 146, edited by N. Untersteiner, Martinus Nijhoff, Dordrecht, Netherlands, 395–463.

McConville MJ, Mitchell C, Wetherbee R (1985) Patterns of carbon assimilation in a microalgal community from annual sea ice, East Antarctica. Polar Biol 4:135–41.

McConville MJ, Wetherbee R, Bacic A (1999) Subcellular location and composition of the wall and secreted extracellular sulphated polysaccharides/proteoglycans of the diatom *Stauroneis amphioxys* Gregory. Protoplasma 206:188–200.

McMinn A, Ashworth C, Ryan KG (2000) *In situ* net primary productivity of an Antarctic fast ice bottom algal community. Aquat Micro Ecol 21:177–185.

McMinn A, Hegseth EN (2003) Early Spring pack ice algae fron the Arctic and Antarctic: how different are they? Backhuys Publishers, 27 Aug - 1 Sep 2001, Vrije Universiteit, Amsterdam: 182 – 186. ISBN 90-5782-079-X.

McMinn A, Hegseth EN (2004) Quantum yield and photosynthetic parameters of marine microalgae from the Southern Arctic Ocean, Svalbard. J Mar Biol Ass UK 84:865–871.

McMinn A, Martin A (2013) Dark survival in a warming world. Proc R Soc B 280(1755) doi: 10.1098/rspb.2012.2909.

McMinn A, Pankowskii A, Ashworth C, Bhagooli R, Ralph P, Ryan K (2010) In situ net primary productivity and photosynthesis of Antarctic sea ice algae, phytoplankton and benthic algal communities. Mar Biol 157:1345–1356.

McMinn A, Ryan K, Grademann R (2003) Diurnal changes in photosynthesis of Antarctic fast ice algal communities determined by pulse amplitude modulation fluorometry. Mar Biol 143:359–367.

McMinn A, Ryan KG, Ralph PJ, Pankowski A (2007) Spring sea ice photosynthesis, primary productivity and biomass distribution in eastern Antarctica, 2002 – 2004. Mar Biol 151:985–995.

McMinn A, Skerratt J, Trull T, Ashworth C (1999) Nutrient stress gradient in the bottom 5 cm of fast ice, McMurdo Sound, Antarctica. Polar Biol 21:220–227.

Mehta SK, Gaur JP (2007) Use of algae for removing heavy metal ions from wastewater: Progress and prospects. Crit Rev Biotechnol 25:113–152.

Meiners K, Brinkmeyer R, Granskog MA, Lindfors A (2004) Abundance, size distribution and bacterial colonization of exopolymer particles in Antarctic sea ice (Bellingshausen Sea). Aquat Micro Ecol 35:283–296.

Meiners K, Gradinger R, Fehling J, Civitarese G, Spindler M (2003) Vertical distribution of exopolymer particles in sea ice of the Fram Strait (Arctic) during autumn. Mar Ecol Prog Ser 248:1–13.

Meiners KM, Krembs C, Gradinger R (2008) Exopolymer particles: Microbial hotspots of enhanced bacterial activity in Arctic fast ice (Chukchi Sea). Aquat Microb Ecol 52:195–207.

Meiners KM, Norman L, Granskog MA, Krell A, Heil P, Thomas DN (2011) Physico-ecobiogeochemistry of East Antarctic pack ice during the winter-spring transition. Deep Sea Res II 58:1172 – 1181.

Meiners KM, Papadimitriou S, Thomas DN, Norman L, Dieckmann GS (2009) Biogeochemical conditions and ice algal photosynthetic parameters in Weddell Sea ice during early spring. Pol Biol 32:1055–1065.

Meiners KM, Vancoppenolle M, Thanassekos S, Dieckmann GS, Thomas DN, Tison J-L, Arrigo KR, Garrison DL, McMinn A, Lannuzel D, van der Merwe P, Swadling KM, Smith Jr WO, Melnikov I, Raymond B (2012) Chlorophyll *a* in Antarctic sea ice from historical ice core data. Geophys Res Lett 39(L21602) doi:10.1029/2012GL053478.

Michael KJ, Higgins J (2014) Diffuse attenuation coefficients for East Antarctic pack ice and snow at ultraviolet and visible wavelengths. IEEE Trans Geosci Remote Sens 52(7):4455–4461.

Mishra A, Jha B (2009) Isolation and characterization of extracellular polymeric substances from micro-algae *Dunaliella salina* under salt stress. Bioresource Technol 100:3382–3386.

Mitchell BG, Brody EA, Holm-Hansen O, McMlain C, Bishop J (1991) Light limitation of phytoplankton biomass and macronutrient utilization in the Southern Ocean. Limnol Oceanogr 36(8):1662–1677.

Mock T (2002) *In situ* primary production in young Antarctic sea ice. Hydrobiologia 470:127–132.

Mock T, Thomas DN (2005) Recent advances in sea-ice microbiology. Environ Microbiol 7(5):605–619.

Mock T, Valentin K (2004) Photosynthesis and cold acclimation: Molecular evidence from a polar diatom. J Phycol 40:732–741.

Mohamed ZA (2001) Removal of cadmium, and manganese by a non-toxic strain of the freshwater cyanobacterium *Gloethece manga*. Water Res 35:4405–4409.

Moore JK, Abbott MR (2000) Phytoplankton chlorophyll distributions and primary production in the Southern Ocean. J Geophys Res 105: 28709–28722.

Myklestad S (1977) Production of carbohydrates by marine plankton diatoms. II. Influence of the N/P ratio in the growth medium on the assimilation ratio, growth rate, and production of cellular and extracellular carbohydrates by *Chaetoceros affinis* var. *willei* (Gran) Hustedt and *Skeletonema costatum* (Grev.) Cleve. J Exp Mar Biol Ecol 29(2):161–179.

Myklestad S, Holm-Hansen O, Vårum KM, Volcani BE (1989) Rate of release of extracellular amino acids and carbohydrates from the marine diatom *Chaetoceros affinis*. J Plank Res 11:763–773.

Myklestad SM, Børsheim KY (2007) Dynamics of carbohydrates in the Norwegian Sea inferred from monthly profiles collected during 3 years at 66°N 2°E. Mar Chem 107:475–485.

Nelson DM, Smith Jr Wo (1991) Sverdrup revisited: critical depths, maximum chlorophyll levels, and the control of southern ocean productivity by the irradiance mixing regime. Limnol Oceanogr 36:1650–1661.

Norman L, Thomas DN, Stedmon CA, Granskog MA, Papadimitriou S, Krapp RH, Meiners KM, Lannuzel D, van der Merwe P, Dieckmann GS (2011) The characteristics of dissolved organic matter (DOM) and chromophoric dissolved organic matter (CDOM) in Antarctic sea ice. Deep Sea Res II 58(9–10):1075–1091.

Oppenheim DR, Ellis-Evans JC (1989) Depth-related changes in benthic diatoms assemblages of a maritime Antarctic lake. Polar Biol 9:525–532.

Pakulski JD, Benner R (1994) Abundance and distribution of dissolved carbohydrates in the ocean. Limnol Oceanogr 39:930–940.

Palmisano AC, Garrison DL (1993) Microorganisms in Antarctic sea ice. In: Friedmann EI (ed) Antarctic microbiology. Wiley-Liss, New York 167–218.

Palmisano AC, SooHoo JB, Sullivan CW (1985) Photosynthesis-irradiance relationships in sea ice microalgae from McMurdo Sound, Antarctica. J of Phycol 21(3):341–346.

Palmisano AC, Sullivan CW (1983) Sea ice microbial communities (SIMCO). Polar Biol 2(3):171–177.

Papadimitriou S, Thomas DN, Kennedy H, Kuosa H, Deickmann GS (2009) Inorganic carbon removal and isotopic enrichment in Antarctic sea ice gap layers during early austral summer. Mar Ecol Prog Ser 386:15–27.

Papadimitriou S, Thomas DN, Kennedy H, Kuosa H, Krell A, Dieckmann GS (2007) Biogeochemical composition of natural sea ice brines from the Weddell Sea during early austral summer. Limnol Oceanogr 52:1809–18223.

Park MG, Yang SR, Kang S-H, Chung KH, Shim JH (1999) Phytoplankton biomass and primary production in the marginal ice zone of the northwestern Weddell Sea during austral summer. Polar Biol 21:251–261.

Perkins RG, Underwood GJC, Brotas V, Snow GC, Jesus B, Ribeiro L (2001) Responses of microphytobenthos to light: primary production and carbohydrate allocation over an emersion period. Mar Ecol Prog Ser 223:101–112.

Petrich C, Eicken H (2010) Growth, structure and properties of sea ice. In: Sea ice (2nd ed), DN Thomas and G S Dieckmann (eds), Wiley–Blackwell, Oxford, UK 23–77.

Petrou K, Ralph PJ (2011) Photosynthesis and net primary productivity in three Antarctic diatoms: possible significance for their distribution in the Antarctic marine ecosystem. Mar Ecol Prog Ser 437:27–40.

Platt T, Gallegos CL, Harrison WG (1980) Photoinhibition of photosynthesis in natural assemblages of marine phytoplankton. J Marine Res 38:687–701.

Ploug H, Grossart H-P (1999) Bacterial production and respiration in suspended aggregates – A matter of the incubation method. Aquat Microb Ecol 20:21–29.

Ploug H, Jørgensen B B (1999) A net-jet flow system for mass transfer and microsensor studies of sinking aggregates. Mar Ecol Prog Ser 176:279–290.

Popp BN, Trull T, Kenig F, Wakeham SG, Rust TM, Tilbrook B, Griffiths B, Wright SW, Marchant HJ, Bidigare RR, Laws EA (1999) Controls on the carbon isotopic composition of Southern Ocean phytoplankton. Global Biogeochem Cycles 13:827–843.

Qain J, Mopper K (1996) An automated, high performance, high temperature combustion dissolved organic carbon analyser. Anal Chem 68(18):3090–3097.

Ralph PJ, Gademann R (2005) Rapid light curves: a powerful tool to assess photosynthetic activity. Aquat Bot 82:222–237.

Redfield AC, Ketchum BH, Richards FA (1963) The influence of organisms on the composition of sea-water. In: The Sea (v. 2), MN Hill, John Wiley and Sons, New York 26–77.

Reeburgh (1984) Fluxes associated with brine motion in growing sea ice. Polar Biol 3:29–33.

Riebesell U, Wolf-Gladrow DA, Smetacek V (1993) Carbon dioxide limitation of marine phytoplankton growth rates. Nature 361:249–251.

Riedel A, Michel C, Gosselin M (2006) Seasonal study of sea-ice exopolymeric substances on the Mackenzie shelf: Implications for transport of sea-ice bacteria and algae. Aquat Micro Ecol 45:195–206.

Riedel A, Michel C, Gosselin M, LeBlanc B (2007) Enrichment of nutrients, exopolymeric substances and microorganisms in newly formed sea ice on the Mackenzie shelf. Mar Ecol Prog Ser 342:55–67.

Riedel A, Michel C, Gosselin M, LeBlanc B (2008) Winter-spring dynamics in sea-ice carbon cycling in the coastal Arctic Ocean. J Mar Syst 74(3–4):918–932.

Roukaerts AL, Cavagna A-J, Fripiat F, Lannuzel D, Meiners K, Dehairs F (submitted) Sea-ice algal primary production and nitrogen uptake rates off East Antarctica. Deep Sea Res II.

Roy RN, Roy LN, Vogel KM, Porter-Moore C, Pearson T, Good C, Millero FJ, Campbell DM (1993) The dissociation constants of carbonic acid in seawater at salinities 5 to 45 and temperatures 0 to 45 °C. Mar Chem 44(2-4):249–267.

Ryan KG, Hegseth EN, Martin A, Davy SK, O'Tool R, Ralph PJ, McMinn A, Thorn CJ (2006) Comparison of the microalgal community within fast ice at two sites along the Ross Sea coast, Antarctica. Ant Sci 18(4):583–594.

Ryan KG, Ralph P, McMinn A (2004) Acclimation of Antarctic bottom-ice algal communities to lowered salinities during melting. Polar Biol 27:679–686.

Saenz BT, Arrigo KR (2014) Annual primary production in Antarctic sea ice during 2005-2006 from a sea ice state estimate. J Geophys Res-OC 119(6):3645–3678.

Sakshaug E, Bricaud A, Dandonneau Y, Falkowski PG, Kiefer DA, Legendre L, Morel A, Parslow J, Takahshi M (1997) Parameters of photosynthesis: definitions, theory and interpretation of results. J Plankton Res 19:1637–1670.

Sakshaug E, Holm-Hansen O (1986) Photoadaptiation in Antarctic phytoplankton: Variations in growth rate, chemical composition and *P* verses *I* curves. J Plankton Res 8:450–473.

Sakshaug E, Slagstad D (1991) Factors controlling the development of phytoplankton blooms in the Antarctic Ocean – a mathematical model. Mar Chem 35(1–4):259–271.

Sambrotto RN, Mace BJ (2000) Coupling of biological and physical regimes across the Antarctic Polar Front as reflected by nitrogen production and recycling. Deep Sea Res II 47:3339–3367.

Sarthou G, Timmermanns KR, Blain S, Treguer P (2005) Growth physiology and fate of diatoms in the ocean: a review. J Sea Res 53:25–42.

Schnack-Schiel SB, Dieckmann GS, Kattner G, Thomas DN (2004) Copepods in summer platelet ice in the eastern Weddell Sea, Antarctica. Polar Biol 27:502–506.

Schreiber U (2003) Pulse amplitude (PAM) fluorometry and saturation pulse method. In: Papageorgiou, G., Govindjee (eds) Chorophyll fluorescence: A signature of photosynthesis. Advances in photosynthesis and respiration series. Kluwer Academic Publishers, Dordrecht, The Netherlands.

Scott P, McMinn A, Hosie G (1994) Physical parameters influencing diatom community structure in eastern Antarctic sea ice. Polar Biol 14:507–517.

Servais P, Casamayor EO, Courties C, Catala P, Parthuisot N, Lebaron P (2003) Activity and diversity of bacterial cells with high and low nucleic acid content. Aquat Micro Ecol 33:41–51.

Sharp JH (1977) Excretion of organic matter by marine phytoplankton: Do healthy cells do it? Limnol Oceanogr 22:381–399.

Smith DJ, Underwood GJC (1998). Exopolymer production by intertidal epipelic diatoms. Limnol Oceanogr 43(7):1578–1591.

Smith DJ, Underwood GJC (2000) The production of extracellular carbohydrates by estuarine benthic diatoms: The effects of growth phase and light and dark treatment. J Phycol 36:321–333.

Smith Jr WO, Comiso JC (2008) Influence of sea ice on primary production in the Southern Ocean: A satellite perspective. Geophys Res 113(C5) DOI: 10.1029/2007JC004251.

Smith Jr WO, Nelson DM (1986) The importance of ice-edge phytoplankton production in the Southern Ocean. BioScience 36:251–257.

Smith REH, Anning J, Clement P, Cota G (1988) Abundance and production of ice algae in Resolute Passage, Canadian Arctic. Mar Ecol Prog Ser 48:251–261.

Smith REH, Demers S, Hattori H, Kudoh S, Legendre L, Michel C, Gosselin M, Robineau B, Suzuki S, Takahashi M, Therriault JC, Juniper SK, Sime-Ngando T (1995) Biological and chemical investigations of the Saroma-Resolute project in ice-covered Resolute Passage, 1992. Can Data Rep Hydrogr Ocean Sci 137:vvi–19.

Smith WO, Gordon LI (1997) Hyperproductivity of the Ross Sea (Antarctica) polynya during austral spring. Geophys Res Lett 24:233–236.

Staats N, Stal LJ, Mur LR (2000) Exopolysaccharide production by the epipelic diatom *Cylindrotheca closterium*: effects of nutrient concentrations. J Exp Mar Biol Ecol 249:13–27.

Sullivan CW, Palmisano AC (1984) Sea ice microbial communities: distribution, abundance, and diversity of ice bacteria in McMurdo Sound, Antarctica, in 1980. Appl Environ Microbiol 47:788–795.

Sullivan CW, Palmisano AC, Kottmeier S, McGroath Grossi S, Moe R (1985) The influence of light on growth and development of the sea-ice microbial community of McMurdo Sound. In: Siegfried WR, Condy PR, Laws RM (eds) Antarctic nutrient cycles and food webs. Springer, Berlin Heidelberg, New York. 78–83.

Taylor GT, Sullivan CW (2008) Vitamin B12 and cobalt cycling among diatoms and bacteria in Antarctic sea ice microbial communities. Limnol Oceanogr 53:1862–1877.

Thomas DN, Dieckmann GS (2002) Antarctic sea ice – a habitat for extremophiles. Science 295(5555):641–644.

Thomas DN, Dieckmann GS eds. (2010) Sea ice. Second edition. Oxford, Wiley-Blackwell.

Thomas DN, Kattner G, Engbrodt R, Giannelli V, Kennedy H, Haas C, Dieckmann GS (2001) Dissolved organic matter in Antarctic sea ice. Ann Glaciol 33:297–303.

Thomson PG, Davidson AT, van den Enden R, Pearce I, Seuront L, Paterson JS, Williams GD (2010) Distribution and abundance of marine microbes in the Southern Ocean between 30 and 80°E. Deep Sea Res II 57:815–827.

Tilzer MM, Elbrächter M, Gieskes W, Beese B (1986) Light-temperature interactions in the control of photosynthesis in Antarctic phytoplankton. Polar Biol 5:105–111.

Tison J-L, Worby A, Delille B, Barabant F, Papadimitriou S, Thomas D, de Jong J, Lannuzel D, Haas C (2008) Temporal evolution of decaying summer first-year sea ice in the Western Weddell Sea, Antarctica. Deep Sea Res II 55(8–9):975–987.

Trenerry L, McMinn A, Ryan K (2002) In situ oxygen microelectrode measurements of bottom ice algal production in McMurdo Sound, Antarctica. Polar Biol 25(1):72–80.

Trevena AJ, Jones GB, Wright SW, van den Enden RL (2000) Profiles of DMSP, algal pigments, nutrients and salinity in pack ice from eastern Antarctica. J Sea Res 43(3-4):265–273.

Ugalde SC, Martin A, Meiners KM, McMinn A, Ryan KG (2014). Extracellular organic carbon dynamics during a bottom-ice algal bloom (Antarctica). Aquat Microb Ecol doi: 10.3354/ame01717.

Ugalde SC, Meiners KM, Davidson AT, Westwood KJ, McMinn A (2013) Photosynthetic carbon allocation of an Antarctic sea ice diatom (*Fragilariopsis cylindrus*). J Exp Mar Biol Ecol 446:228–235.

Underwood GJ, Aslam SN, Michel C, Niemi A, Norman L, Meiners KM, Laybourn-Parry J, Paterson H, Thomas DN (2013) Broad-scale predictability of carbohydrates and exopolymers in Antarctic and Arctic sea ice. Proc Natl Acad Sci 110(39):15734–15739.

Underwood GJC, Boulcott M, Raines CA, Waldron K (2004) Environmental effects on exopolymer production by marine benthic diatoms: dynamics, changes in composition, and pathways of production. J Phycol 40:293–304.

Underwood GJC, Fietz S, Papadimitriou S, Thomas DN, Dieckmann GS (2010) Distribution and composition of dissolved extracellular polymeric substances (EPS) in Antarctic sea ice. Mar Ecol Prog Ser 404:1–9.

Underwood GJC, Paterson DM (2003) The importance of extracellular carbohydrate production by marine epipelic diatoms. Adv Bot Res 40:183–240.

Underwood GJC, Paterson DM, Parkes RJ (1995) The measurement of microbial carbohydrate exopolymers from intertidal sediments. Limnol Oceanogr 40(7):1243–1253.

Underwood GJC, Smith DJ (1998) Predicting epipelic diatom exopolymer concentrations in intertidal sediments from sediment chlorophyll *a*. Microb Ecol 35:116–125.

van der Merwe P, Lannuzel D, Mancuso Nichols CA, Meiners K, Heil P, Norman L, Thomas DN, Bowie AR (2009) Biogeochemical observations during the winter-spring transition in East Antarctic sea ice: evidence of iron and exopolysaccharide controls. Mar Chem 115:163–175.

van Oijen T, van Leeuwe MA, Granum E, Weissing FJ, Bellerby RGJ, Gieskes WWC, de Baar HJW (2004) Light rather than iron controls photosynthate production and allocation in Southern Ocean phytoplankton populations during austral autumn. J Plankton Res 26(8):885–900.

Vancoppenolle M, Goosse H, de Montety A, Fichefet T, Tremblay B, Tison J-L (2010) Modeling brine and nutrient dynamics in Antarctic sea ice: The case of dissolved silica. J Geophys Res 115(C02005) doi:10.1029/2009JC005369.

Vancoppenolle M, Meiners KM, Michel C, Bopp L, Brabant F, Carnat G, Delille B, Lannuzel D, Madec G, Moreau S, Tison J-L, van der Merwe P (2013) Role of sea ice in global biogeochemical cycles: emerging views and challenges. Quat Sci Rev 79:207–230.

Waite AM, Olson RJ, Dam HG, Passow U (1976) Sugar-containing compounds on the cell surfaces of marine diatoms measured using concanacalin A and flow cytometry. J Phycol 31:925–933.

Wang D, Henrichs SM, Guo L (2006) Distributions of nutrients, dissolved organic carbon and carbohydrates in the western Arctic Ocean. Cont Shelf Res 26:1654–1667.

Wedborg M, Hoppema M, Skoog A (1998) On the relation between organic and inorganic carbon in the Weddell Sea. J Mar Syst 17:59–76.

Weeks WF, Ackley SF (1986) The growth, structure, and properties of sea ice. In: Untersteiner N (eds.) The geophysics of sea ice. Plenum Press, New York. 9–164.

Weissenberger J, Grossmann S (1998) Experimental formation of sea ice: importance of water circulation and wave action for incorporation of phytoplankton and bacteria. Polar Biol 20:178–188.

Wolfstein K, Stal L (2002) Production of extracellular polymeric substances (EPS) by benthic diatom: effect of irradiance and temperature. Mar Ecol Prog Ser 236:13–22.

Worby AP, Geiger CA, Paget MJ, van Woert ML, Ackley SF, DeLiberty TL (2008) Thickness distribution of Antarctic sea ice. J Geophys Res 113(C05S92) doi:10.1029/2007JC004254.

Worby AP, Steer, A, Lieser JL, Heil P, Yi D, Markus T, Allison I, Massom RA, Galin N, Zwally J (2011) Regional-scale sea-ice and snow thickness distributions from in situ and satellite measurements over East Antarctica during SIPEX 2007. Deep Sea Res II 58(9–10):1125–1136.

Wright SW, van den Enden RL, Pearce I, Davidson AT, Scott FJ, Westwood KJ (2010) Phytoplankton community structure and stocks in the Southern Ocean (30–80°E) determined by CHEMTAX analysis of HPLC pigment signatures. Deep Sea Res II 57:758–778.

Zinkevich V, Bogdarina I, Kang H, Hill MAW, Tapper R, Beech IB (1996) Characterisation of exopolymers produced by different isolates of marine sulphate-reducing bacteria. Int Biodeterior Biodegrad 5:163–172.